

X-581-74-

PREPRINT

NASA TM X-70728

**RADIO ASTRONOMY EXPLORER-B
POSTLAUNCH
ATTITUDE OPERATIONS
ANALYSIS**

(NASA-TM-X-70728) RADIO ASTRONOMY
EXPLORER-B POSTLAUNCH ATTITUDE OPERATIONS
ANALYSIS (NASA) 143 p HC \$10.25

N74-32261

CSCL 22C

Unclas

G3/30

46674

JULY 1974



GODDARD SPACE FLIGHT CENTER
GREENBELT, MARYLAND

RADIO ASTRONOMY EXPLORER-B

POSTLAUNCH

ATTITUDE OPERATIONS

ANALYSIS

R. D. Werking

R. Berg

K. Brokke

T. Hattox

G. Lerner

D. Stewart

R. Williams

ABSTRACT

In June 1973, the Radio Astronomy Explorer-B (RAE-B) spacecraft was launched from the Eastern Test Range on a journey which resulted in a near-circular lunar orbit. This document describes the attitude support activities provided by the Attitude Determination and Control Section of Goddard Space Flight Center and Computer Sciences Corporation during the RAE-B mission. The performance of the spacecraft hardware and support software also is discussed. Because the RAE-B spacecraft was placed in lunar orbit as opposed to the Earth orbit of RAE-1, many changes to the attitude systems of the RAE-1 mission were made for the RAE-B mission. These changes included: (1) a cold-gas attitude control system to replace the magnetic control system, (2) a panoramic attitude sensor (PAS) to replace the magnetometers, and (3) a new attitude support software package using interactive graphics.

The RAE-B attitude support software used the recently developed Multi-Satellite Attitude Program System (MAPS). The MAPS/RAE-B system relied heavily on the use of interactive graphics. This interactive capability allowed the user to control the flow of data through the system, to review the quality of data as processing continued, and to provide a pictorial representation of the events as they occurred. The various plots in this report are reproductions of displays which were used during the support activities. The use of interactive graphics proved itself by allowing the support function to provide the quality control necessary to ensure mission success in an environment where flight-simulated ground testing of all spacecraft hardware cannot be performed.

The PAS proved to be a very flexible sensor for use in attitude determination activities. Although difficulties were encountered during some phases of the sensor operation, the device has a great deal of potential and has been recommended for use on the International Ultraviolet Explorer (IUE).

TABLE OF CONTENTS

<u>Section 1 - The Mission and the Spacecraft</u>		1-1
1.1	Mission Overview	1-1
1.2	Spacecraft Subsystems	1-2
1.2.1	Spacecraft Configuration	1-2
1.2.2	Experiments	1-4
1.2.3	Solar Aspect Sensor System	1-4
1.2.4	Panoramic Attitude Sensor System	1-5
1.2.5	Attitude Control System	1-6
1.2.6	Velocity Correction Propulsion Subsystem	1-7
1.3	Mission and Attitude Determination Requirements	1-7
1.3.1	Mission Requirements	1-7
1.3.2	Attitude Determination and Control Section Requirements . .	1-8
1.4	Conclusions and Recommendations	1-9
1.4.1	Spacecraft Hardware	1-10
1.4.2	Attitude Support Software	1-13
 <u>Section 2 - Mission Profile</u>		 2-1
2.1	Introduction	2-1
2.2	Launch	2-1
2.3	Translunar Cruise	2-9
2.4	Lunar Insertion	2-18
2.5	Orbit Correction	2-27
2.6	Dipole Calibration	2-28
2.7	Boom Deployment	2-29
 <u>Section 3 - Attitude Determination and Control Hardware Evaluation</u> . .		 3-1
3.1	Introduction	3-1
3.2	Attitude Determination Sensors--Spin Mode	3-1
3.2.1	Prelaunch Specifications and Alignment	3-1
3.2.2	Postlaunch Sensor Operation	3-9
3.3	Attitude Determination Sensors--Planar Mode	3-38
3.3.1	Prelaunch Specifications and Alignment	3-38
3.3.2	PAS Hardware Malfunctions	3-43
3.3.3	SAS Hardware Malfunctions	3-43
3.4	Attitude Control Hardware Evaluation	3-44
3.4.1	Hardware Malfunctions	3-45
3.4.2	Hardware Calibration	3-49

TABLE OF CONTENTS (Cont'd)

<u>Section 4 - Software Evaluation</u>	4-1
4.1 MAPS/RAE-B System Evaluation	4-1
4.2 Performance Evaluation of Analytical Algorithms	4-2
4.2.1 Solution Restoration	4-2
4.2.2 Horizon-Terminator Checking	4-4
4.2.3 Solution Pairing	4-4
4.2.4 Bit Overflow Restoration	4-5
4.2.5 ACS Performance Parameter Evaluation	4-8
4.2.6 Predicted-Observed Telemetry Data Plot	4-8

Appendix A - Explanation of Column Headings for Tabular Displays

Appendix B - Dipole Calibration Data Analysis

References

LIST OF ILLUSTRATIONS

Figure

1-1	Geometric Structure of the RAE-B Spacecraft	1-3
2-1	Single Frame Solutions From Earth at Launch	2-3
2-2	Sensor Data From the Moon Using Scanner 2	2-6
2-3	Single Frame Solutions From Moon at Launch	2-7
2-4	Block Average Attitude Using Moon Data at Launch	2-8
2-5	Sensor Data From Moon During Translunar Cruise	2-10
2-6	Block Average Attitude Using Moon During Translunar Cruise	2-11
2-7	Block Average Editing	2-12
2-8	Cone Intersection Geometry Prior to Midcourse Correction	2-14
2-9	PAS1 Performance at 2200 on June 13	2-16
2-10	Moon Geometry at 2200 on June 13	2-17
2-11	Moon Geometry Prior to Lunar Insertion Precess, 1700 GMT June 14	2-19
2-12	Attitude Data Obtained During Precession Maneuver	2-20
2-13	Moon Geometry After Precess Maneuver, 2044 GMT June 14	2-21
2-14	Attitude Determination, 2044 GMT June 14	2-22
2-15	Moon Geometry at 0357 GMT June 15	2-23
2-16	Moon Geometry at 0510 GMT June 15	2-24
2-17	Moon Geometry at 0523 GMT June 15	2-25
2-18	Moon Geometry at 0547 GMT June 15	2-26
2-19	Data Availability Profile--Attitude Chosen To Provide Fair Coverage for D1 and D2	2-30
2-20	Data Availability Profile--Attitude Chosen To Provide Maximum Coverage for D1	2-31
2-21	Pitch Solutions Prior to Deployment at 1453 GMT	2-34
2-22	Roll Solutions Prior to Deployment at 1453 GMT	2-35
2-23	Yaw Solutions Prior to D1 Deployment at 1453 GMT	2-36
2-24	Yaw Solutions Prior to D1 at 1453 GMT	2-37
2-25	Predicted-Observed Body Sun Angles	2-38
2-26	Attitude Solutions (No Shadow)	2-45
2-27	Attitude Solutions (Shadow)	2-46
3-1	RAE-B Spacecraft Geometry	3-2
3-2	PAS Scanner Head	3-3
3-3	PAS Scanner Optics	3-4
3-4	PAS Telescope and Encoder Details	3-5

LIST OF ILLUSTRATIONS (Cont'd)

Figure

3-5	PAS Alignment Details	3-8
3-6	Spherical Mode Sun Sensor Operation	3-10
3-7	Upper and Lower Spherical Mode Sun Sensor Alignment	3-11
3-8	Spherical SAS Alignment Details	3-12
3-9	Central Body Geometry at Launch	3-14
3-10	Azimuth Angles Versus Time at Launch	3-15
3-11	Earth-Sun Interference at Launch	3-16
3-12	Moon Data at Launch	3-17
3-13	Moon Data, 1.7-Degree PAS2 Zero Bias	3-18
3-14	Moon Data, 0.7-Degree PAS2 Zero Offset	3-19
3-15	Double-Crossing Solutions (MOD1, MOD2, and MOD3)	3-21
3-16	PAS1 Malfunction	3-22
3-17	Attitude Determination Off Moon	3-24
3-18	PAS2 Asymmetric Sun Acceptance for Positive and Negative Encoder Angles	3-26
3-19	PAS2 Performance at 2145 on June 11	3-28
3-20	PAS2 Performance at 2000 on June 12	3-29
3-21	PAS2 Performance at 0730 on June 13	3-30
3-22	Attitude Determination Off Moon at 2103 GMT June 14 Before Lunar Insertion Trim	3-32
3-23	Attitude Determination Off Moon at 2227 GMT June 14 Before Lunar Insertion Trim	3-33
3-24	Attitude Determination Off Moon at 2400 GMT June 14 After Lunar Insertion Trim	3-34
3-25	Geometry Prior to Lunar Insertion	3-35
3-26	Graphical Attitude Determination Off Lunar Terminator	3-36
3-27	Central Body Geometry During Dipole Calibration	3-37
3-28	Attitude Determination Off Earth From Lunar Orbit	3-39
3-29	Summary of RAE-B Solid Angle Sensor (SAS) Alignment Checks	3-42
3-30	ACS Register Shift During Small Precess Maneuver	3-47
3-31	Predicted-Observed Sun Angles During ACS Maneuver Using Uncalibrated Hardware	3-51
3-32	Predicted-Observed Spin Rates During ACS Maneuver Using Uncalibrated Hardware	3-52
3-33	Initialization Display for ACS Performance Evaluation	3-53
3-34	Display of Results From ACS Performance Evaluation	3-54
3-35	Predicted-Observed Sun Angles Following ACS Performance Evaluation	3-55

LIST OF ILLUSTRATIONS (Cont'd)

Figure

3-36	Predicted-Observed Spin Rates Following ACS Performance Evaluation	3-56
4-1	Restored Single-Crossing Solutions From Moon	4-3
4-2	Pairs of Unidentified Crossings Yielding One Correct and One Incorrect Single-Crossing Solution	4-6
4-3	Block Average Selection of Correct Solutions From Pairs	4-7

LIST OF TABLES

Table

2-1	Attitude Control Events With Main Mission Events	2-2
3-1	RAE-B Biases--Spin Mode	3-40

SECTION 1 - THE MISSION AND THE SPACECRAFT

1.1 MISSION OVERVIEW

The RAE-B spacecraft was launched on June 10, 1973 from the Eastern Test Range (ETR) and placed into a near-circular lunar orbit. The spacecraft's experiments make directional radio-frequency measurements in the 0.025- to 13.1-megahertz range. A follow-on to the RAE-1, an Earth-orbiting spacecraft, the RAE-B is free from magnetospheric shielding, and can use the Moon itself as an occultation disk and as a shield against terrestrial magnetospheric and solar interference. Specific scientific objectives include the following:

- To map the galaxy, free from perturbing effects of the Earth's ionosphere
- To make observations of radio sources free from Earth-radiated signals
- To improve identification and positioning of radio sources by using the Moon as an occulting disk
- To study radiation from the Earth's magnetosphere at lunar distance
- To evaluate conditions needed for long-range planning of Earth-orbiting versus lunar-based radio observatories

The following is a schedule of major mission events; a more detailed description of these events is given in Section 2.

<u>Event</u>	<u>Date (Time)</u>
Launch	10 June (1413)
Translunar Injection	10 June (1428)
Midcourse Orbit Correction	11 June (1800)
Lunar Orbit Insertion	15 June (0721)

<u>Event</u>	<u>Date (Time)</u>
First Orbit Circularization	19 June (0000)
Second Orbit Circularization	20 June (0000)
Dipole Deployment	20 June (1800)
Third Orbit Circularization	9 July (1800)
Main Boom Deployment (183 meters)	
D1	12 July (1453)
D2	12 July (1615)
Damper	12 July (1725)
Final Deployment (229 meters)	13 November (1245)

The mission plan included a spindown to 12 rpm prior to the first midcourse correction with a second midcourse correction 20 hours prior to lunar orbit insertion. The intent of the spin-down was to conserve Attitude Control System (ACS) fuel if extensive maneuvers were necessary during the translunar phase. The mission was close enough to nominal at the time of the first midcourse correction that the spin-down was deleted. Also, the second midcourse was later deleted, confirming the decision not to despin.

1.2 SPACECRAFT SUBSYSTEMS

Major spacecraft systems are described in this subsection. Attitude determination and control systems are introduced here, but described in more detail in Section 3.

1.2.1 Spacecraft Configuration

The geometric structure of the RAE-B spacecraft, as shown in Figure 1-1, is a cylinder 92 centimeters in diameter and 79 centimeters in height, capped at the ends by truncated cones. The lunar insertion motor (LIM) is housed in the forward end; the Velocity Correction Propulsion System (VCPS) and spacecraft separation interface are mounted at the other end.

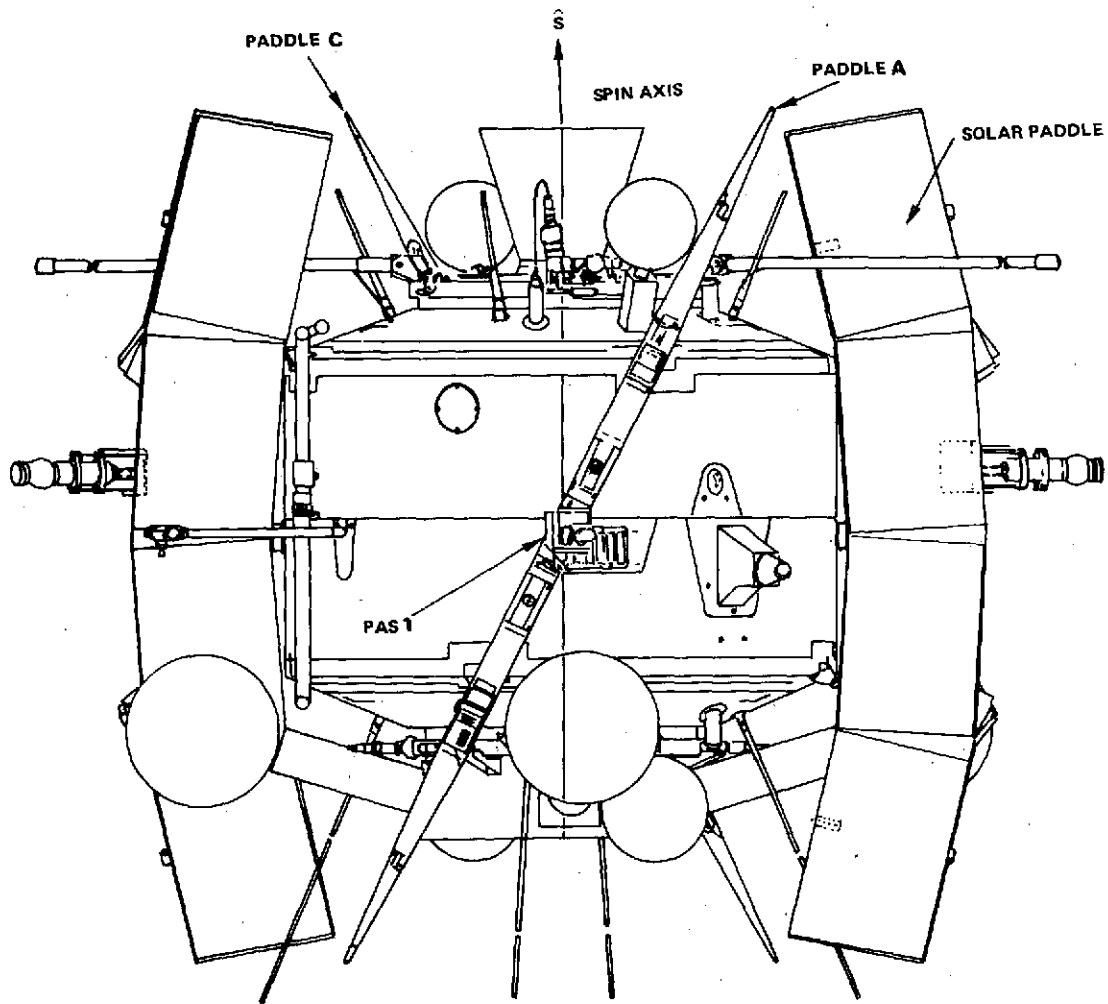


Figure 1-1. Geometric Structure of the RAE-B Spacecraft

Four fixed paddles are mounted on the main body of the spacecraft. The paddles are canted at an angle of 26.5 degrees to maintain a relatively constant power output over a wide range of spacecraft Sun angles. The solar aspect sensor (SAS) and panoramic attitude sensor (PAS) systems are mounted on the paddles. Overall spacecraft measurements are 183 centimeters \times 160 centimeters \times 147 centimeters high. (The last dimension is the paddle tip-to-tip measurement.)

1.2.2 Experiments

The experiments consist of two 9-channel step-frequency Ryle-Vonberg (RV) radiometers, three burst receivers, and an impedance probe. One RV radiometer and one burst receiver are used to measure noise simultaneously on each of the two acute-angle V-antennas. The third burst receiver is used to measure the signals received by a short dipole antenna.

The experiment antennas comprise two back-to-back V-antennas formed by deploying, up to a maximum length of 229 meters, four elements 1.5 centimeters in diameter, and a dipole deployed normal to the spacecraft Z-axis. The V-antennas are deployed at an angle (at the spacecraft body) of 30 degrees with respect to the spacecraft Z-axis, two elements pointing in the +Z direction and two in the -Z direction. As the spacecraft is gravity-gradient oriented, one V-antenna points toward the Moon at all times while the other scans the celestial sphere. The antenna system is essentially omnidirectional between 0.03 and 1 megahertz and is somewhat directional (approximately 15-decibel front-to-back ratio) in the range 1 to 20 megahertz.

1.2.3 Solar Aspect Sensor System

The SAS system functions in two modes, spin and solid. The mode is selected by ground command: spin mode is used above approximately 3 rpm; solid mode, at spin rates below approximately 1 rpm.

Two fan-shaped sensors located on the outer edge of one solar paddle are used for spin mode operation. Solar elevation is measured at the second Sun sighting from the start of alternate telemetry frames. Spin period is measured as

the time between the first and second Sun sightings. The system supplies Sun azimuth information in the form of a Sun pulse to other onboard systems during spin mode. (Two solar gates associated with the panoramic sensors can also supply the Sun pulse. Selection is by ground command.)

Eight sensors are used for solid mode operation. Each has a field of view shaped as an inverted pyramid, with a 120-degree dihedral angle between opposite faces. Two sensors are mounted on each of the four solar paddles and oriented to cover the entire celestial sphere. The Sun angles are read out from the most intensely illuminated sensor, which is automatically selected by an onboard circuit. The reading is taken at a known time interval after the beginning of every other telemetry frame.

1.2.4 Panoramic Attitude Sensor System

The PAS system consists of two fixed-plane panoramic scanners and associated electronics equipment. The field of view of each scanner is 0.75 degree. This field is scanned 360 degrees in a plane parallel to the spin axis. The scan planes of the two scanners intersect at an angle of 54 degrees. The scanners operate in two modes: spherical and planar, which correspond to the spin and solid modes, respectively, of the SAS system operation.

In spherical mode, ground command may select either one of the two scanners. The scanner is advanced in steps of 0.7 degree at each Sun pulse from whichever sensor has been selected to supply the spacecraft Sun pulse. The Sun-pulse advance is inhibited upon scanner acquisition of a lit body (Sun, Earth, or Moon). The scanner is then advanced one step after each measurement. The Sun-pulse advance is resumed when lit-body acquisition is lost. A ground-commanded advance of 16 steps is also available.

In planar mode the two scanners alternate. A scan is initiated at the beginning of every second telemetry frame. The operating scanner advances at the constant rate of 100 steps per second. The status of the scanner is set to light or

dark when four consecutive steps indicate the same value (light or dark), and an acquisition or loss (as appropriate) is recorded when the status changes. The angles of first acquisition and last loss are transmitted. The Sun and panoramic sensor data are recorded in the same telemetry frame, although they are transmitted in alternate frames.

1.2.5 Attitude Control System

The ACS provides both spin rate and spin axis attitude control. The system uses a cold-gas propellant of Freon-14 plus 10 percent helium. The propellant is stored in two tanks; it passes through a regulator to either of two ACS booms located 180 degrees apart about the spin axis. Each boom has three nozzles: spin up, spin down, and orient. All nozzles produce a nominal 0.2-pound thrust except one of the orient nozzles, which produces a nominal 0.1-pound thrust.

The spin control functions in two modes: continuous and pulse. In continuous mode, the system is commanded on for an interval of time set in increments of either 1.28 or 2.56 seconds to a maximum of 21.5 or 43 minutes. The spin rate changes at about 0.15 rpm per second. In pulsed mode, the system is commanded on for a 300-millisecond pulse to trim the spin rate.

The orient control also functions in both continuous and pulsed modes. In continuous mode, the selected orient jet operates for one spin period, from one Sun pulse to the next. In pulsed mode, the selected orient jet operates once per revolution for an interval of time set in the same timer used for continuous spin control. (Spin and orient commands are not executed simultaneously.)

Direct ground control over the time interval can also be exercised. Ground commands are used to set the delay between the Sun pulse and the initiation of the ACS pulse and to select the pulse duration from three available widths (nominally 80 milliseconds, 350 milliseconds, and 950 milliseconds).

1.2.6 Velocity Correction Propulsion Subsystem

The VCPS is a hydrazine-fueled thruster which provides velocity corrections after payload separation from the third-stage motor. It is packaged on the transtage that is mounted between the spacecraft and the third-stage flight adapter. The VCPS is nonsteerable; the spacecraft must be oriented to obtain a particular thrust direction. The subsystem is jettisoned after final lunar orbit corrections are made, prior to main antenna deployment.

1.3 MISSION AND ATTITUDE DETERMINATION REQUIREMENTS

The Attitude Support System was designed to satisfy general RAE-B mission requirements as well as specific requirements of the Attitude Determination and Control Section. These requirements, in the following subsections, were considered in the evaluation of RAE-B hardware and software.

1.3.1 Mission Requirements

The primary requirement of the RAE-B mission was to place a gravity-gradient stabilized spacecraft in a circular lunar orbit. To accomplish this, the following were required.

1. The spacecraft must be spin stabilized in a lunar transfer trajectory.
2. The spacecraft must perform spin-up/spin-down maneuvers upon ground command.
3. The ACS and VCPS must be operated by ground command for mid-course corrections and reorientations to satisfy thermal and power constraints.
4. The ACS and the fourth-stage retromotor must be operated by ground command to attain an elliptical lunar orbit.
5. The ACS and VCPS must be operated by ground command to circularize the lunar orbit.

6. The dipoles must be extended by ground command, calibrated, and then retracted by ground command.
7. The ACS must be operated by ground command to orient the spin axis to the proper attitude in the orbit plane for boom deployment.
8. The ACS must be operated by ground command to despin the spacecraft to 1/4 rpm.
9. Attitude confirmation based on real-time data must be made to determine/predict the time when the pitch, roll, and yaw of the spacecraft will be within a specified tolerance for the first deployment of the 750-foot booms.
10. The main antenna must be deployed in a double deadbeat sequence.
11. Attitude confirmation must be made between each deadbeat step to determine proper tolerances for subsequent deployment.
12. The damper assembly, damper booms, and dipoles must be deployed by ground command.

1.3.2 Attitude Determination and Control Section Requirements

1.3.2.1 Translunar and Lunar

The following displays were required within the Attitude Support System:

1. Predicted versus observed Earth width
2. Right ascension and declination (from quick-look results)
3. Predicted and observed spin rates and Sun angles (real time) during maneuvers
4. Intermediate analytical results

Other requirements for translunar and lunar processing were to

1. Operate in batch processing mode
2. Compute nutation amplitude and period
3. Compute commands to maneuver spacecraft
4. Predict fuel consumption
5. Access orbit, Sun, and lunar files
6. Provide the following files for communication with other systems:
 - a. Attitude file (on command)
 - b. Attitude status file (on command)
 - c. Telemetry status file (continuously)

1.3.2.2 Pre- and Post-Boom Deployment

Requirements for pre- and post-boom deployment processing were to

1. Provide real-time determination and displays of pitch, roll, and yaw before and during boom deployment
2. Provide attitude rates in pitch, roll, and yaw during boom deployment
3. Calculate the counts required for boom deployment
4. Access orbit, Sun, and lunar files
5. Provide the following files for communication with other systems:
 - a. Attitude file (on command)
 - b. Attitude status file (continuously)
 - c. Telemetry status file (continuously)

1.4 CONCLUSIONS AND RECOMMENDATIONS

The mission and attitude requirements defined in the preceding sections were generally satisfied throughout the mission. Specific observations relating to

both software and hardware were noted during system development and post-launch support. Conclusions derived from the observations discussed in Sections 2 through 4, and recommendations based on them, are discussed in detail below.

1.4.1 Spacecraft Hardware

Of the attitude determination and control hardware, only the spin mode Sun sensor functioned as expected throughout the mission. However, all problems with the other systems were ultimately resolved more or less satisfactorily.

1.4.1.1 Attitude Control Subsystem

The ACS was designed for maximum flexibility, allowing precession in a nearly arbitrary direction, and either continuous or pulsed spin commands. In this respect, it fully satisfied mission requirements. Except for calibration maneuvers and maneuvers for critical velocity corrections, precession maneuvers were accomplished with a single command sequence. Spin rate control also was adequate to meet requirements. Differences between performance in ground-based tests and in actual operation were corrected by support software.

Two malfunctions occurred which were intermittent and could not be predicted. In one case, the counter which determined the sectoring of a precession pulse shifted in midmaneuver, changing the direction of the precession. This counter shift was observed twice, with the same hardware combination in use both times. The combination in question was not used after the second occurrence, and the problem did not recur. In the other case, the spin system, while in pulsed mode, remained on instead of terminating after a preset time interval. This occurred twice. The system was successfully shut off manually both times, but in the second instance only after the spacecraft had despun through 0 rpm to a negative spin rate.

The precession malfunction was almost certainly electronic in nature. The spin malfunction may have been electronic or mechanical, perhaps involving

sticking valves. The satisfactory performance of the system in other respects would justify further analysis of the problems if similar systems are needed on later missions.

1.4.1.2 Solid Mode Sun Sensors

The solid mode Sun sensors apparently worked properly under design conditions (spin rate less than 1 rpm). At spin rates higher than the design rate, a malfunction (discussed in Section 4; also in Appendix B, a reprint of Reference 1) occurred which may have arisen in the sensor selection circuit. Analyses of data at higher spin rates indicate that the malfunction may include uncertainty in the data sampling time, which uncertainty may extend to low spin rates (below 1 rpm). While insignificant following completion of boom deployment, this uncertainty would have complicated the problem of manual initiation of boom deployment, had that been necessary. An analysis of the circuitry is indicated if operation of a multisensor system above 1 rpm is contemplated.

1.4.1.3 Panoramic Attitude Sensors

The design of the PAS was based on the desire to use the same hardware in both spin-stabilized and gravity-gradient-stabilized modes. The result was a flexible system, particularly in spin mode, which allowed attitude determination at almost any time a target was available. For instance, acquisition of the Moon shortly after launch provided a quick confirmation of the injection attitude without needing accurate spacecraft orbit information.

The sensors did however suffer throughout the mission with a larger than intended Sun acceptance angle. The sensitivity of the detector was partly responsible, in that the scanner was designed to detect the Moon from the vicinity of the Earth.

Additional problems arose during the mission. Spurious triggerings, probably resulting from reflections within the scanner head, limited the region of the

celestial sphere in which the Earth and the Moon could be detected. A final spin mode problem occurred with one of the two scanners, in which the output from the solar gate on the scanner apparently was coupled into the output from the scanner detector, probably through the power supply which is common to the PAS detector and the associated solar gate. In planar mode, the scanner selector mechanism frequently malfunctioned, selecting only one of the two scanners. This usually happened at times when the scanner in question was not detecting valid (lunar horizon) transitions.

Despite these problems, the PAS provided attitude data sufficient to meet mission requirements. In spin mode, a sensor combination could usually be found to provide attitude data; while in planar mode, data was obtained for part of every orbit, and Sun angle data could be used for attitude confirmation at other times.

The flexibility of a variable-mounting-angle telescope has commended the use of the PAS design on other missions. The problem of Sun triggerings remains, however, and could be serious under certain conditions. Short of a complete redesign to eliminate the window believed to be the source of most of the problem, three possibilities suggest themselves:

1. Record and transmit more than one acquisition of signal (AOS) and loss of signal (LOS) per spin period. This would increase the probability that a valid target is detected if present. The problem of separating Sun acquisitions from others would rest with the support software, but would probably not be serious.
2. Provide additional solar gates for triggering the PAS counter. Probably two gates per PAS would be sufficient if properly oriented with respect to PAS Sun acceptance angles.
3. Provide a sectoring count under ground control (similar to ACS sectoring) to delay PAS activation relative to the Sun pulse. This

would provide maximum flexibility, but at the expense of additional operational complexity.

Because the Sun acceptance problems caused the PAS to trigger at every mounting angle, the manual scanner command, which advanced the scanner mounting angle by 16 0.7-degree steps per command, was invaluable. A modification to the circuit which sets the planar mode to zero might be more useful, however. This circuit compares the output of the shaft angle encoder with a hard-wired code to determine the end of the scan. A command similar to the manual advance command could be used to advance the scanner to such a predetermined position. If the code were placed in a ground-controlled register rather than being hard wired, a target in any relatively fixed location could be repetitively scanned with a minimum number of commands.

If operation of a multiscanner system corresponding to RAE-B planar mode is anticipated, the circumstances of the malfunction in the scanner selector circuit should be analyzed.

1.4.2 Attitude Support Software

The MAPS/RAE-B Attitude Support System was designed and developed to satisfy the mission and Attitude Determination and Control Section requirements discussed in Sections 1.3.1 and 1.3.2. The system functioned in an exceptional manner throughout the mission despite spacecraft hardware problems and stringent real-time operational requirements. The system was designed under the Multi-Satellite Attitude Determination (MSAD) Executive System which facilitated the design and the development of such a large system. The RAE-B System illustrates the demanding analytical and software requirements placed upon the GSFC Attitude Determination and Control Section in supporting future spacecraft missions.

SECTION 2 - MISSION PROFILE

2.1 INTRODUCTION

This section details the sequence of mission events and attitude software support for the RAE-B spacecraft from launch through main boom deployment.

Table 2-1 lists attitude control events with main mission events. Times are Greenwich Mean Time (GMT) and are approximate. Initial, desired, and final right ascension and declination are given for precession maneuvers with the great circle arc length connecting initial and final points. Spin rate changes, when not expressly commanded, resulted from other spacecraft operations. Most comments are amplified in the text.

2.2 LAUNCH

The spacecraft was launched from the ETR on June 10, 1973, at 1413 GMT. Attitude data was received by the control center at 1443 GMT, approximately 15 minutes after a nominal translunar injection. The initial data (PAS2-SAS configuration) was spotty and consisted mainly of Sun sightings, several of which were attributed to the Moon or Earth by the attitude system because of the anomalous behavior of the PAS scanner (see Section 3). A tentative Moon triggering at 1447 GMT resulted in an attitude of right ascension (α) = +164.6 degrees and declination (δ) = -15 degrees, which was quite close to the nominal attitude value of $\alpha_0 = +165.9$ degrees and $\delta_0 = -14.2$ degrees.

The spacecraft clock was switched from 200 Hertz to 800 Hertz at 1503 GMT, and a series of Earth triggerings was obtained as shown in Figure 2-1. (See Figures 3-9 through 3-11 for a plot of central body geometry shortly after

Table 2-1. Attitude Control Events With Main Mission Events

EVENT	TIME MM/DD/HHMM	RIGHT ASCENSION (DEGREES)			DECLINATION (DEGREES)			LENGTH (DEGREES)	SPIN RATE (RPM)			COMMENTS	
		INITIAL	DESIRED	FINAL	INITIAL	DESIRED	FINAL		INITIAL	DESIRED	FINAL		
LAUNCH	06/10/1413												
TRANSLUNAR INJECTION	1428												
PRECESSION	2130	164.9	168.2	N.D.	-12.0	-12.7	N.D.	3.3			50.4	ACS TEST	
PRECESSION	2200	168.2	179.0	176.2	-12.7	-14.5	-10.0	8.3			50.4	ACS TEST REGISTER SHIFT	
PRECESSION	06/11/1200	176.2	200.1	178.4	-10.0	-17.9	- 7.9	3.0			50.4	PRECESS TO VCS ATTITUDE REGISTER SHIFT	
PRECESSION	1245	178.4	200.1	197.6	- 7.9	-17.9	-21.9	23.2			50.3	PRECESS TO VCS ATTITUDE	
PRECESSION	1420	197.6	200.4	200.6	-21.9	-18.0	-18.4	4.5			50.2	TRIM MANEUVER FOR VCS	
MIDCOURSE ORBIT CORRECTION	1800										51.8	SPIN RATE INCREASE FROM VCS FIRING	
PRECESSION	1840	200.6	179.2	179.8	-18.4	-12.0	-12.8	20.8			51.8	SUNBATHE MANEUVER	
PRECESSION	06/14/1915	179.8	217.0	214.9	-12.8	26.0	24.7	50.8			51.5	PRECESS TO LUNAR INSERTION ATTITUDE	
PRECESSION	2345	214.9	216.7	216.7	24.7	26.0	26.1	2.2			51.1	TRIM MANEUVER FOR LUNAR INSERTION	
LUNAR ORBIT INSERTION	06/15/0721										51.4	FOURTH-STAGE FIRING	
SPIN DOWN	06/18/1700		217.3			26.8				51.4	10.5	SPIN RATE OVERSHOOT FROM CALIBRATION	
SPIN TRIM	1730									10.5	12.2	TWENTY-TWO SPIN-UP PULSES COMMANDED	
PRECESSION	1817	217.3	231.0	230.9	26.8	32.7	32.4	13.1			12.2	PRECESS TO CIRCULARIZATION ATTITUDE	
FIRST ORBIT CIRCULARIZATION	06/19/0000										12.3		
PRECESSION	1306	230.9	51.0	52.3	32.4	-32.5	34.1	177.9			12.3	PRECESS TO SECOND CIRCULARIZATION	
PRECESSION	1727	52.3	50.7	50.0	-34.1	-32.7	-32.0	2.8			12.4	TRIM MANEUVER FOR CIRCULARIZATION	
SECOND ORBIT CIRCULARIZATION	06/20/0000										12.4		
PRECESSION	1400	50.0	9.0	7.7	-32.0	3.5	4.3	54.1			12.6	PRECESS INTO ECLIPTIC PLANE	
SPIN UP	1438			7.7			4.3			12.6	15.0	INCREASE SPIN RATE FOR DIPOLE DEPLOYMENT	
DIPOLE DEPLOYMENT	1800									17.5	17.5		
SPIN DOWN	06/29/0400			7.7			4.3			4.7	3.0	3.1	
SPIN UP	07/09/1055			7.7			4.3			4.7	12.0	12.0	
										11.4	12.0	12.0	
PRECESSION	1135	7.7	269.0	267.4	4.3	38.0	37.0				12.0	DECREASE SPIN RATE TO TEST SUN SENSORS	
THIRD ORBIT CIRCULARIZATION	1800										12.0	SPIN RATE INCREASE TO USE HIGHER CLOCK RATE (DIPOLES PREVIOUSLY RETRACTED)	
PRECESSION	07/10/1746	267.4	217.7	219.2	37.0	29.6	30.5	40.2			12.0	PRECESS TO THIRD CIRCULARIZATION	
SPIN DOWN	07/11/1240			219.2			30.5				12.0	VCS EJECTED AFTER FIRING	
SPIN DOWN	1320			219.2			30.5		12.0	3.8	3.8	PRECESS TO BOOM DEPLOYMENT ATTITUDE	
SPIN UP	1415			219.2			30.5			0.25	-6.5	CONTINUOUS SPIN DOWN TO 3 RPM	
SPIN DOWN	1430			219.2			30.5			1.15	1.11	PULSED SPIN DOWN, MALFUNCTION	
										1.11	0.25	0.39	
MAIN BOOM DEPLOYMENT													SPIN UP TO ACHIEVE CORRECT SPIN DIRECTION
D1	07/12/1453												FINAL SPIN DOWN, COMMANDED EIGHT OF NINE PLANNED PULSES
D2	1615												MAIN ANTENNA DEPLOYMENT TO 183 METERS
DAMPER	1725												IN SINGLE DEADBEAT SEQUENCE, FOLLOWED BY DAMPER BOOM DEPLOYMENT
FINAL DEPLOYMENT	11/13/1245												FINAL DEPLOYMENT TO 229 METERS

2-2

```

***** M S A D *****
*** DISPLAY ***** 73.161.11.37.28 ***
**
** SGLRES SINGLE CROSS SOLUTIONS **
**
** ISGL--SGLCRS IND. (NO,YES) YES **
**
** IWEIGHT--WEIGHTING OPT. (1-SPIN,2-ARC) 1 **
** TRMCHK--HORIZON CHECK(0-H,1-H+U,2-ALL) 1 **
** CBWID--MIN. RHO FOR TRMCHK (DEG) 0.300 **
**
** BLOCK REFERENCE TIME (YYDDD) 73161 **
**
** BLOCK LIMITS-- IOUT1 1 **
** IOUT2 46 **
**
** CB - CENTRAL BODY (E,M,S,U) **
** HT - HORIZON/TERM. (H,T,U) **
**
** F TIME C H SUN SOL. ONE SOL. TWO R NO. **
** L HMMSS B T BETA GAMMA ALPHA1 DELTA1 WGT1 ALFA2 DELTA2 WGT2 F SOL **
** 145331 U U 92.4 152.7 999.00 999.00 0.0 999.00 999.00 0.0 0 **
** 145331 U U 92.4 152.7 999.00 999.00 0.0 999.00 999.00 0.0 0 **
** 145721 M T 92.4 33.6 164.56 -14.98 0.16 999.00 999.00 0.0 * 1 **
** 145721 M T 92.4 33.6 999.00 999.00 0.0 999.00 999.00 0.0 0 **
** 152023 S U 92.4 126.5 999.00 999.00 0.0 999.00 999.00 0.0 0 **
** 152023 S U 92.4 126.5 999.00 999.00 0.0 999.00 999.00 0.0 0 **
** 152054 S U 92.4 130.0 999.00 999.00 0.0 999.00 999.00 0.0 0 **
** 152054 S U 92.4 130.0 999.00 999.00 0.0 999.00 999.00 0.0 0 **
** 152109 S U 92.4 130.7 999.00 999.00 0.0 999.00 999.00 0.0 0 **
** 152109 S U 92.4 130.7 999.00 999.00 0.0 999.00 999.00 0.0 0 **
** 152125 S U 92.4 131.4 999.00 999.00 0.0 999.00 999.00 0.0 0 **
** 152125 S U 92.4 131.4 999.00 999.00 0.0 999.00 999.00 0.0 0 **
** F 152140 E H 92.4 132.1 999.00 999.00 0.0 999.00 999.00 0.0 0 **
** 152140 E H 92.4 132.1 173.10 4.94 0.42 999.00 999.00 0.0 * 1 **
** 152155 E H 92.4 132.8 999.00 999.00 0.0 999.00 999.00 0.0 0 **
** 152155 E H 92.4 132.8 172.62 3.82 0.39 999.00 999.00 0.0 * 1 **
** F 152211 E H 92.4 133.5 999.00 999.00 0.0 999.00 999.00 0.0 0 **
** 152211 E H 92.4 133.5 172.16 2.76 0.36 999.00 999.00 0.0 * 1 **
** F 152226 E H 92.4 134.2 999.00 999.00 0.0 999.00 999.00 0.0 0 **
** 152226 E H 92.4 134.2 171.64 1.54 0.32 999.00 999.00 0.0 * 1 **
** F 152242 E H 92.4 136.3 999.00 999.00 0.0 999.00 999.00 0.0 0 **
** 152242 E H 92.4 136.3 169.98 -2.37 0.22 999.00 999.00 0.0 * 1 **
** F 152257 E H 92.4 137.0 999.00 999.00 0.0 999.00 999.00 0.0 0 **
** 152257 E H 92.4 137.0 169.09 -4.47 0.16 999.00 999.00 0.0 * 1 **
** F 152312 E H 92.4 137.7 999.00 999.00 0.0 999.00 999.00 0.0 0 **
** 152312 E H 92.4 137.7 167.67 -7.81 0.09 999.00 999.00 0.0 * 1 **
** 152328 E H 92.4 138.4 166.35 -10.90 0.07 999.00 999.00 0.0 1 **
** 152328 E H 92.4 138.4 162.82 -18.85 0.03 999.00 999.00 0.0 * 1 **
** 152343 E H 92.4 139.1 165.89 -11.96 0.19 999.00 999.00 0.0 1 **
** 152343 E H 92.4 139.1 165.38 -13.12 0.04 167.94 -7.17 0.05 2 **
** 152358 E H 92.4 139.8 165.84 -12.06 0.32 999.00 999.00 0.0 1 **
** 152358 E H 92.4 139.8 165.80 -12.15 0.12 170.10 -2.09 0.13 2 **
**
** CPOINT=SGLCRS WHAT NOW NEXT CALL DISPLAY CISP 1 OF 1 **
**
***** M S A D *****
***** DISPLAY *****

```

```

SUBROUTINE CCINIT ENTERED. JFLOW= -1
SUBROUTINE PRECAL ENTERED. JFLOW= -1

```

Figure 2-1. Single Frame Solutions From Earth at Launch

launch.) An attitude was obtained based on the data in Figure 2-1 and was written to the status file as follows:

RAE-B BLOCK AVERAGE ATTITUDE SOLUTION SUMMARY

TIME OF SOLUTION	730610.	151237.		
ATTITUDE ANGLE	CALCULATED	UNCERTAINTY	DESIRED	
RIGHT ASCENSION	164.00	10.64	165.87	DEGREES
DECLINATION	-16.25	10.21	-14.17	DEGREES
SUN ANGLE	92.50	SPIN RATE	50.71	(RPMS)
HALF-ANGLE ERROR	3.40	DEGREES		
CALCULATED - DESIRED	ARC LENGTH DIFFERENCE	2.75	DEGREES	
ORBIT LEVEL 2 USED	(-1 INDICATES ORBIT GENERATOR)			
10 SOLUTIONS USED BY BLOCK AVERAGE	FROM	10		
WRITTEN TO GENERAL ATTITUDE FILE	LEVEL	3		

Because of the highly unfavorable Earth geometry, it was decided to use the Moon as the primary body for attitude determination. The apparent diameter of the Moon from the vicinity of the Earth is 0.52 degree compared to the PAS stepsize of 0.7 degree; this implies that Moon sightings would be rare because the scanner logic requires two sightings before a measurement is made. One sighting halts the encoder advance, and one provides the AOS and LOS register counts. In the presence of even slight spacecraft nutation, simulations indicated very few valid measurements would be obtained. No significant nutation was observed in the early data at 50 rpm, but there was concern that an unacceptable level of nutation might appear if the spacecraft were spun down to 12 rpm as had been originally planned. This concern, combined with early orbit data indicating that a minimum of attitude maneuvering would be required in the translunar flight, led to a decision to maintain the spin rate at 50 rpm. A series of scanner-advance commands was sent to the spacecraft to maximize the amount of lunar data. These efforts resulted in six sightings from

1604 to 1710 GMT, and a precise attitude of $\alpha = 165.9$ degrees and $\delta = -12.1$ degrees was obtained. The data are shown in Figures 2-2 through 2-4. (Tabulated parameters on all displays are defined in Appendix A.)

Several measurements were made to determine biases in the attitude sensors (see Section 3) prior to the critical midcourse and lunar insertion VCPS maneuvers. The PAS1 scanner was malfunctioning and was not used.

At 2130 GMT, a series of ACS maneuvers was initiated to calibrate and test the hardware for subsequent critical maneuvers. A very short precession (3.3 degrees) was performed at 2130 GMT using the smallest pulse width (80 milliseconds) to verify that the ACS was operating properly and that the spacecraft was precessing in the desired direction. A 10.6-degree precession maneuver was then initiated (2200 GMT) using the optimum ACS hardware combination (350-millisecond pulse width) for the 50 rpm spin rate. An ACS malfunction occurred during this maneuver when the ACS register shifted from its preset value. This problem is discussed in Section 3.4.1.1. These first two maneuvers were both aimed toward the attitude required for the first midcourse correction.

At 1200 GMT on June 11, the main precess maneuver (24.5 degrees) to the first midcourse attitude was initiated using the hardware combination for which the register shift occurred. At 1.5 minutes into the precession, the ACS register again shifted and the maneuver was immediately terminated. Attitude was quickly redetermined, and a maneuver to the desired attitude was executed using the 80-millisecond pulse width. No problem with the ACS register was encountered this time. However, preflight calibrations for this hardware combination were inaccurate, and the targeted attitude was not attained. After using the software capability for in-flight updating of ACS performance characteristics, a trim maneuver to the desired attitude was computed and executed at 1420 GMT.


```

***** H S A D *****
*** ***** DISPLAY ***** 73.240.17.14.58 ***
**
**      BLKOUT          BLOCK AVERAGE RESULTS
**-----
**      IBLK - BLCK AVERAGE INDICATOR          OS
**      (NO,0,OS,DIN,ODUT,S,IN,OUT)
**-----
**      BLKAVE PLANAR MODE IND.          MODE1
**      (MODE1,MODE2)
**-----
**      BLKAVE TERM. CHECK (YES,NO)          NO
**      A PRIORI RIGHT ASCENSION          164.500
**      A PRIORI DECLINATION              -15.000
**-----
**      IAPICR - A PRIORI ATTITUDE INDICATOR  4
**      (0-NONE,4-USE LAST,8-USE FIRST)
**-----
**      ITMAX - MAXIMUM ITERATIONS IN SPNV    5
**      SPNSIG - REJECTION TOL. (TIMES STDV)  3.00
**      SPNTOL - REJECTION TOL. (RADIAN)     0.100
**-----
**      BLKAVE ARRAY POINTERS
**      IBSTRT - START ELEMENT               1
**      IEND - ENDING ELEMENT               18
**-----
**      SSPAVG - AVERAGE SPIN RATE (RPM)     50.704
**      SOLAVG - AVERAGE SUN ANGLE          92.500
**-----
**
**      *** BLOCK AVERAGE RESULTS ***
**-----
**      ALPHAV - AVERAGE RIGHT ASCENSION     165.910
**      DELTAV - AVERAGE DECLINATION         -12.112
**-----
**      AVERAGE THETA (DEG)                 102.112
**      AVERAGE PHI (DEG)                   255.910
**-----
**      SDEV - STANDARD DEVIATION             0.2802
**      SIG3A - 3 SIGMA ERROR IN RT. ASC.    0.85567
**      SIG3D - 3 SIGMA ERROR IN DECLINATION  0.84065
**      NUSEFL - NO. OF GCCD SAMPLES USED    18
**      BLOCK REFERENCE DATE (YYMMDD)       730610.
**      TIME (HHMMSS.SSS)                   163726.405
**-----
**      BLOCK LIMITS
**      START DATE OF BLOCK (YYMMDD)         730610.
**      TIME (HHMMSS.SSS)                   160440.468
**      LAST DATE OF BLOCK (YYMMDD)         730610.
**      TIME (HHMMSS.SSS)                   171012.342
**-----
**
**      MCCN SOLUTIONS. SCANNER 2. MODE3 DOUBLECROSS
**      CPOINT=BLKRES WHAT NOW          CALL DISPLAY          DISP 1 OF 1
**-----
***** H S A D *****
***** ***** DISPLAY *****

```

Figure 2-4. Block Average Attitude Using Moon Data at Launch

2.3 TRANSLUNAR CRUISE

After the trim maneuver at 1420 GMT on June 11, an effort was made to confirm the attitude prior to the first velocity correction. A series of lunar events was recorded between 1430 and 1745 GMT as shown in Figure 2-5. Several of these events, denoted by a δ , are believed to be caused by reflections from the inertia boom. An attitude was obtained (see Figure 2-6) with a standard deviation of 0.7 degree and an error of less than 0.3 degree from the desired attitude of $\alpha = 200.4$ degrees and $\delta = -18$ degrees. Note that the attitudes computed from suspected boom reflections were eliminated in the editing procedure (Figure 2-7). The computed spacecraft spin axis was approximately 1 degree from the great circle defined by the intersection of the celestial sphere with the plane defined by the spacecraft, Sun, and Moon. An alternate description is shown in Figure 2-8. Note that for a conic intersection solution to exist the Sun-to-Moon nadir angle must satisfy the relation

$$|\beta - n| \leq \pi - \eta \leq \beta + n$$

where equality denotes tangent cones.

The ambiguity resulting from the two possible cone intersections is resolved by comparing the observed dihedral angle from the spin-axis-Sun plane to the spin-axis-Moon plane with the angles computed from each intersection vector. As the cones approach tangency, the ambiguous vectors coalesce as do the associated dihedral angles. Whenever the difference between the computed dihedral angles is of the same order as the observed resolution, the ambiguity is not resolvable, but in this case the two vectors are nearly equal so that no precision is lost. The geometry ($\beta = 125.4$ degrees and $\gamma = 20.4$ degrees) prior

PRRSLT		PRECAL RESULTS											
BASETIME (YYDD)		73162											
TIME OF FIRST OF NEW DATA (HHMMSS)		174340											
REJECTED 0(NONE)/1(EARTH)/2(MOON)		0											
AA,SS,CC,EE=ANGLY,CBODY,HORIZ,OVRFWS													
REKHN MANUAL OVERRIDE OF EE YES/NO.		NO											
SET COLUMN BB TO U TO SUPPRESS DATA													
SET COLUMN EE TO OVERRIDE OVERFLOWS													
TIME	A	B	C	PAS	BODY	CLCK	SPNRT	SUN-	KKKK	KKKK	E	A	ALPHA
HHMMSS	A	B	C	BETA	GAM	RADIUS	RATE (RPM)	CBODY	0123	4567	E	A	ALPHA
143024	0	M	T	125.5	19.0	0.55	200.	12.53	107.5	1000	0000	0	332.8 108.2
143024	0	M	T	125.4	19.0	0.55	200.	12.53	107.5	1000	0000	0	335.4 107.9
143040	0	M	T	125.4	15.5	0.55	200.	12.53	107.5	1000	0000	0	8.9 110.1
143040	0	M	T	125.4	15.5	0.55	200.	12.53	107.5	1000	0000	0	8.9 110.1
143243	0	M	T	125.4	19.0	0.55	200.	12.53	107.5	1000	0000	0	332.5 108.3
143243	0	M	T	125.4	19.0	0.55	200.	12.53	107.5	1000	0000	0	335.5 107.9
143851	0	M	T	125.4	19.0	0.55	200.	12.53	107.4	1000	0000	0	332.8 108.2
143851	0	M	T	125.4	19.0	0.55	200.	12.53	107.4	1000	0000	0	335.4 107.9
143907	0	M	T	125.4	15.5	0.55	200.	12.53	107.4	1000	0000	0	4.7 110.0
143907	0	M	T	125.4	15.5	0.55	200.	12.53	107.4	1000	0000	0	4.7 110.0
144110	0	M	T	125.4	19.0	0.55	200.	12.53	107.4	1000	0000	0	332.0 108.3
144110	0	M	T	125.4	19.0	0.55	200.	12.53	107.4	1000	0000	0	335.0 108.0
154017	0	M	T	125.4	19.7	0.56	200.	12.92	107.0	1000	0000	0	332.4 107.6
154017	0	M	T	125.4	19.7	0.56	200.	12.92	107.0	1000	0000	0	335.5 107.2
154236	0	M	T	125.4	19.0	0.56	200.	12.98	107.0	1000	0000	0	333.7 108.1
154236	0	M	T	125.4	19.0	0.56	200.	12.98	107.0	1000	0000	0	334.9 108.0
154251	0	M	T	125.4	19.7	0.56	200.	12.98	107.0	1000	0000	0	332.9 107.6
154251	0	M	T	125.4	19.7	0.56	200.	12.98	107.0	1000	0000	0	334.9 107.3
174224	0	M	T	125.4	20.4	0.57	200.	12.98	106.3	1000	0000	0	333.4 106.8
174224	0	M	T	125.4	20.4	0.57	200.	12.98	106.3	1000	0000	0	336.2 106.5
174442	0	M	T	124.4	19.7	0.57	200.	12.98	106.3	1000	0000	0	334.1 106.4
174442	0	M	T	124.4	19.7	0.57	200.	12.98	106.3	1000	0000	0	335.3 106.3
174457	0	M	H	124.4	20.4	0.57	200.	12.98	106.3	1000	0000	0	333.3 105.9
174457	0	M	H	124.4	20.4	0.57	200.	12.98	106.3	1000	0000	0	334.9 105.7

Figure 2-5. Sensor Data From Moon During Translunar Cruise

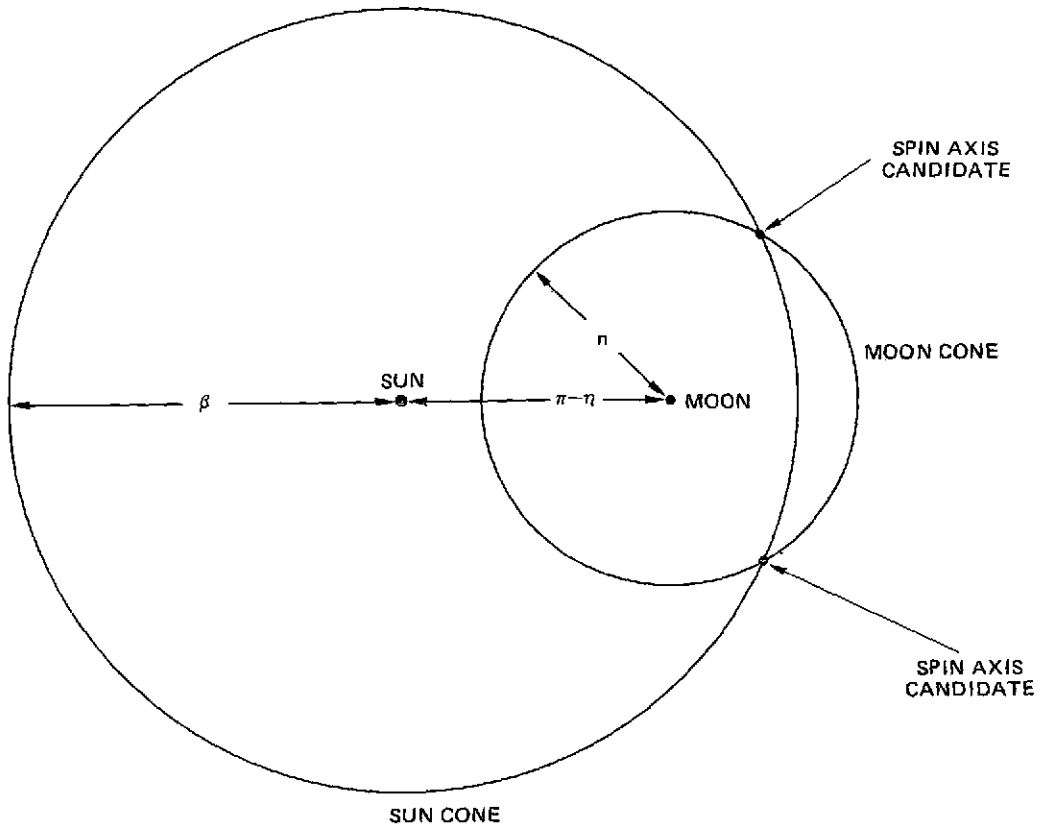

```

*****
*** RAE-B TRANSLUN ***** N S A D ***** 73.247.17.03.34 ***
*** D I S P L A Y *****

**
**          BLKINT          BLOCK AVERAGE INPUT ARRAYS          **
**
**  IBLK - BLOCK AVERAGE INDICATOR          DS          **
**  (NO,D,DS,DIN,DOUT,S,IN,OUT)          **
**  IDBL - DBLCK5 IND. (NO,MOD1,MOD2,MOD3)  MOD3          **
**  ISGL - SGLCK5 IND. (NO,YES)          YES          **
**  REFERENCE DATE (YYDD)          73152          **
**  A PRIORI RIGHT ASCENSION          200.000          **
**  A PRIORI DECLINATION          -18.000          **
**
**  IAPIOR - A PRIORI ATTITUDE INDICATOR    8          **
**  (0-NONE,4-USE LAST,8-USE FIRST)          **
**  BLKAVE ARRAY POINTERS          **
**  IBSTR - START ELEMENT          1          **
**  IEND - ENDING ELEMENT          33          **
**  INPUT ARRAY POINTERS IBOUT1          1          **
**  IBOUT2          24          **
**  GEN. BLKAVE DISPLAY ARRAYS (YES,NO)    YES          **
**  FRAM #R NO. SOL. ONE SOL. TWO CHOIC SPNDEV          **
**  NO: ID SOL ALPHA1 DELTA1 WTB1 ALPHA2 DELTA2 WTB2          **
**  1 J 1 201.53 -16.63 0.13 999.00 999.00 0.0 1 1.70          **
**  1 I 1 201.16 -17.92 0.18 999.00 999.00 0.0 1 0.55          **
**  2 J 2 201.07 -18.03 0.52 201.26 -17.40 0.88 1 0.44          **
**  3 J 1 202.78 -11.51 2.79 999.00 999.00 0.0 0 *****          **
**  4 J 1 202.87 -11.54 2.72 999.00 999.00 0.0 0 *****          **
**  5 J 1 201.90 -16.63 0.13 999.00 999.00 0.0 1 1.68          **
**  5 I 1 201.09 -17.96 0.18 999.00 999.00 0.0 1 0.47          **
**  6 J 2 201.08 -17.99 0.59 201.27 -17.37 0.84 1 0.46          **
**  7 J 1 201.53 -16.54 0.12 999.00 999.00 0.0 1 1.77          **
**  7 I 1 201.11 -17.99 0.18 999.00 999.00 0.0 1 0.51          **
**  8 J 2 201.09 -17.97 0.38 201.24 -17.47 0.51 1 0.47          **
**  9 J 1 202.77 -11.50 2.79 999.00 999.00 0.0 0 *****          **
**  10 J 1 202.86 -11.53 2.72 999.00 999.00 0.0 0 *****          **
**  11 J 1 201.55 -16.48 0.12 999.00 999.00 0.0 1 1.84          **
**  11 I 1 201.13 -17.84 0.17 999.00 999.00 0.0 1 0.55          **
**  12 J 2 201.10 -17.94 0.09 201.17 -17.69 0.11 1 0.48          **
**  13 J 1 201.24 -17.49 0.16 999.00 999.00 0.0 1 0.84          **
**  13 I 1 200.87 -18.70 0.21 999.00 999.00 0.0 1 0.66          **
**  14 J 2 200.97 -18.37 1.55 201.24 -17.49 1.98 1 0.45          **
**  15 I 1 201.41 -16.94 0.13 999.00 999.00 0.0 1 1.37          **
**  17 J 1 201.25 -17.43 0.16 999.00 999.00 0.0 1 0.89          **
**  17 I 2 200.86 -18.73 0.08 200.93 -18.51 0.10 2 0.52          **
**  18 J 2 200.93 -18.51 1.15 201.17 -17.71 1.61 1 0.52          **
**  19 J 1 201.21 -17.37 0.16 999.00 999.00 0.0 1 0.77          **
**  19 I 2 200.82 -18.89 0.08 200.88 -18.67 0.09 2 0.64          **
**  20 J 2 200.94 -18.48 1.55 201.19 -17.62 1.97 1 0.51          **
**  21 J 1 200.06 -17.77 0.20 999.00 999.00 0.0 1 0.62          **
**  21 I 2 199.82 -18.55 1.58 200.09 -17.65 2.09 2 0.66          **
**  22 J 2 199.91 -18.25 2.07 200.19 -17.33 2.10 1 0.70          **
**  M204 NUMBER(S) TO BIG FOR FORMAT (*)          **
**  CPOINT=BLKRES WHAT NOW NEXT CALL DISPLAY DISP I OF I          **
**
*****
*** D I S P L A Y *****
*****

```

Figure 2-7. Block Average Editing (1 of 2)



WHERE $\pi - \eta$ = SUN-MOON NADIR ANGLE $\approx 108^\circ$
 β = SPIN-SUN NADIR ANGLE $\approx 125^\circ$
 n = SPIN-MOON NADIR ANGLE $\approx 20^\circ$

Figure 2-8. Cone Intersection Geometry Prior to Midcourse Correction

to the midcourse correction (1731 GMT on June 11) was such that the two possible spin vectors were as follows:

<u>Cone Intersection</u>	<u>α</u> <u>(Degrees)</u>	<u>δ</u> <u>(Degrees)</u>	<u>ϕ</u> <u>(Degrees)</u>
1	205.7	-5.6	22.3
2	201.2	-17.6	337.7

Because the measured dihedral or phase angle was 333.5 degrees, the second solution is valid. Note that the 4.2-degree phase error is partly due to sensor resolution, but primarily is an indication of an attitude error. Because of the small lunar nadir angle, errors of ± 1 degree in either γ or β result in a magnified effect on ϕ : $\frac{\partial \phi}{\partial \gamma} \approx -12$ and $\frac{\partial \phi}{\partial \beta} \approx +8$. Assuming $\Delta \gamma = 0.45$ degree and $\Delta \beta = 0.5$ degree, we have $\Delta \phi = 7$ degrees, and solutions 1 and 2 have a dihedral angle of 7σ and 0.5σ , respectively, from the observed value.

An evaluation of the VCPS maneuver was made by the Flight Dynamics Manager. After some initial uncertainty, due in part to sparse range and range rate data, he determined that the maneuver was nominal and that a second midcourse correction would not be necessary. The midcourse attitude determined by the MAPS/RAE-B system was estimated to be within ± 0.2 degree of the true attitude based on a comparison of expected and observed orbit data.

The midcourse velocity correction was made at 1800 GMT, and it was confirmed that the attitude was not perturbed. At 1840 GMT, the spacecraft was reoriented to satisfy thermal and power constraints. A precession maneuver was executed which reduced the Sun angle from 125 degrees to 105 degrees at the maximum rate. No specific attitude was required.

A degradation in the performance of the PAS2 scanner was observed from about 0523 GMT until 1422 GMT on June 13 when a decision was made to use the PAS1 scanner for attitude determination prior to lunar insertion (see Section 3). Figures 2-9 and 2-10 illustrate the PAS1 performance and central

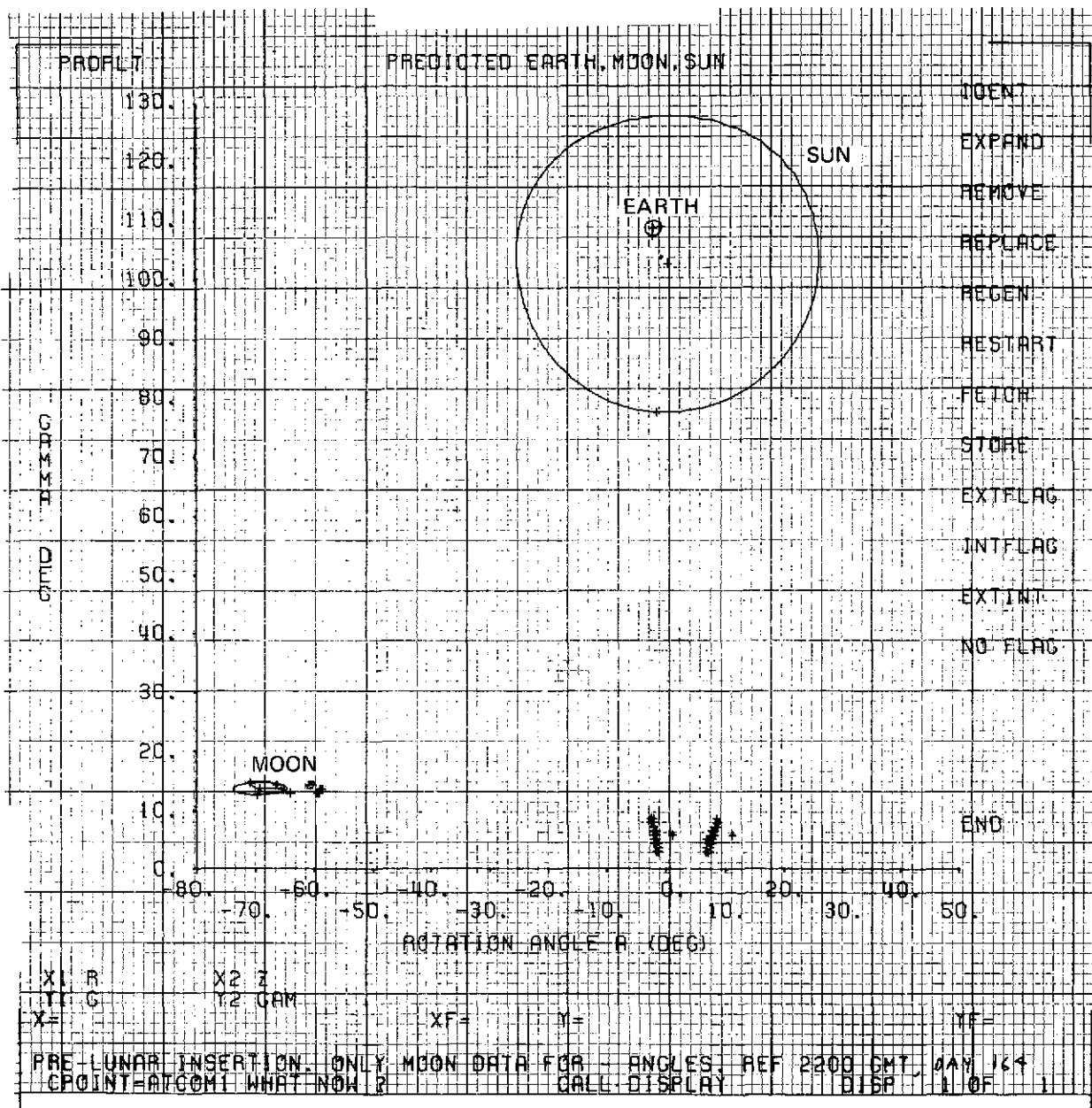


Figure 2-9. PAS1 Performance at 2200 on June 13

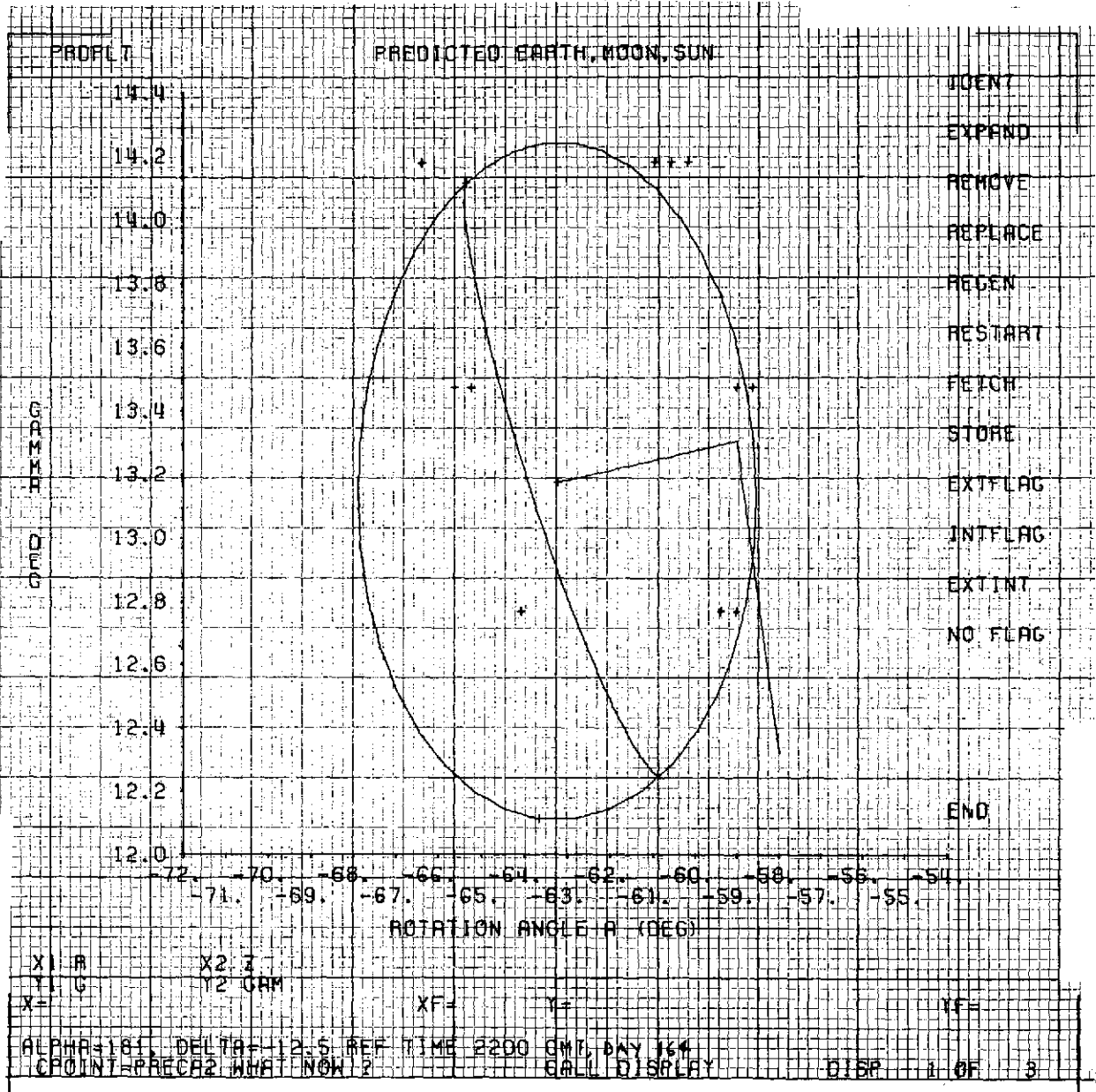


Figure 2-10. Moon Geometry at 2200 on June 13

body geometry, respectively, at 2200 GMT on June 13. (See Section 4.2.6 for a detailed description of the predicted Earth, Moon, Sun plot.) The attitude was $\alpha = 181$ degrees and $\delta = -12.5$ degrees.

2.4 LUNAR INSERTION

Because of the problems associated with the PAS scanners, a decision was made to precess to and confirm the lunar insertion attitude as early as possible. Several attitudes and sensor configurations were studied to satisfy mission requirements; an attitude of $\alpha = 216.7$ degrees and $\delta = 26$ degrees and a sensor configuration PAS1-SAS was selected. This choice would permit attitude determination throughout the remaining translunar cruise. Figures 2-11 through 2-13 illustrate the geometry at the time of the precess to the lunar insertion attitude. A correction of approximately $\delta = -0.6$ degree is required to align the predicted Moon with the observed data in Figure 2-14.

A 53-degree precession maneuver, using a previously calibrated hardware combination (80-millisecond pulse width), was executed at 1915 GMT on June 14. The resulting attitude was within 2.5 degrees of the desired lunar insertion attitude. (The attitude determination procedure prior to lunar insertion is described in detail in Section 3.) The changing geometry on approach to the Moon is shown in Figures 2-15 through 2-18. After the initial precess, the attitude was at $\alpha = 215.0$ degrees and $\delta = 24.5$ degrees with a standard deviation of 0.3 degree. A very short ACS trim maneuver was performed at 2345 GMT on June 14, and an attitude of $\alpha = 216.4$ degrees and $\delta = 25.9$ degrees with a standard deviation of 0.4 degree was obtained. This was the required lunar insertion attitude within the stated uncertainty. For the 6 hours immediately preceding lunar insertion, periodic measurements were made to confirm the spacecraft attitude. The fourth-stage firing for lunar insertion was initiated and confirmed at 0721 GMT on June 15. No attitude change was observed. The spin rate increased from 51.12 rpm to 51.76 rpm, while Sun angle data indicated an induced nutation of about 0.5-degree half-cone angle.

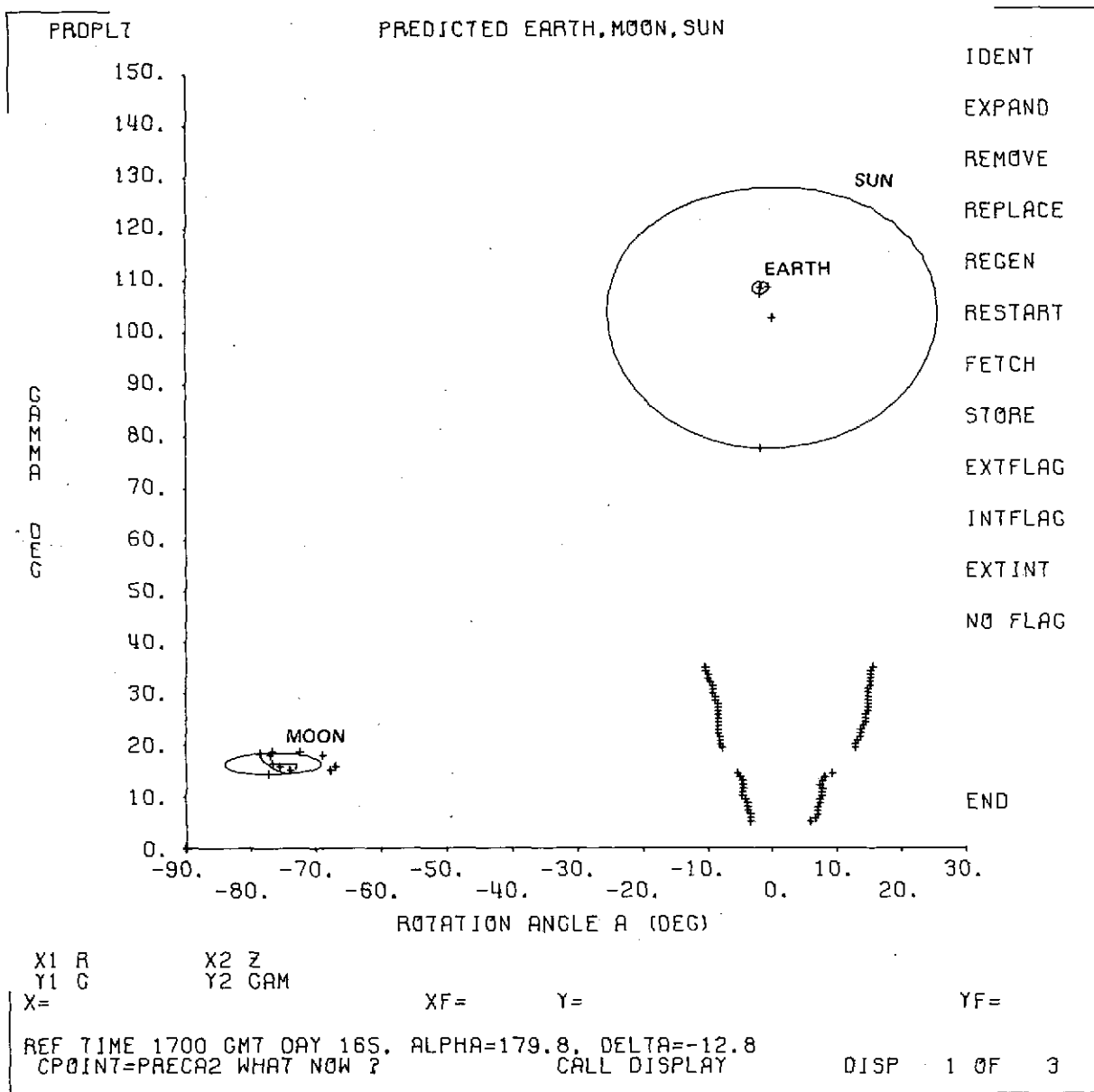


Figure 2-11. Moon Geometry Prior to Lunar Insertion Process, 1700 GMT June 14

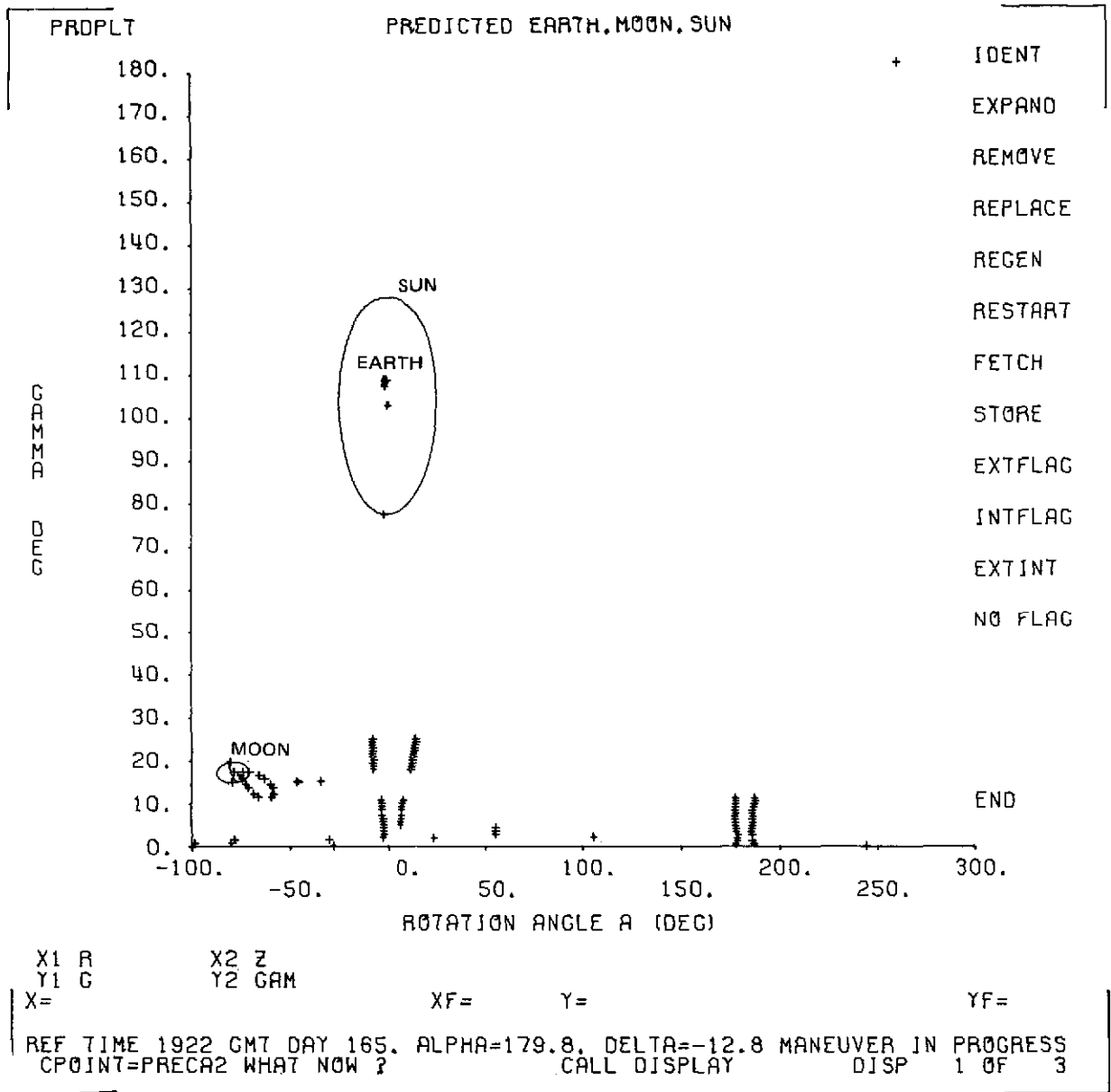


Figure 2-12. Attitude Data Obtained During Precession Maneuver

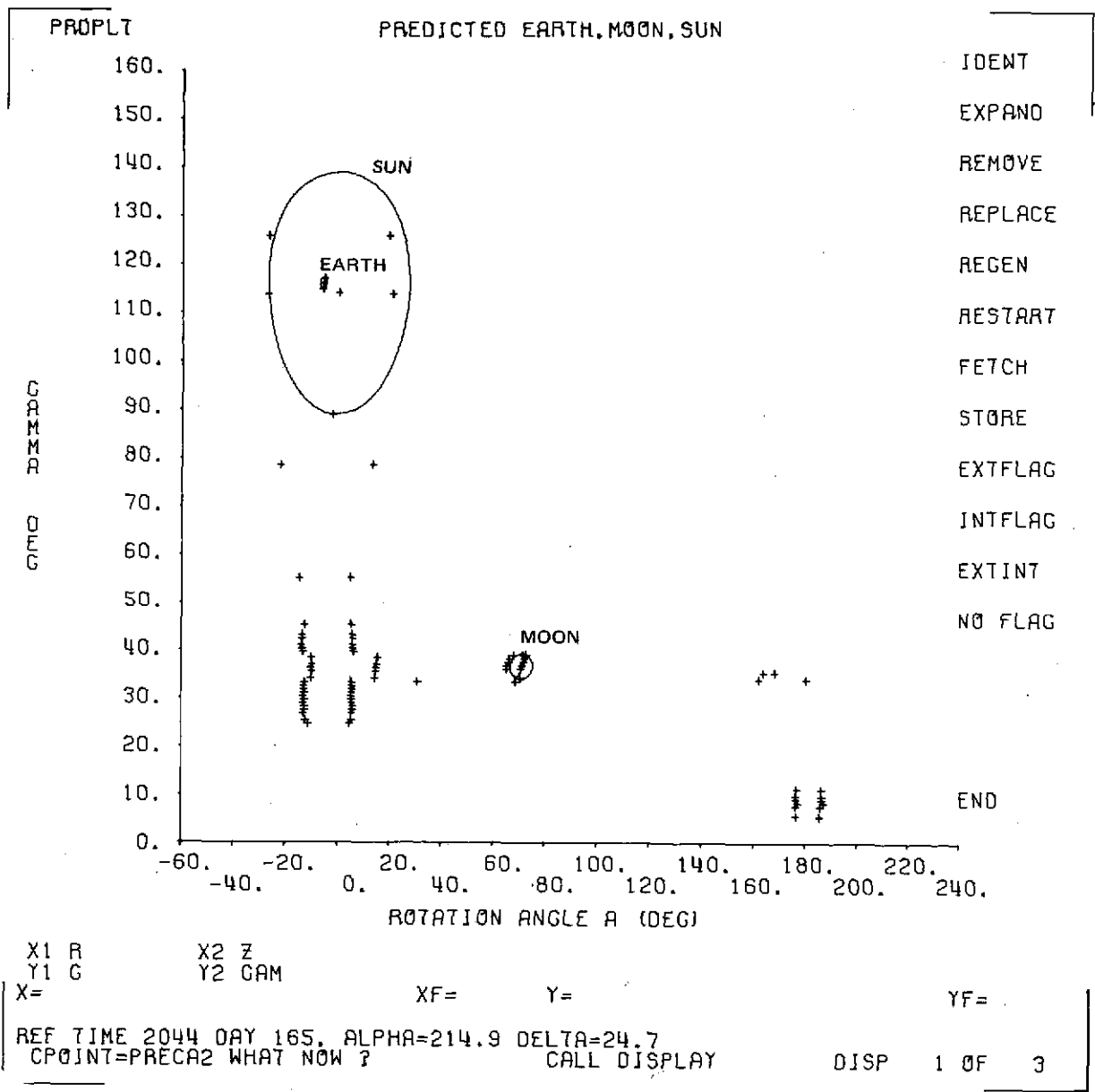


Figure 2-13. Moon Geometry After Precess Maneuver,
2044 GMT June 14

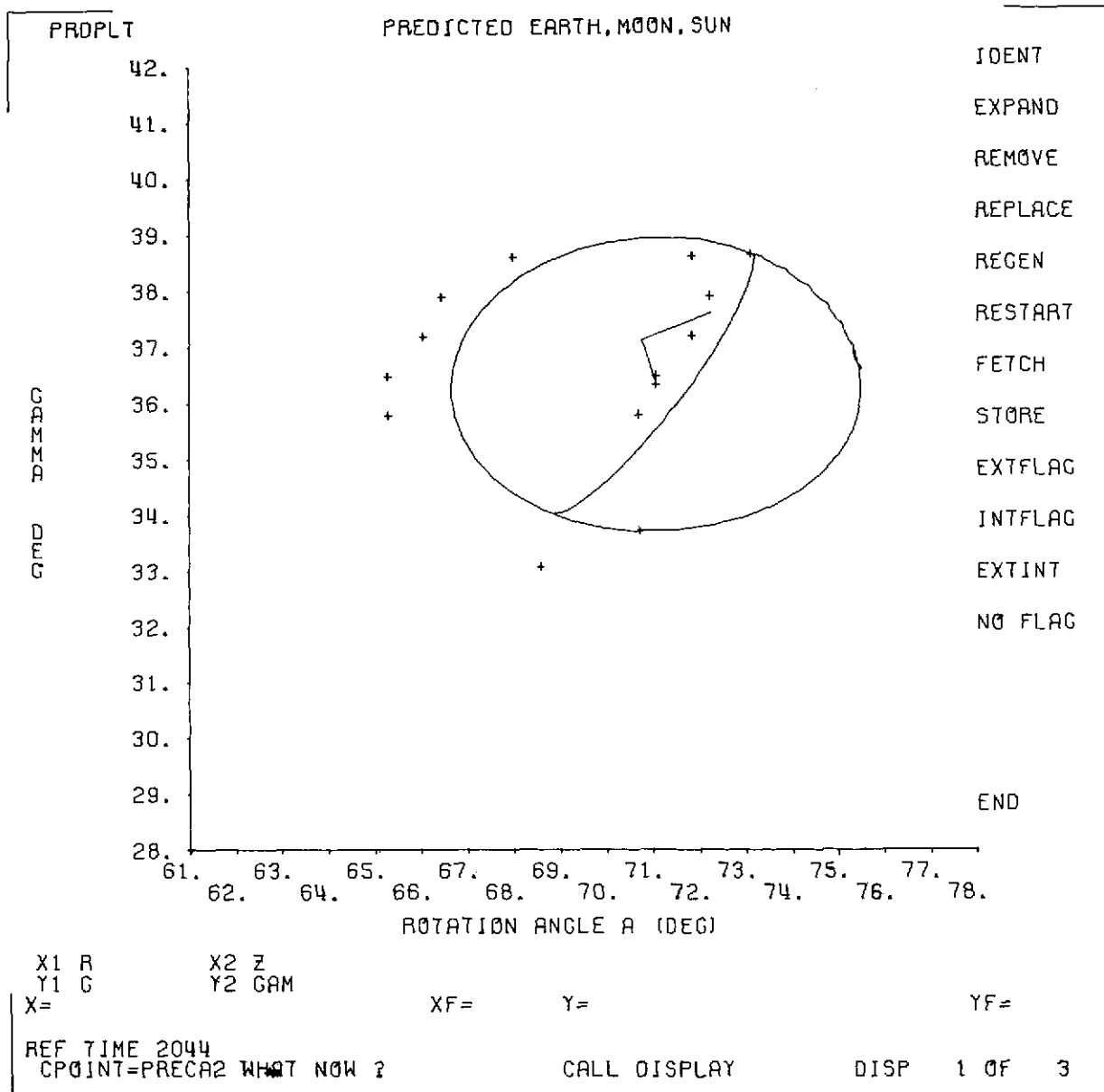


Figure 2-14. Altitude Determination, 2044 GMT June 14

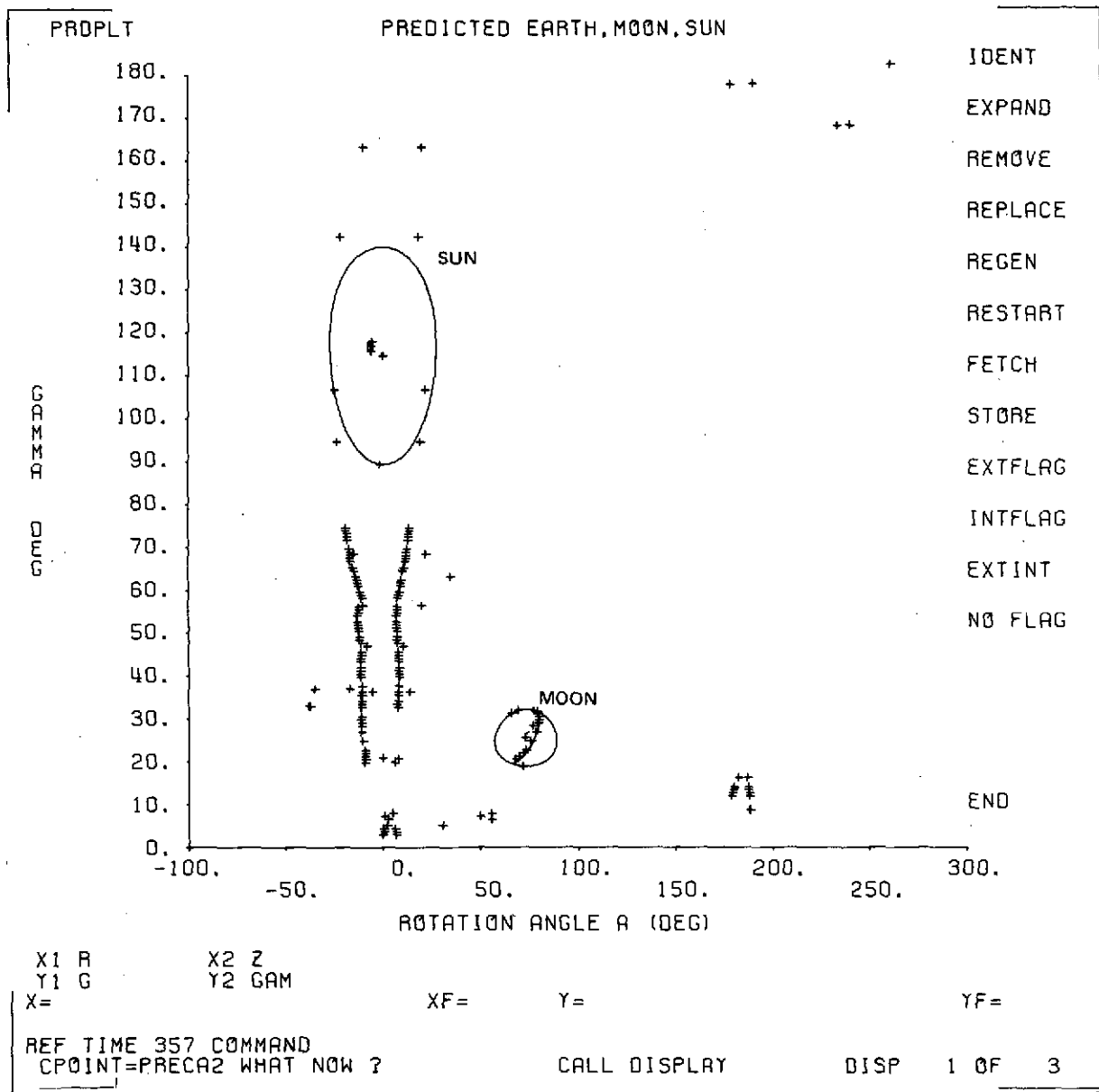


Figure 2-15. Moon Geometry at 0357 GMT June 15

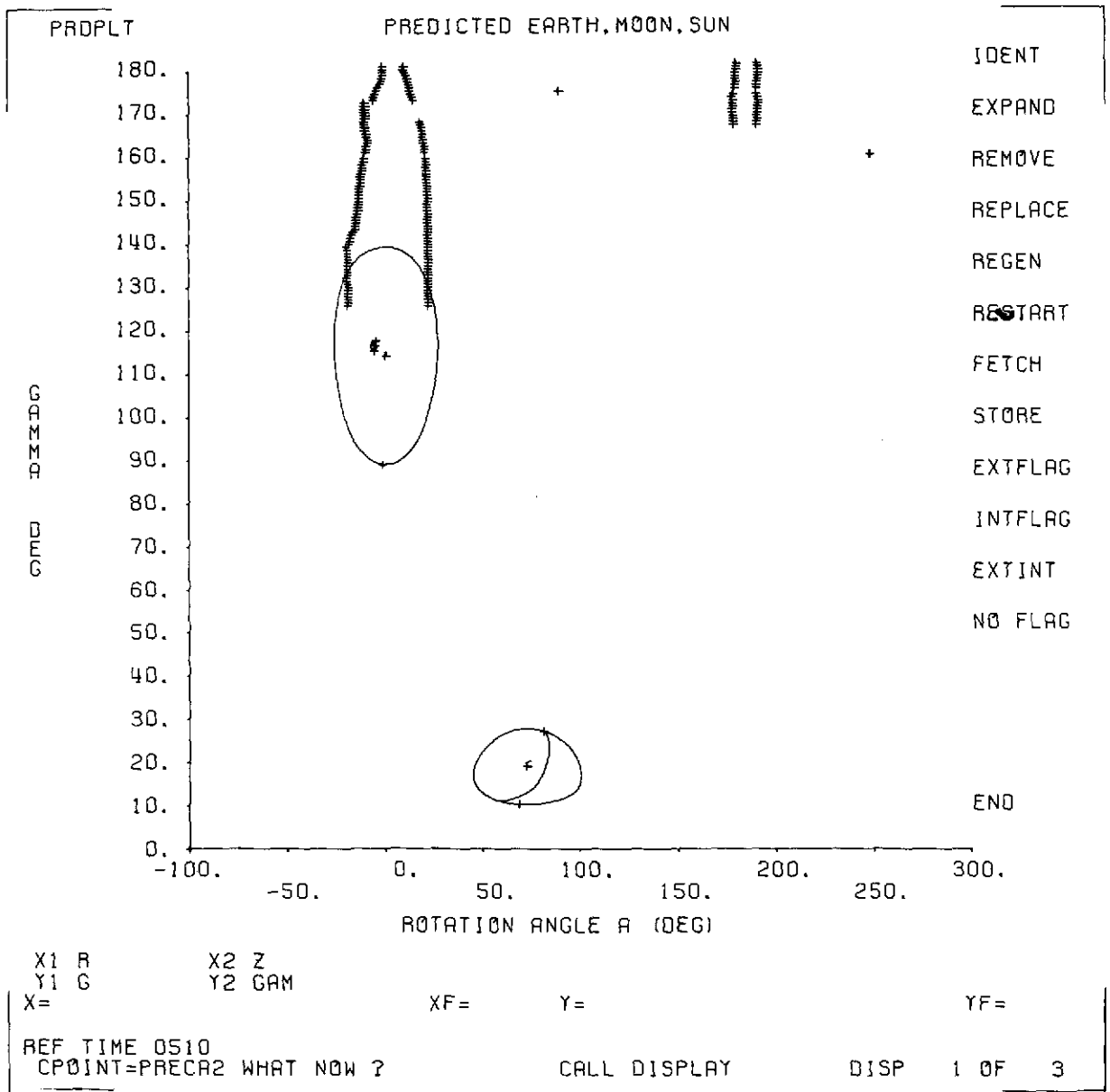


Figure 2-16. Moon Geometry at 0510 GMT June 15

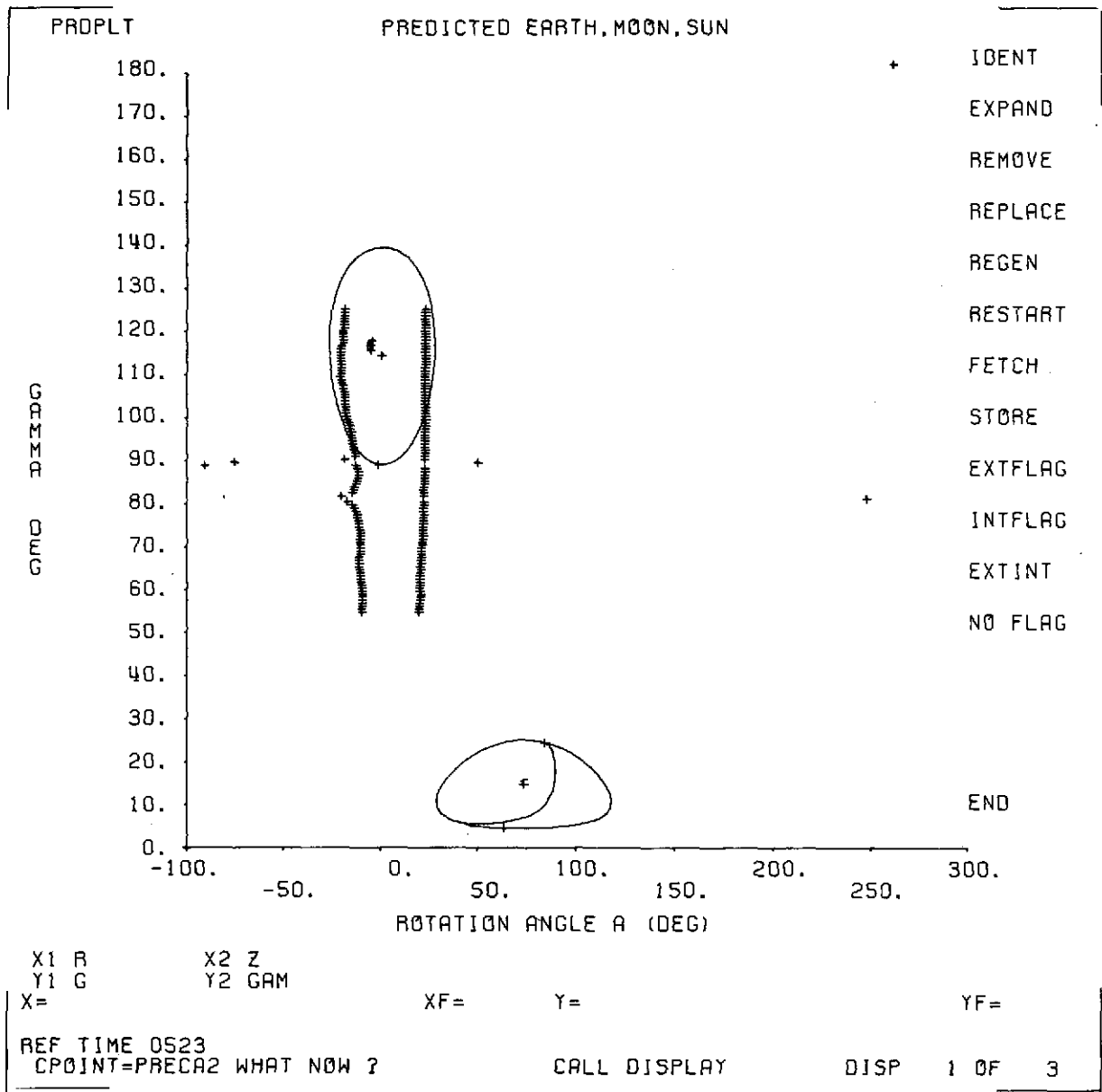


Figure 2-17. Moon Geometry at 0523 GMT June 15

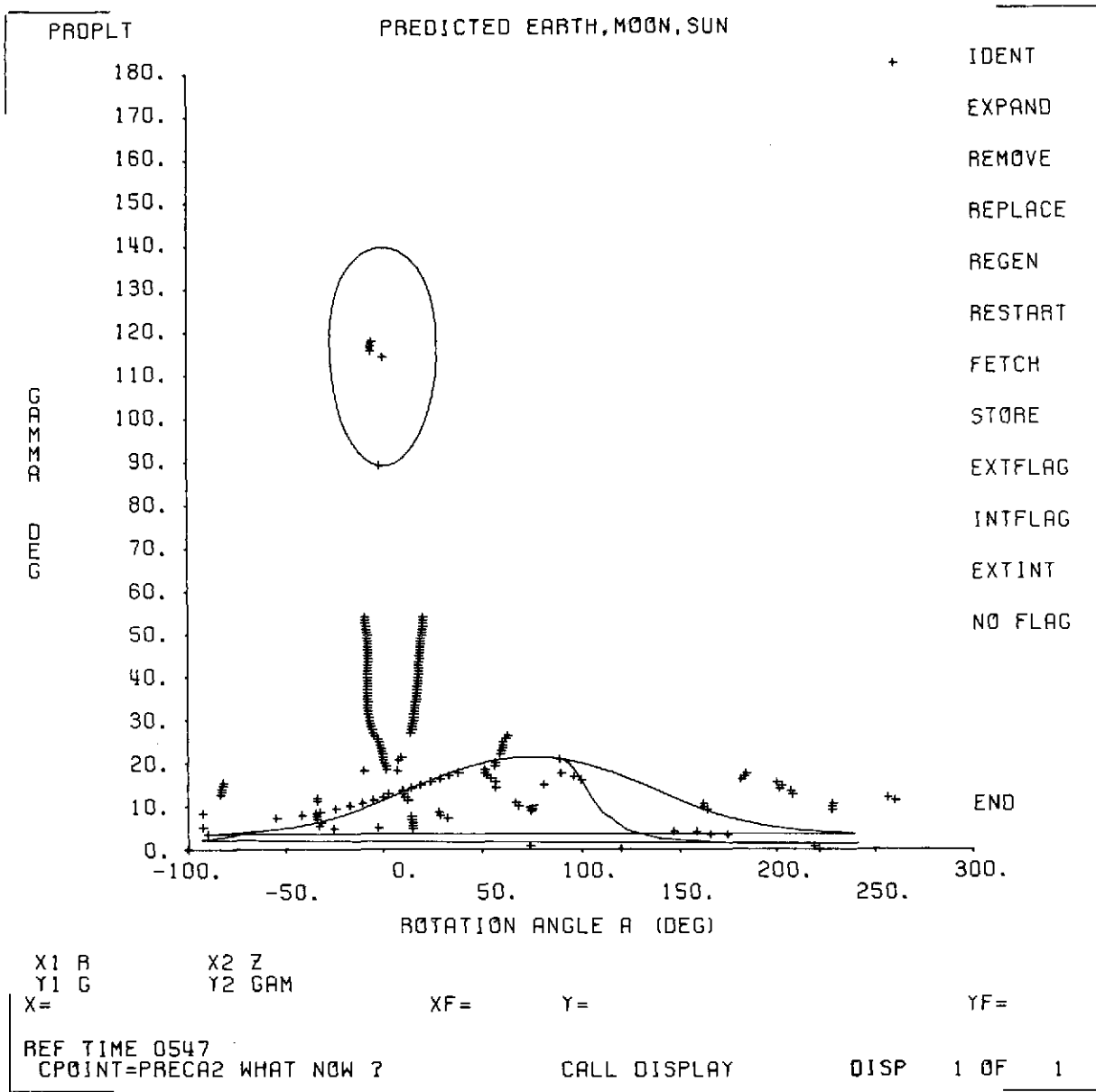


Figure 2-18. Moon Geometry at 0547 GMT June 15

2.5 ORBIT CORRECTION

After lunar insertion, the spacecraft spin rate was to be reduced from the nominal 50 rpm required for fourth-stage firing to approximately 13 rpm to conserve ACS propellant. The fourth stage was ejected at 1630 GMT on June 18, just prior to the spin down. A continuous spin-down maneuver was executed at 1700 GMT, providing the first test of the spin control hardware. The targeted spin rate of 15 rpm was considerably overshoot, resulting in a final spin rate of 10.5 rpm. This miscalculation was caused by preflight calibrations which underrated the thruster strengths of the spin nozzles by approximately 10 percent. Twenty-two spin-up pulses were then commanded, increasing the spin rate to 12.2 rpm.

The attitude chosen for performing the first VCPS orbit circularization maneuver was $\alpha = 231.0$ degrees and $\delta = 32.7$ degrees. A 13.3-degree precession maneuver was initiated at 1817 GMT, using the hardware combination (80-millisecond pulse width) proven and calibrated at 50 rpm. The resulting attitude was determined to be $\alpha = 230.9$ degrees and $\delta = 32.4$ degrees with a standard deviation of 0.45 degree. This was within the stated error of the required attitude; no trim maneuver was necessary. The VCPS burn was performed at 0000 GMT on June 19. The Sun angle of 114 degrees was adequate for thermal and power constraints so that a Sun-bathe maneuver was not required.

The second orbit circularization correction required an attitude of $\alpha = 50.7$ degrees and $\delta = -32.7$ degrees, which was 180 degrees from the current attitude. The 950-millisecond ACS pulse width was used for the first time, so that the maneuver could be performed within a reasonable time. The precession maneuver was initiated at 1306 GMT on June 19, with a planned duration of 27 minutes. Based on real-time graphic plots of predicted versus observed Sun angles and spin rates, it was decided to extend the maneuvering time to 29.25 minutes. The resulting final attitude was within 2 degrees of the targeted position. A trim maneuver was executed at 1727 GMT. Attitude measurements confirmed achievement of the required attitude: $\alpha = 50.3$ degrees and

$\delta = -32.7$ degrees with a standard deviation of 0.1 degree. The VCPS burn for the second orbit circularization was performed at 0000 GMT on June 20.

2.6 DIPOLE CALIBRATION

Dipole calibration required an attitude in the ecliptic plane with an acceptable Sun angle range during the calibration period of 2 to 3 weeks. A 53-degree precession maneuver to the selected attitude of $\alpha = 9$ degrees and $\delta = 3.5$ degrees was initiated at 1400 GMT on June 20. The resulting attitude was near enough to the ecliptic plane that no trim was performed. To ensure that the spacecraft spin rate would not fall below 3 rpm as a result of dipole deployment, it was decided to increase the spin rate from 12.6 rpm to 15 rpm using a series of pulsed spin commands. The pulses were commanded at 15-second intervals beginning at 1419 GMT. On the 27th command, the spin nozzle apparently stuck on until the initiation of the 28th command 15 seconds later. The final two pulses apparently executed properly, but the spin rate had increased to 17.5 rpm because of the hardware malfunction. The dipoles were deployed from this spin rate (17.5 rpm) at 1800 GMT on June 20. The configurational change occurring during deployment caused the spin rate to drop to 4.7 rpm. Originally this period of dipole deployment was to be used only for calibration of the dipole antenna. However, a decision was made by the experimenter to use this period to perform experiments with the dipole antenna. This required the use of the solid-angle Sun sensors to obtain rotation-angle information. At this spin rate (considerably above the design spin rate) the sensors did not function properly. The details of the SAS malfunction are discussed in Section 3. In an attempt to gain more information about the SAS malfunction, the spin rate was reduced from 4.7 rpm to 3.1 rpm by a 25-second continuous despin performed at 0400 GMT on June 29 followed immediately by 20 spin-down pulses. No new information was obtained by this maneuver, and no definitive answer exists as to why the sensors were malfunctioning in the way noted.

The dipoles were retracted at 1030 GMT on July 9, increasing the spacecraft spin rate from 3.1 rpm to 11.4 rpm. A series of eight spin-up pulses was then commanded beginning at 1055 GMT to increase the spin rate to 12 rpm. This allowed a higher frequency clock rate to be used, improving the accuracy of various parameters in the telemetry.

An attitude of $\alpha = 269$ degrees and $\delta = 38$ degrees was required for the third orbit circularization correction. A 96-degree precession maneuver was initiated at 1135 GMT on July 9 and came close enough to the desired attitude to omit a trim maneuver. The VCPS burn for the final orbit circularization was performed at 1800 GMT on July 9.

2.7 BOOM DEPLOYMENT

The VCPS was jettisoned on July 9. After ensuring that the attitude of the spacecraft had not changed due to VCPS ejection, data availability for the boom deployment sequences was examined to determine the best attitude for boom deployment. It was found that an attitude could be chosen so that predicted data availability was good prior to either the D1 sequence or the D2 sequence, but not both. The decision was made to have good data availability prior to D1 at the expense of data availability prior to D2 under the assumption that the D2 start could be adequately predicted using dynamic simulators. Figures 2-19 and 2-20 indicate the predicted data availability for two situations. A decision was made to use an attitude with $\alpha = 217.7$ degrees and $\delta = 29.6$ degrees for boom deployment and precess commands were generated to attain this attitude. The maneuver was initiated at 1746 GMT on July 10 and subsequent spin-mode attitude determination indicated that the attitude reached was $\alpha = 219.2$ degrees and $\delta = 30.5$ degrees. This attitude was close to nominal and no trim maneuver was necessary. At 1240 GMT on July 11, commands were sent to perform a continuous spin down from 12 rpm to 3.8 rpm to start final spin-down operations to attain the nominal 0.25 rpm for boom deployment. Thirty-nine pulsed

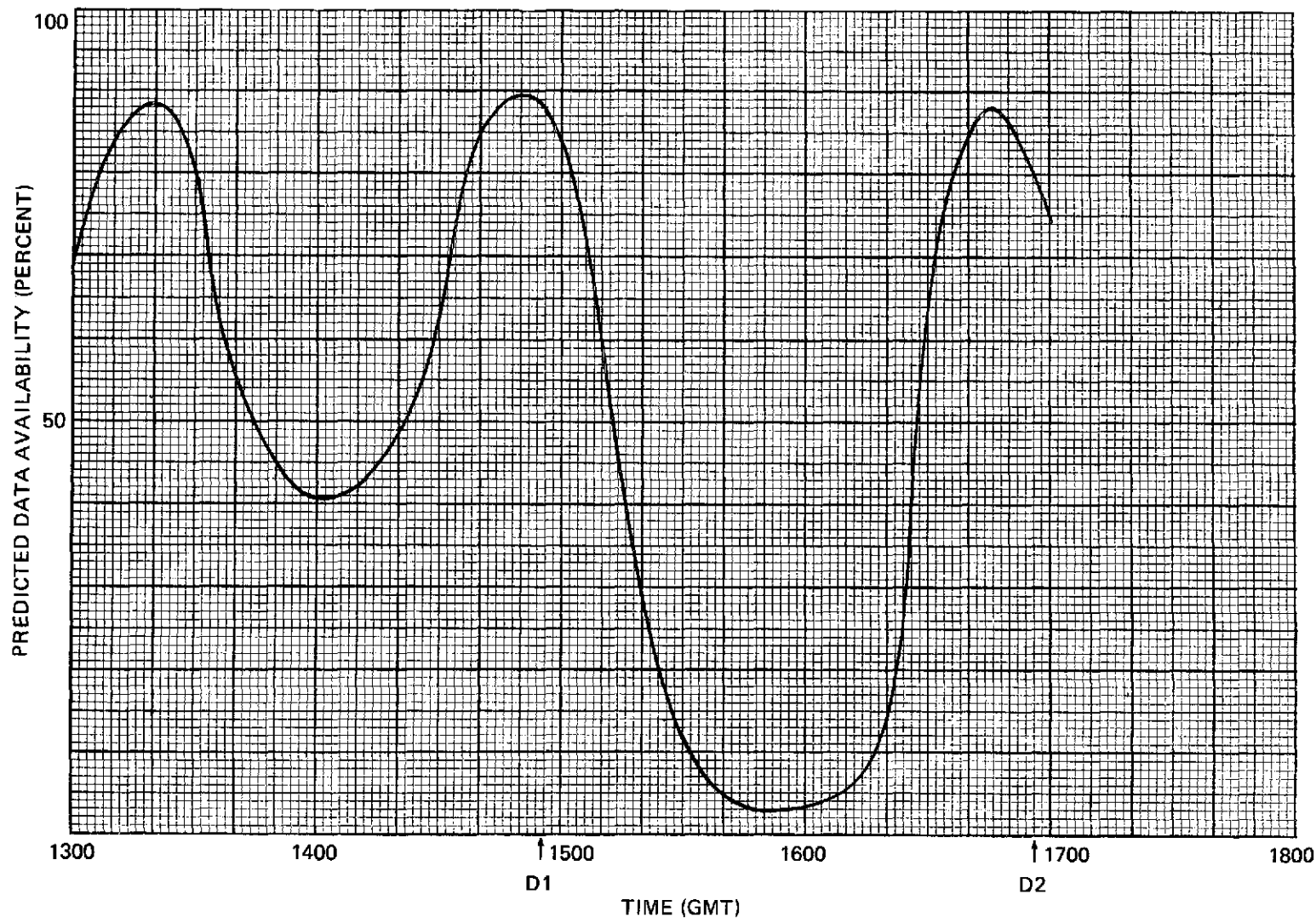


Figure 2-19. Data Availability Profile--Attitude Chosen To Provide Fair Coverage for D1 and D2

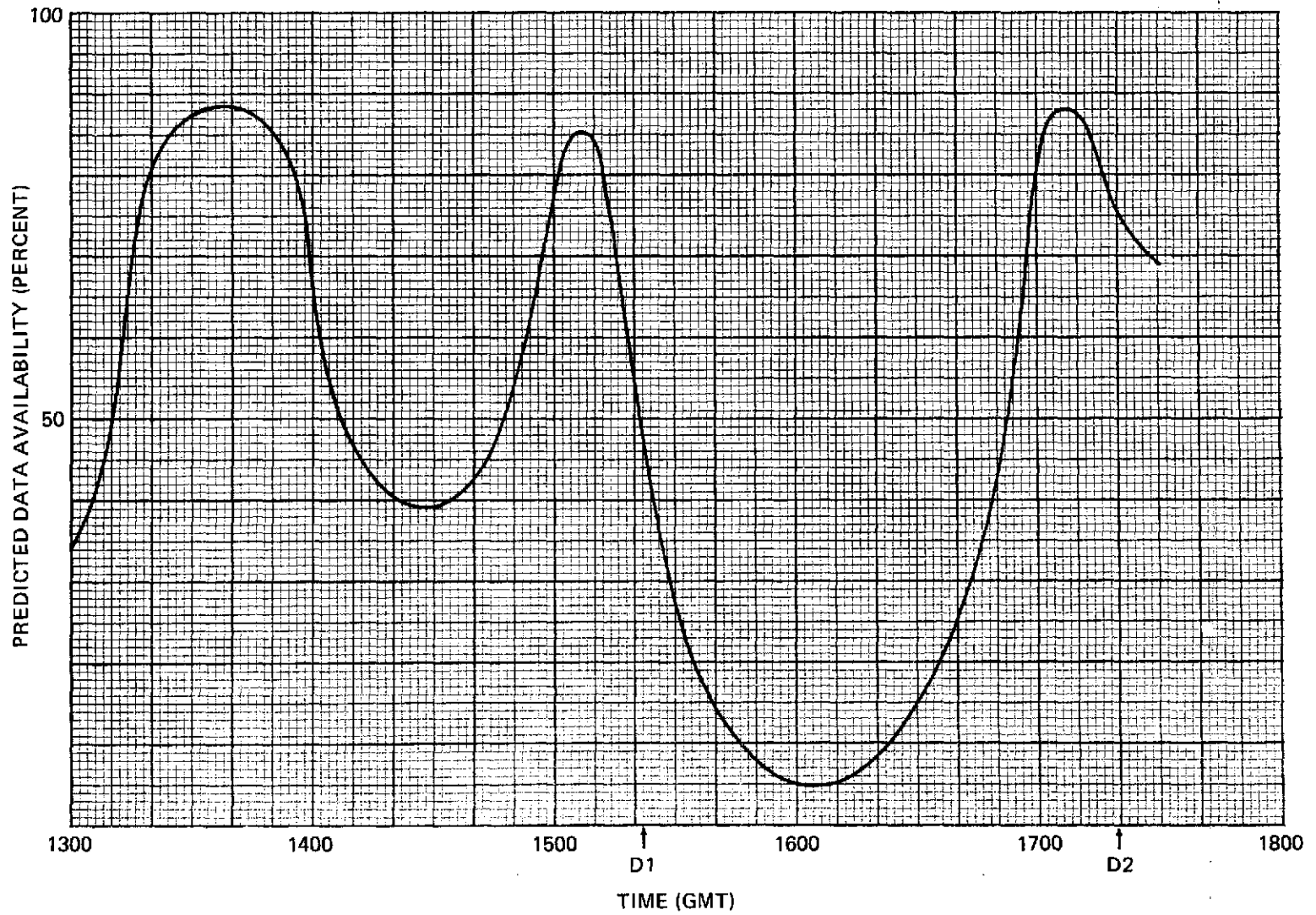


Figure 2-20. Data Availability Profile--Attitude Chosen To Provide Maximum Coverage for D1

spin-down commands were necessary to attain a 0.25-rpm spin rate, and at 1320 GMT the pulse commands were initiated. At the 37th pulse the ACS spin nozzle stuck open and the spacecraft went through 0.0 rpm to -6.5 rpm. At 1415 GMT, a continuous spin-up was initiated to correct the spin direction, and a positive spin rate of 1.11 rpm was attained. Pulsed spin-down commands commenced again at 1430 GMT; eight of nine planned pulses were executed, and the spacecraft reached a final spin rate of 0.39 rpm. The Attitude Computations Analyst decided to stop after eight pulses had been sent because 0.39 rpm was close enough to the nominal spin rate of 0.25 rpm to allow boom deployment operations to continue, and because each command extended the risk of another malfunction.

The solid mode SAS sensors apparently began functioning nominally when the spin rate dropped below approximately 1 rpm, and the problems that plagued the dipole calibration and experimentation period disappeared. Nothing was observed to cause a delay in the scheduled boom deployment sequence as a result of the spin-rate change through 0 rpm; however, subsequent real-time attitude determination showed what appeared to be rather large oscillations in pitch, roll, and yaw indicating that the spacecraft was probably nutating about the deployment attitude with a 5- to 10-degree amplitude. Planned deployment was scheduled for approximately 1800 GMT on July 11. Due to ground-based hardware and software malfunctions, this plan was not carried out. The primary support computer (M&DO's IBM S/360-95) failed approximately 45 minutes before the scheduled time for deployment, and the deployment was rescheduled for the following day.

Attitude operations began again on July 12 and, notwithstanding another failure of the primary support computer, the D1 boom deployment sequence was initiated at 1453 GMT after monitoring pitch, roll, and yaw in real time from the backup computer. Sufficient data was observed to verify that the yaw rate had dropped from 0.39 rpm to near zero after which data availability dropped to

zero. Figures 2-21 through 2-23 show pitch, roll, and yaw solutions just prior to and slightly after D1 start. Figure 2-24 shows in more detail the yaw solution just prior to and just after D1. Pitch and roll oscillations are clearly visible as is yaw capture. The D2 sequence was initiated at 1640 GMT and the damper boom at 1725 GMT.

For some time after the initiation of the D1 sequence, the low data availability and the lack of an accurate a priori attitude limited the number of attitude solutions available. The timing of the D2 sequence and the damper boom deployment were based on results of simulations as calculated attitude results were not available. Only after the observed body Sun angles, measured onboard the spacecraft, provided a semi-independent check on attitude, did a strong confirmation of capture result. The measured Sun declination angle in body coordinates was plotted against the predicted Sun declination assuming a capture with pitch, roll, and yaw of 0 degrees. Figure 2-25 shows predicted and observed Sun angles for about 28 hours following D1. Predicted angles are shown as solid lines; observed angles as a + . The predicted angles were generated using a constant attitude of 0-degrees pitch, 0-degrees roll, and -12-degrees yaw (the nominal capture attitude) except in the first two panels, in which a rigid body integrator was used to predict attitudes during capture. These plots show that the spacecraft achieved capture, but with large librations about the capture attitude.

The capture was not achieved at the expected nominal attitude: pitch, roll, and yaw of 0.0, 0.0, and -12 degrees, respectively. Long-term attitude information indicated that the capture was at pitch, roll, and yaw angles of -8, -5, and -40 degrees, respectively. It is thought that the non-nominal capture attitude was due to the lower trailing boom being bent an excessive amount down toward the Moon. No explanation as to why this occurred is available at this time.

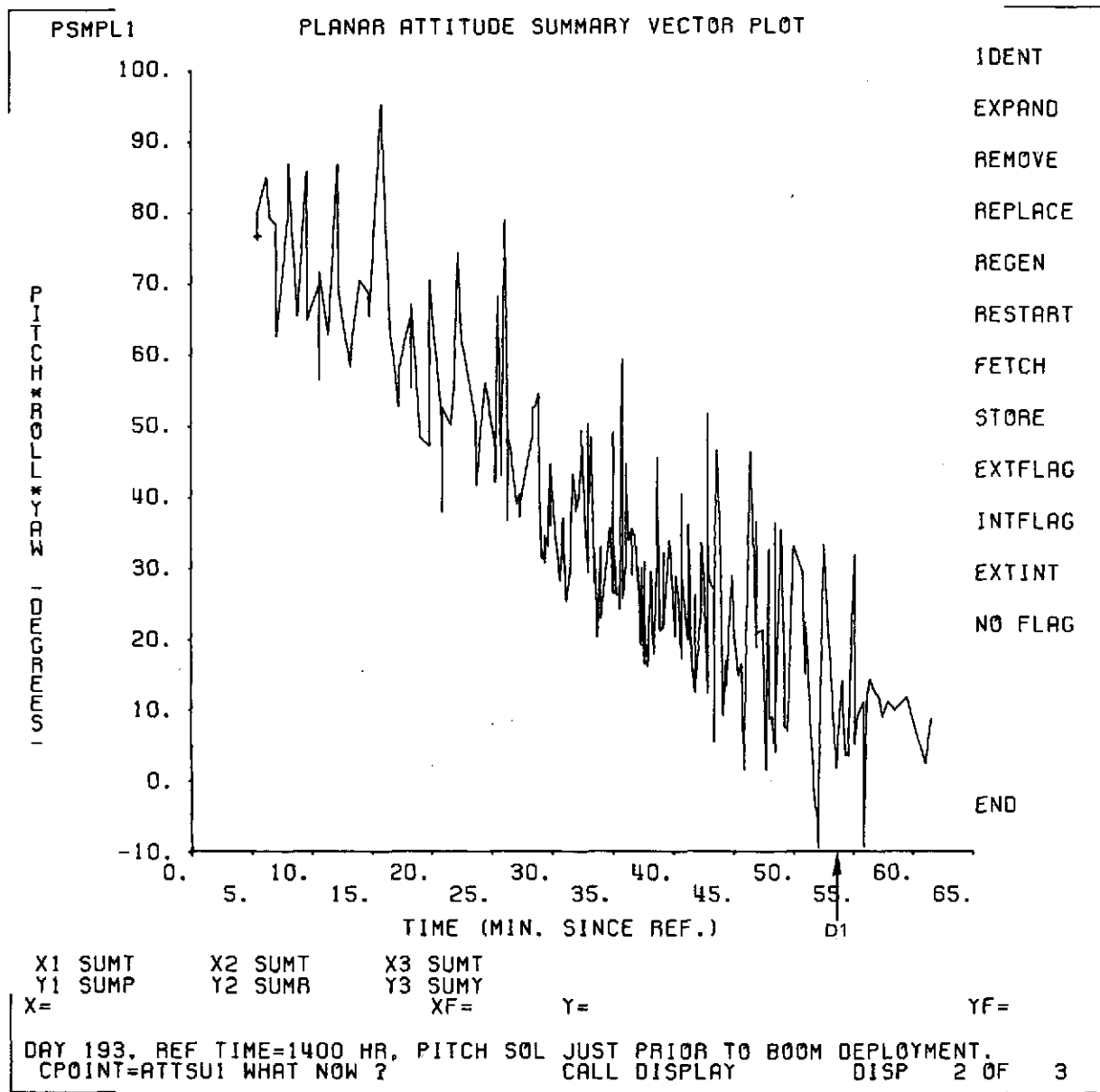


Figure 2-21. Pitch Solutions Prior to Deployment at 1453 GMT
(Reference Time Was 1400 GMT)

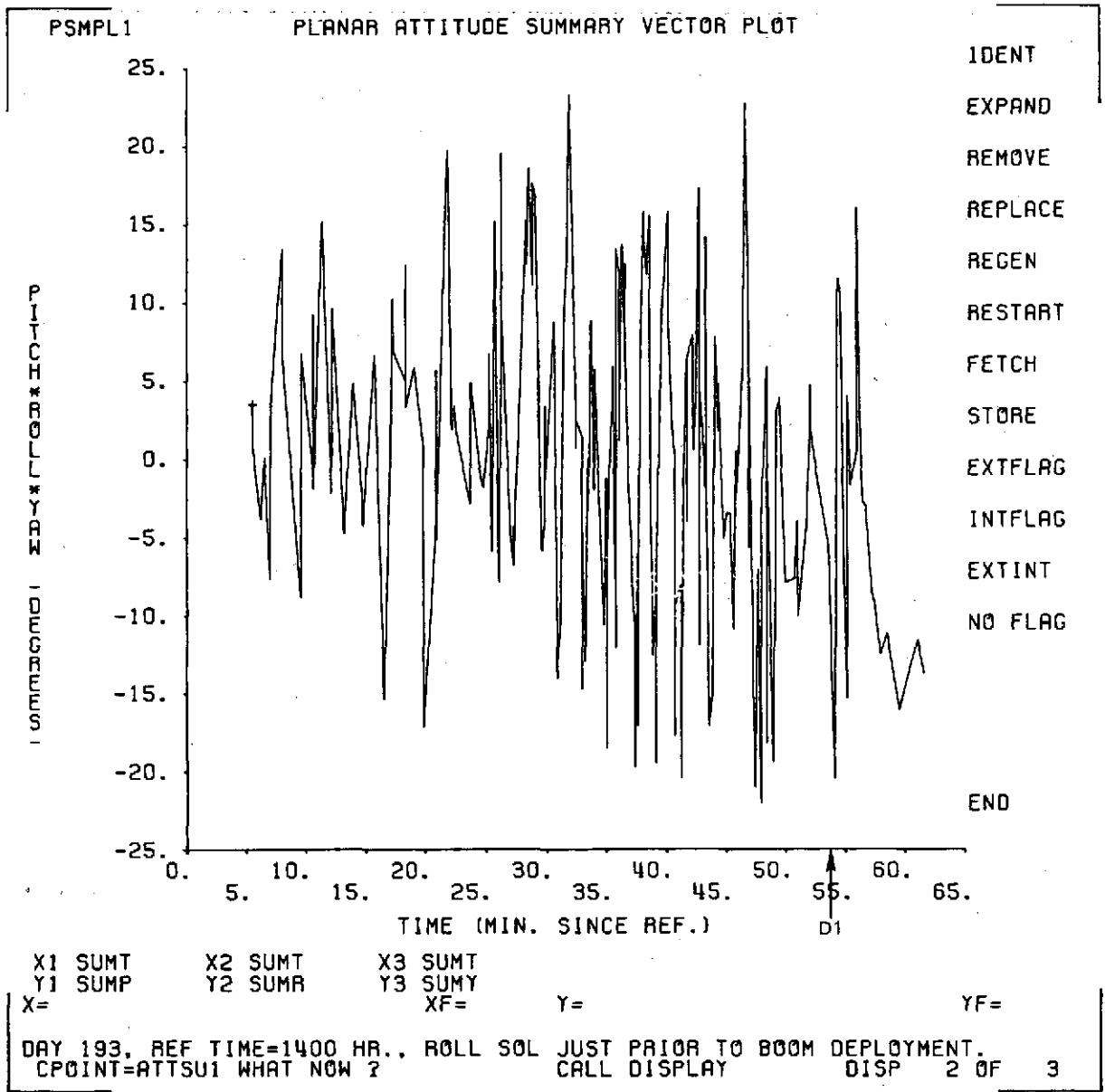


Figure 2-22. Roll Solutions Prior to Deployment at 1453 GMT
(Reference Time Was 1400 GMT)

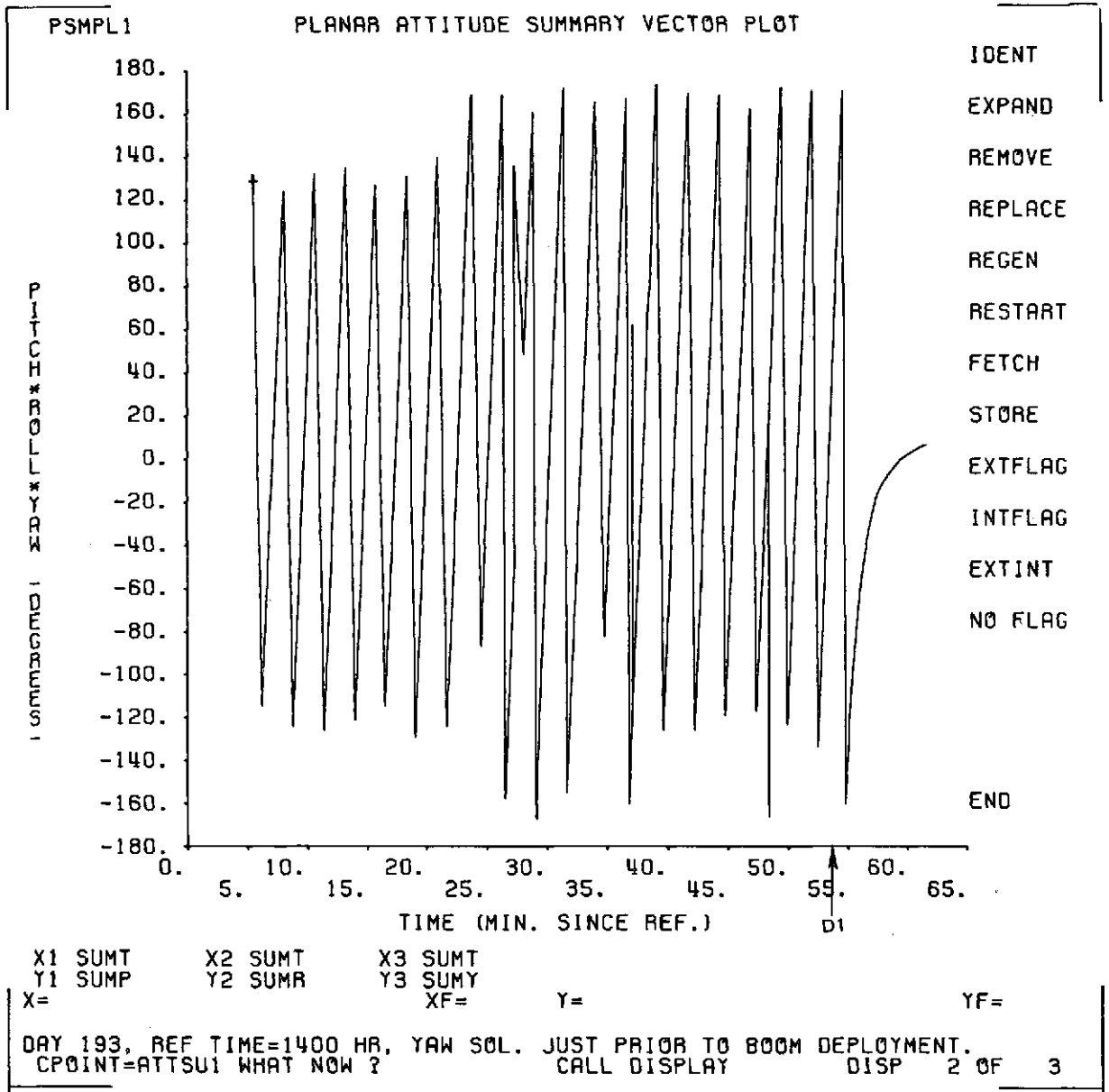


Figure 2-23. Yaw Solutions Prior to D1 Deployment at 1453 GMT
(Reference Time Was 1400 GMT)

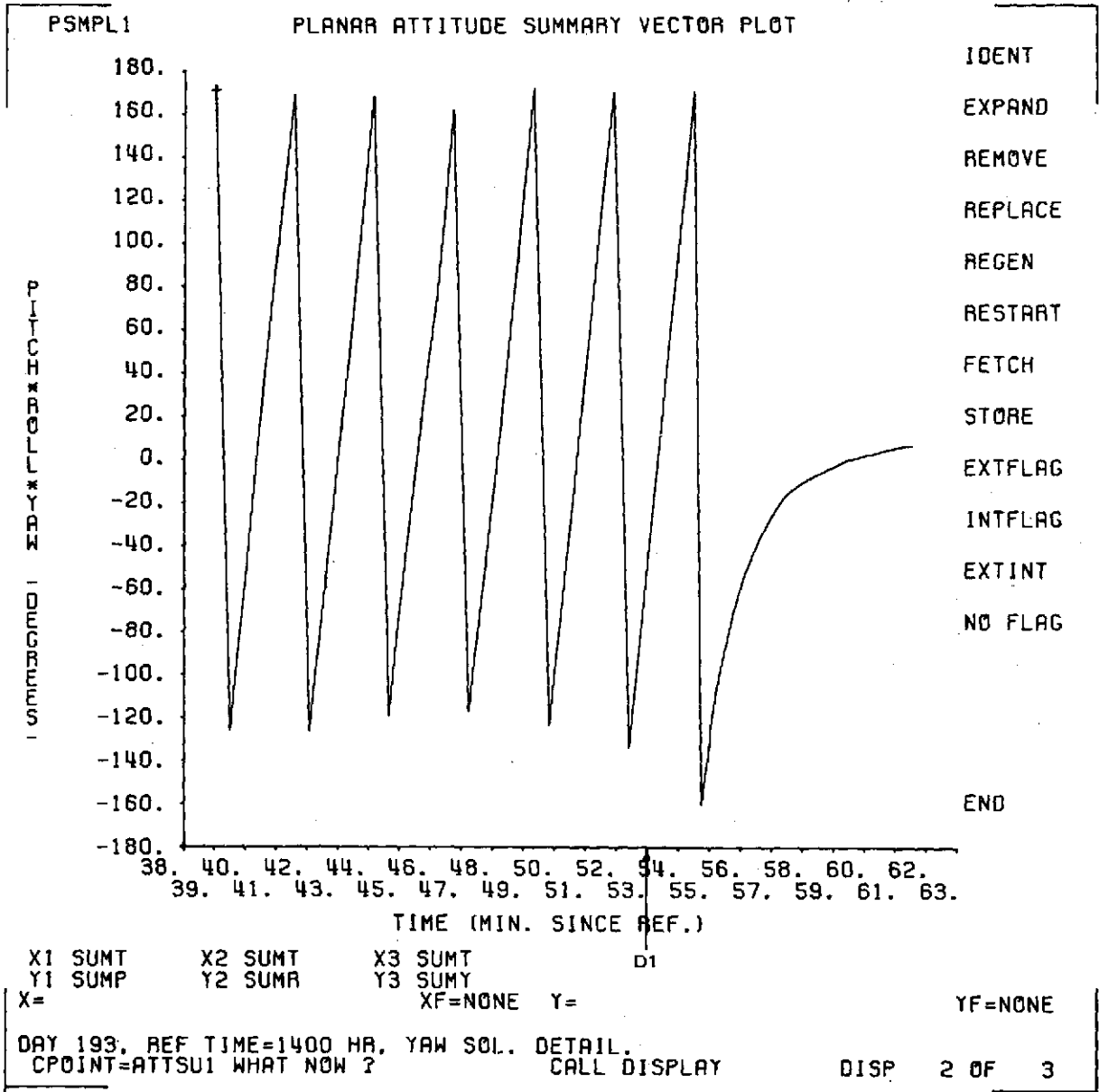


Figure 2-24. Yaw Solutions Prior to D1 at 1453 GMT
(Reference Time Was 1400 GMT)

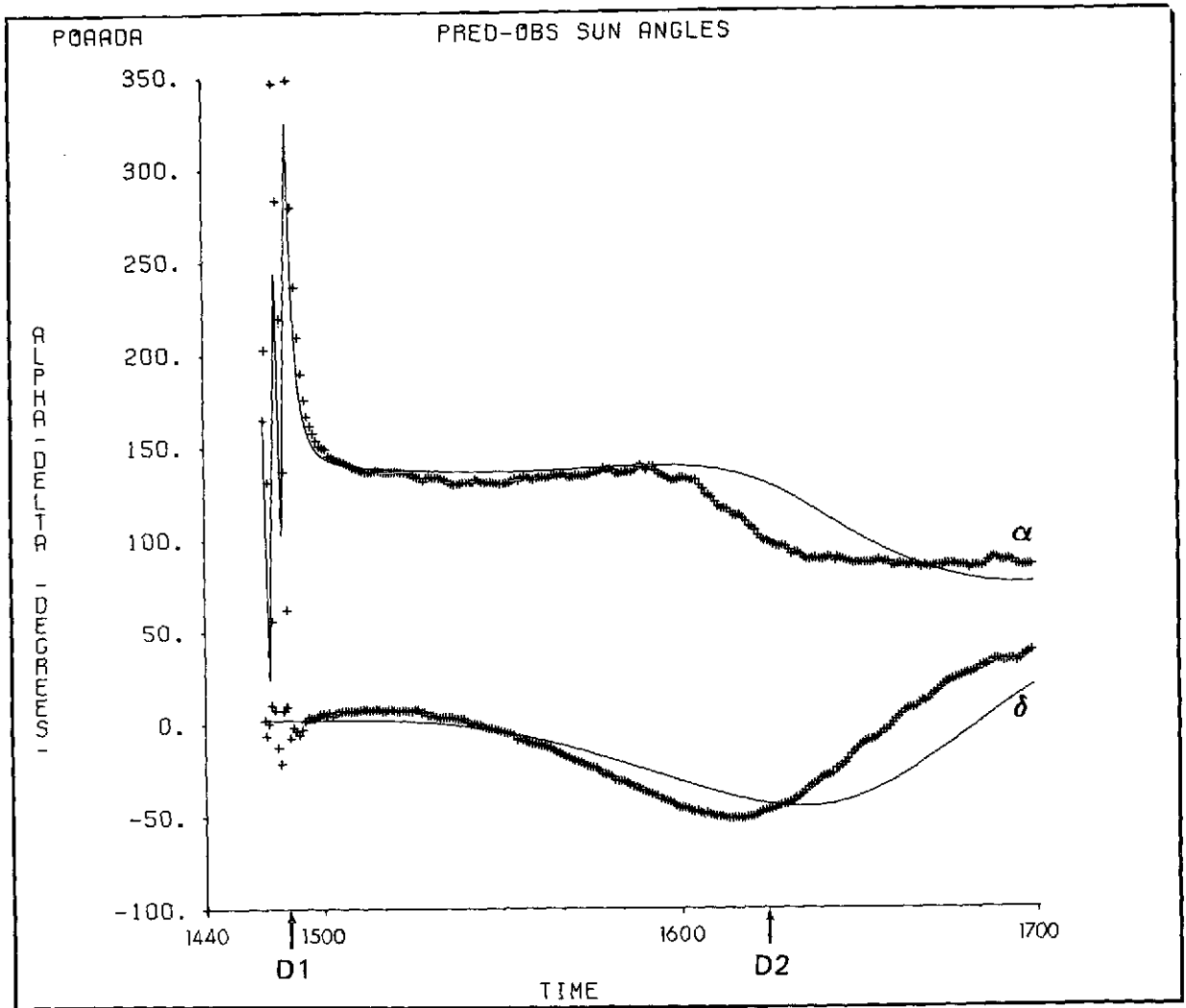


Figure 2-25. Predicted-Observed Body Sun Angles (1 of 6)

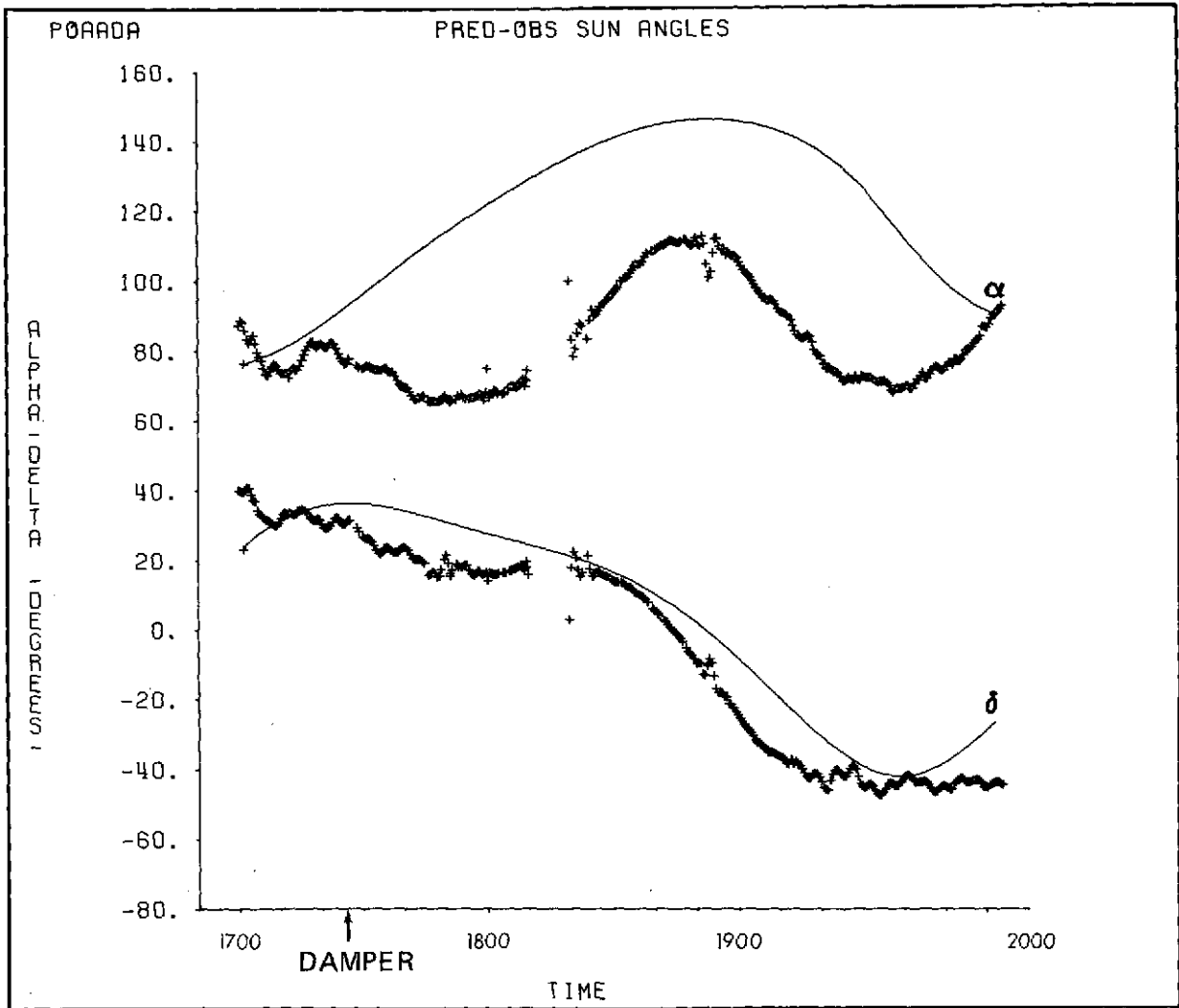


Figure 2-25. Predicted-Observed Body Sun Angles (2 of 6)

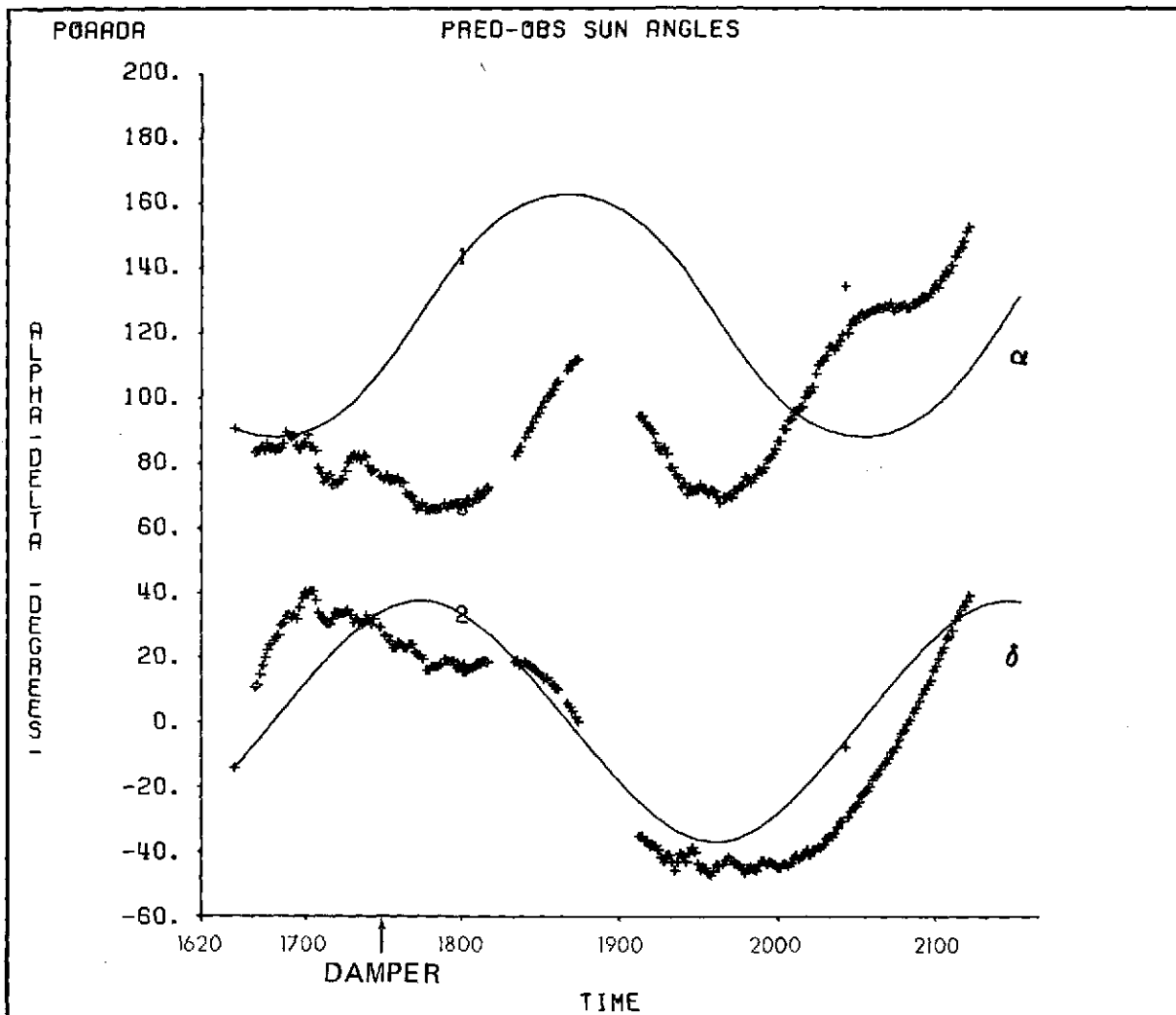


Figure 2-25. Predicted-Observed Body Sun Angles (3 of 6)

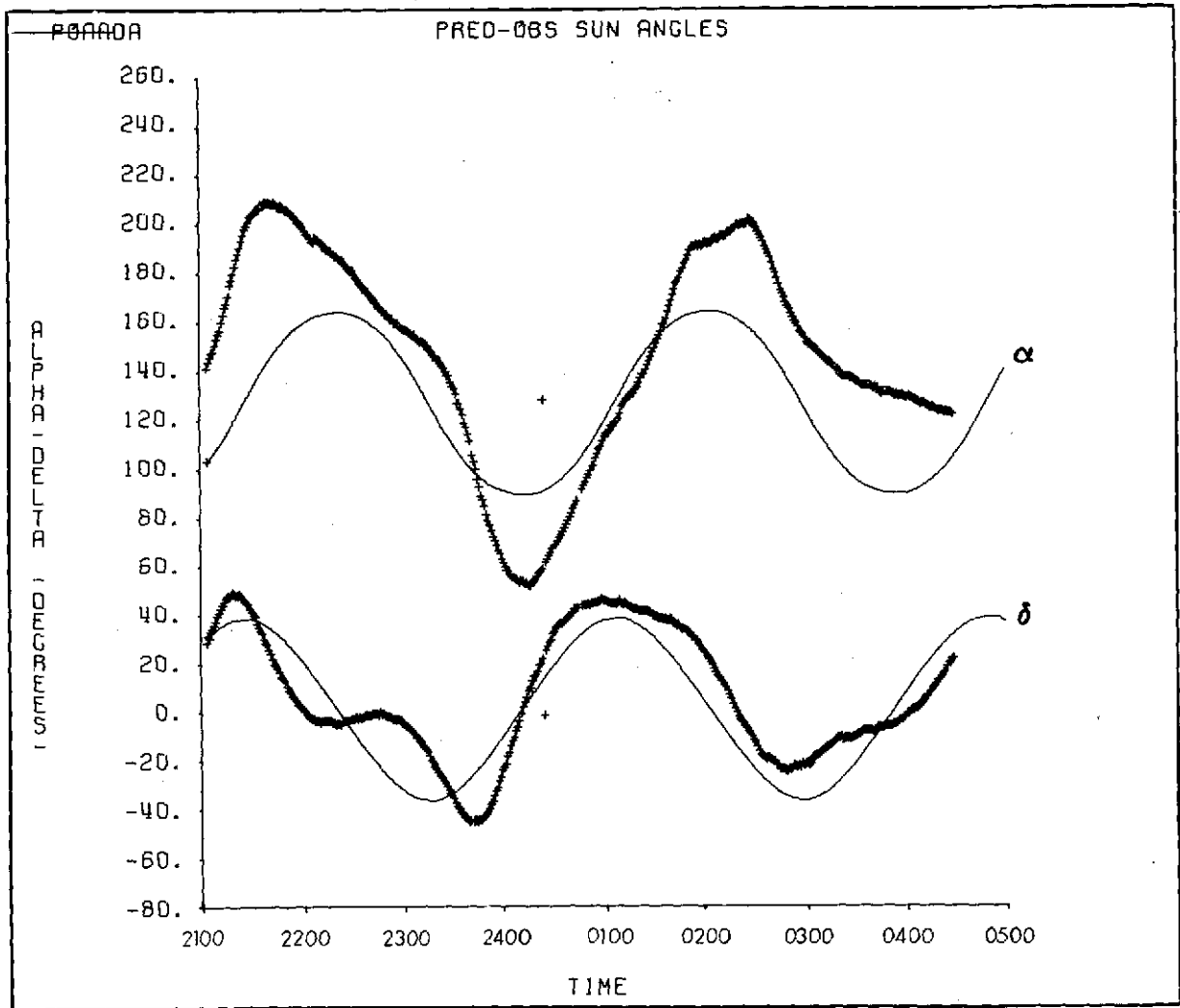


Figure 2-25. Predicted-Observed Body Sun Angles (4 of 6)

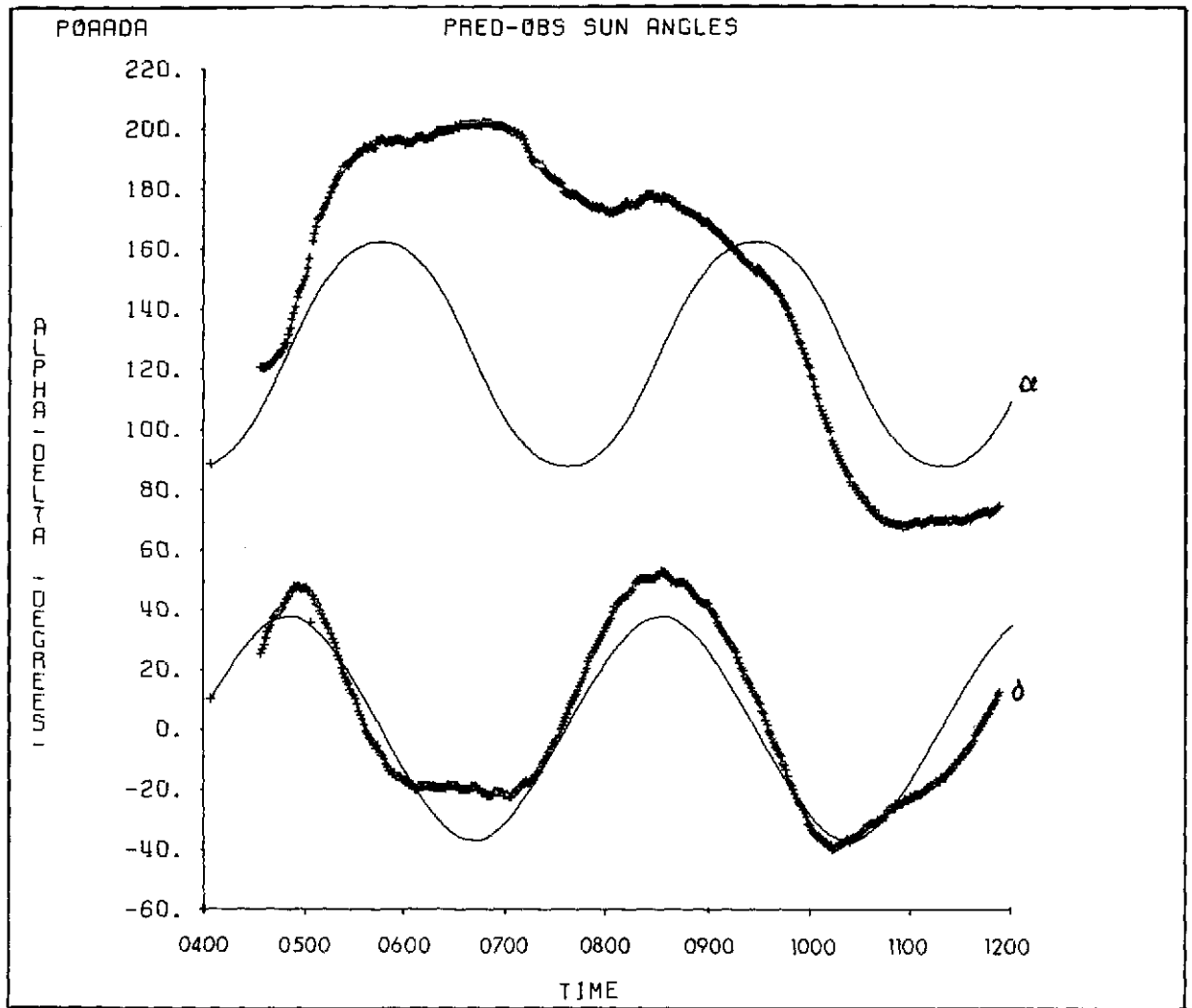


Figure 2-25. Predicted-Observed Body Sun Angles (5 of 6)

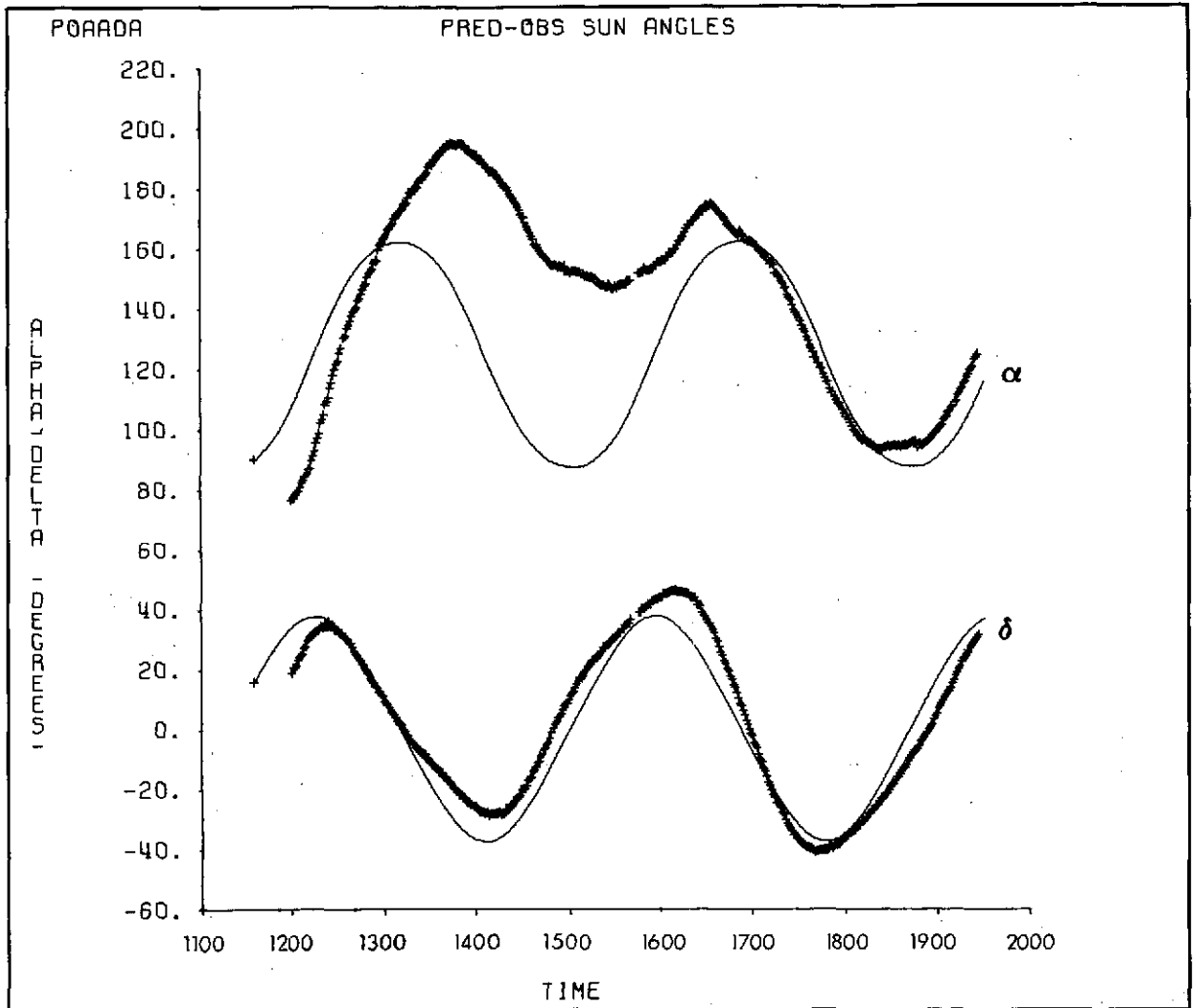


Figure 2-25. Predicted-Observed Body Sun Angles (6 of 6)

Attitude information was processed on a continuous basis from the time of D1 through the period extending to 48 hours after D1. Subsequent to this period, information was processed on a one-orbit-per-day basis until September 8, at which time one orbit per week was processed. During the period after capture a continuing malfunction of the PAS scanners in a way similar to that seen in the translunar phase of the mission was noted. A different type of PAS scanner failure was also noted. Nominally the two PAS scanners are supposed to scan alternately; however, large blocks of telemetry data were received in which the operation of the PAS2 scanner seems to have been suppressed completely. At this time there is no confirmed explanation of either failure. Regular shadow periods started on July 27. The maximum shadow duration lasted approximately 48 minutes. Due to the PAS scanner failures, attitude data during shadow periods were scarce: the average length of the time during an orbit for which valid attitude results could be calculated was approximately 10 to 15 minutes. Figures 2-26 and 2-27 are, respectively, examples of attitude solutions that were calculated for an orbit in which there was no shadow period; and one in which there was significant shadow. Librations seem to be damped considerably during orbits in which a significant amount of shadowing occurs and seem to build up as shadow disappears. Final deployment of the main booms to 750 feet was carried out in three stages beginning on November 8 and ending on November 13, 1973. Only the upper booms were deployed. It was felt, in view of the current lack of understanding of the malfunction that occurred to at least one of these booms, that deployment of the lower booms would endanger the mission. The extension of only the upper booms to 750 feet is sufficient for experimental purposes. No significant changes in attitude were observed due to extending the upper booms.

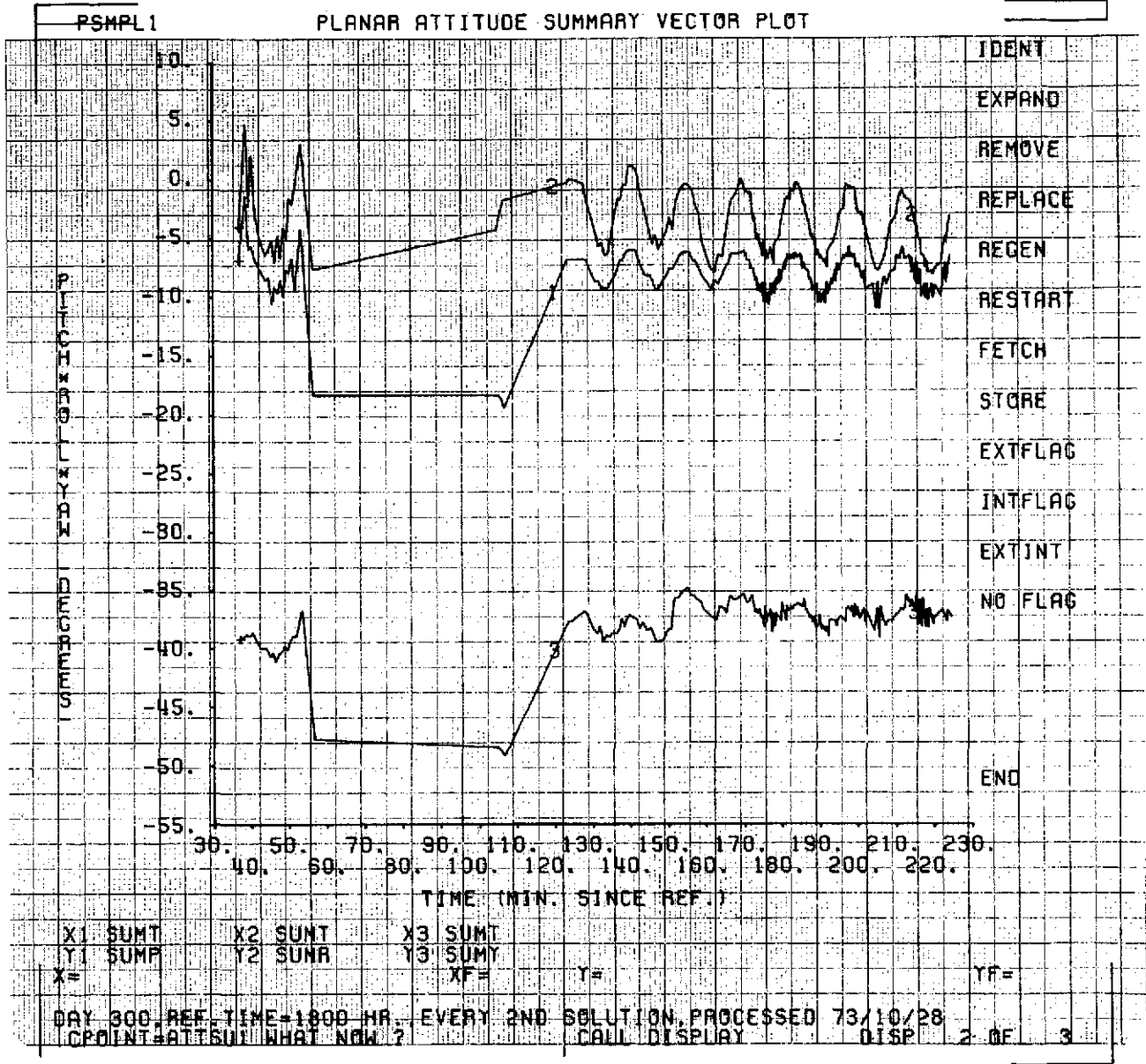


Figure 2-26. Attitude Solutions (No Shadow)

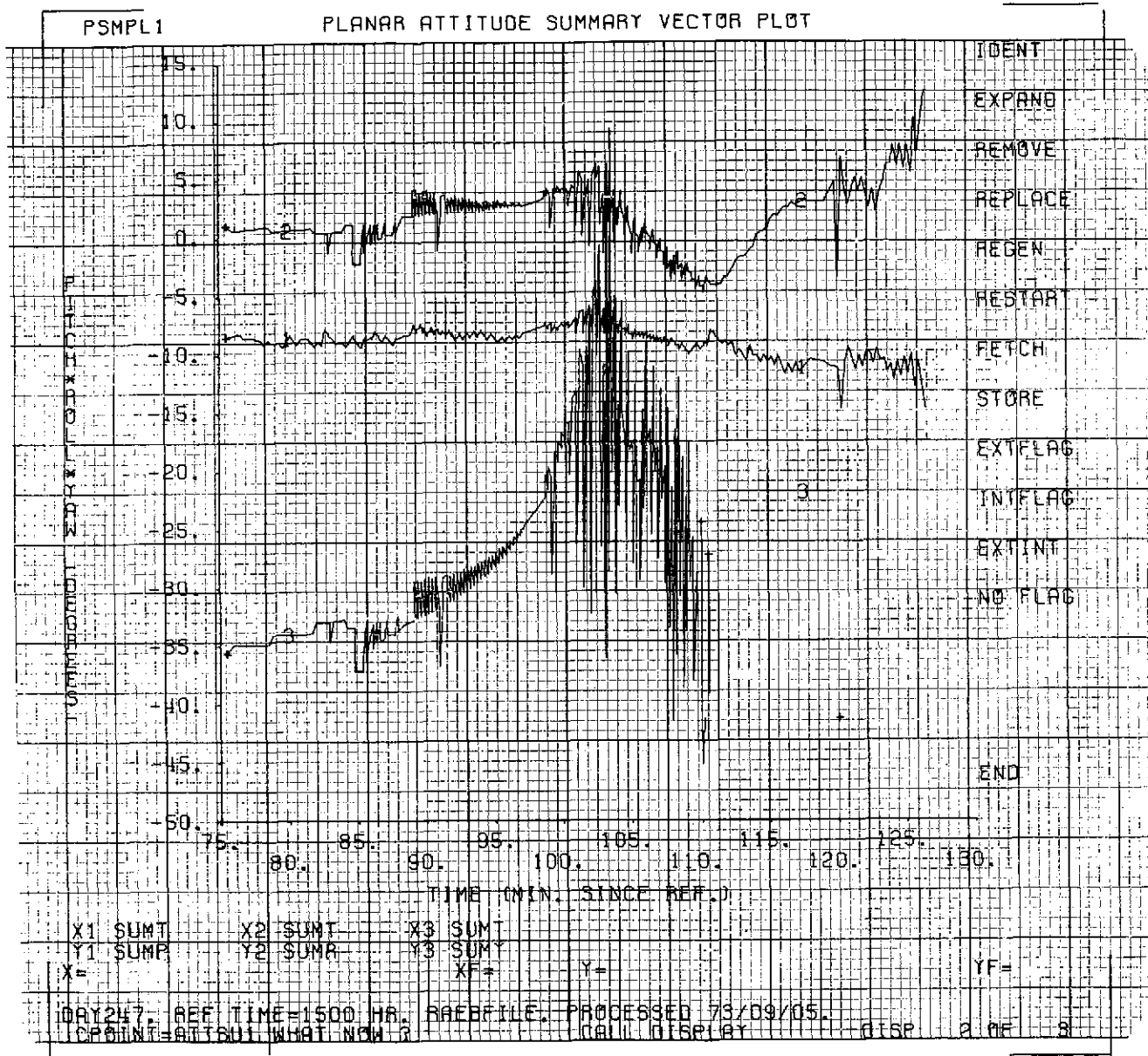


Figure 2-27. Attitude Solutions (Shadow)

SECTION 3 - ATTITUDE DETERMINATION AND CONTROL HARDWARE EVALUATION

3.1 INTRODUCTION

This section describes the operation of the RAE-B spacecraft hardware used to generate data for attitude determination and to maneuver the spacecraft attitude in response to ground commands.

3.2 ATTITUDE DETERMINATION SENSORS--SPIN MODE

3.2.1 Prelaunch Specifications and Alignment

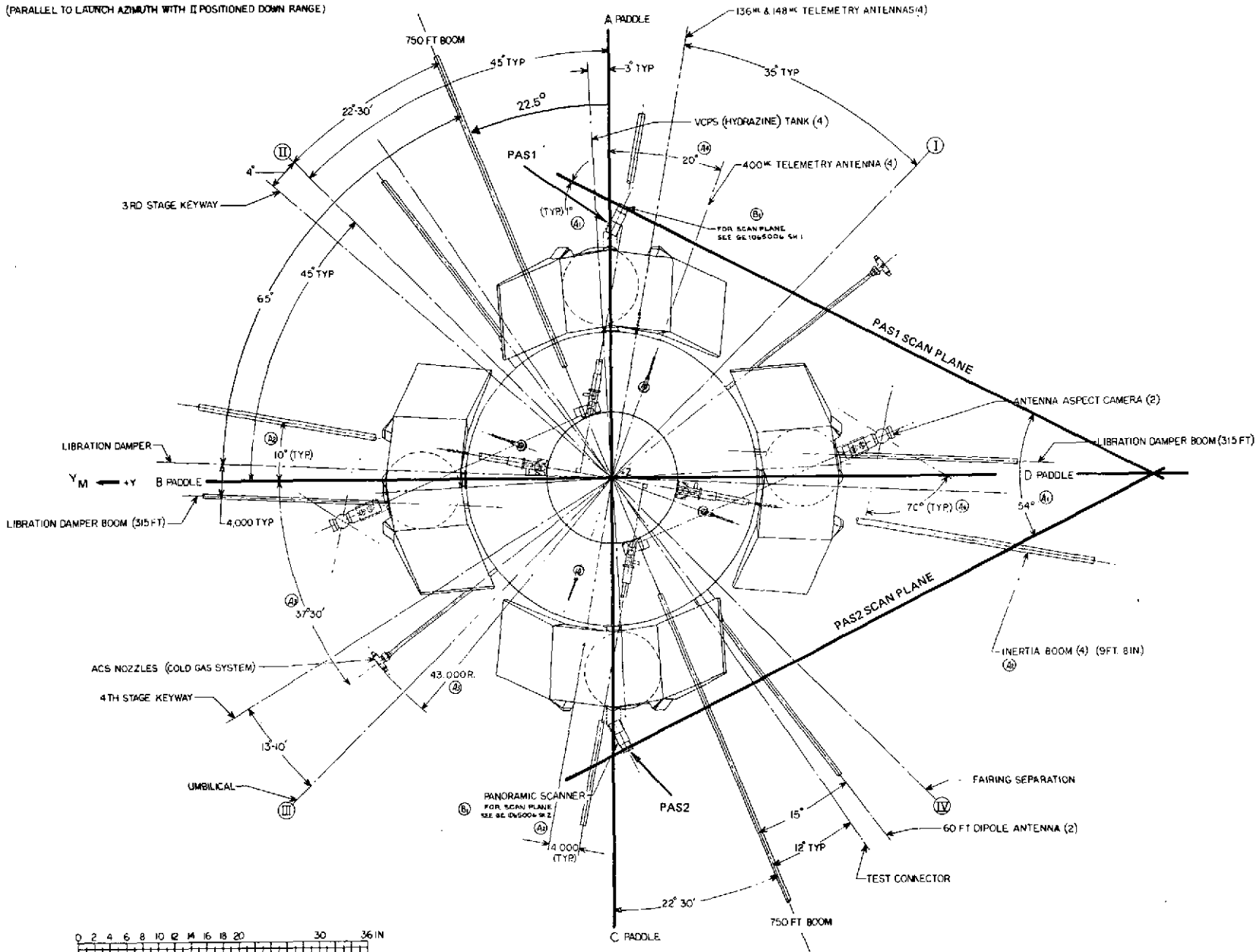
The attitude determination system for the RAE-B spacecraft consists of two PAS scanner heads mounted on paddles A and C and a digital solar sensor mounted on paddle A (Figure 3-1). Each scanner head has two optical sensors: the Sun slit and the scanner as shown in Figure 3-2.

The PAS Sun sensors have a field of view 0.5 degree x 180 degrees and provide only a reference pulse during each revolution of the spacecraft. This pulse is used as a start gate for measuring azimuthal angles, spin rates, and ACS functions.

The scanner is a small telescope consisting of a 60-millimeter focal length objective lens with a photodiode located at the focus. A 90-degree prism, mounted in front of the objective lens, serves as a 45-degree mirror and, with a series of apertures, limits the field of view to a cone of 0.7-degree diameter. The axis of this cone is perpendicular to the telescope axis (Figure 3-3) which rotates 360 degrees so that the locus of the line of sight is a great circle. An encoder provides an 8-bit (0-511) digital representation of the angle from the PAS line of sight to the spacecraft Z-axis. Figure 3-4 shows the telescope's encoder assembly with the nominal zero position in the spacecraft body X-Y plane.

(PARALLEL TO LAUNCH AZIMUTH WITH II POSITIONED DOWN RANGE)

3-2



TOP VIEW

Figure 3-1. RAE-B Spacecraft Geometry

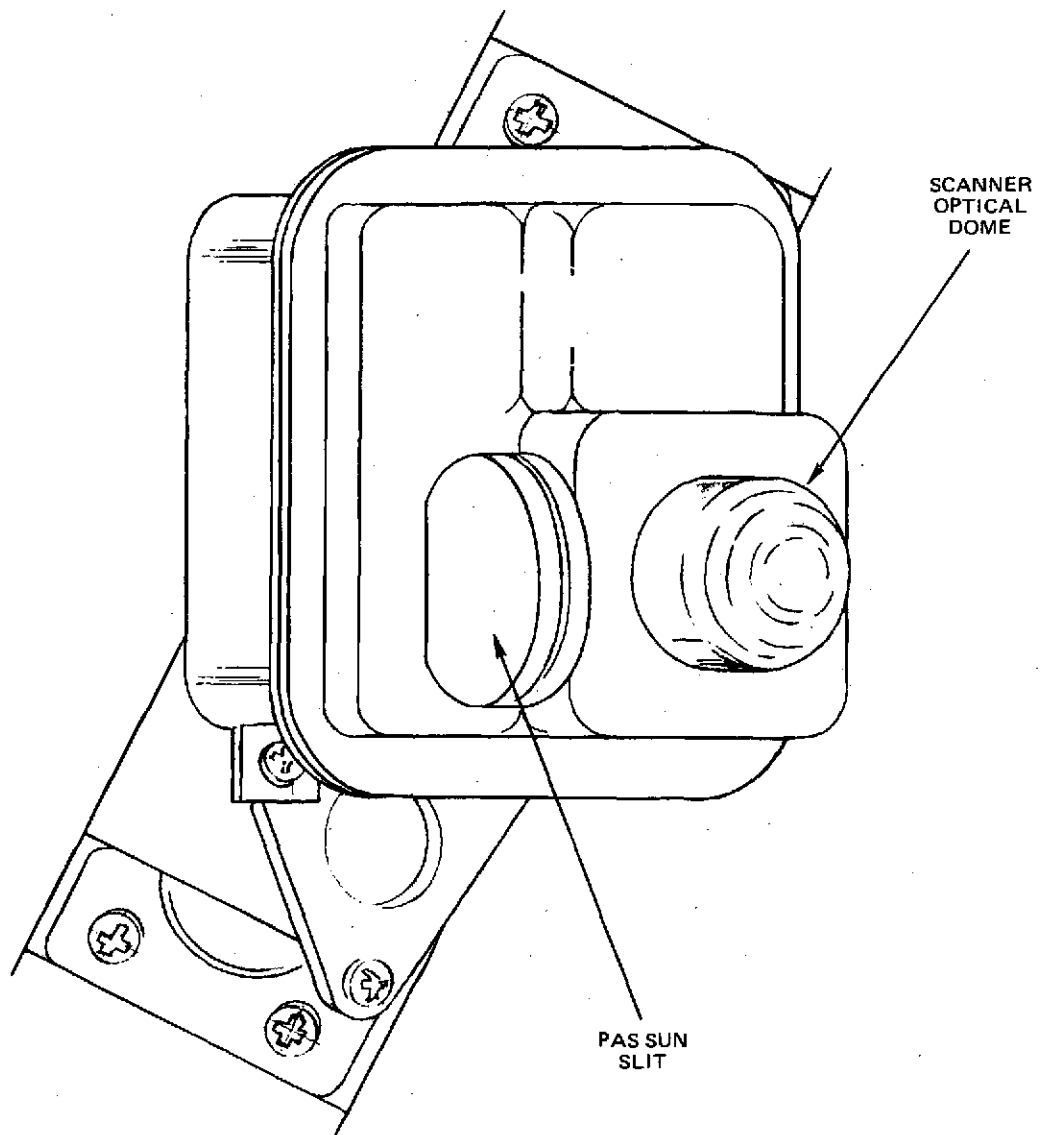


Figure 3-2. PAS Scanner Head

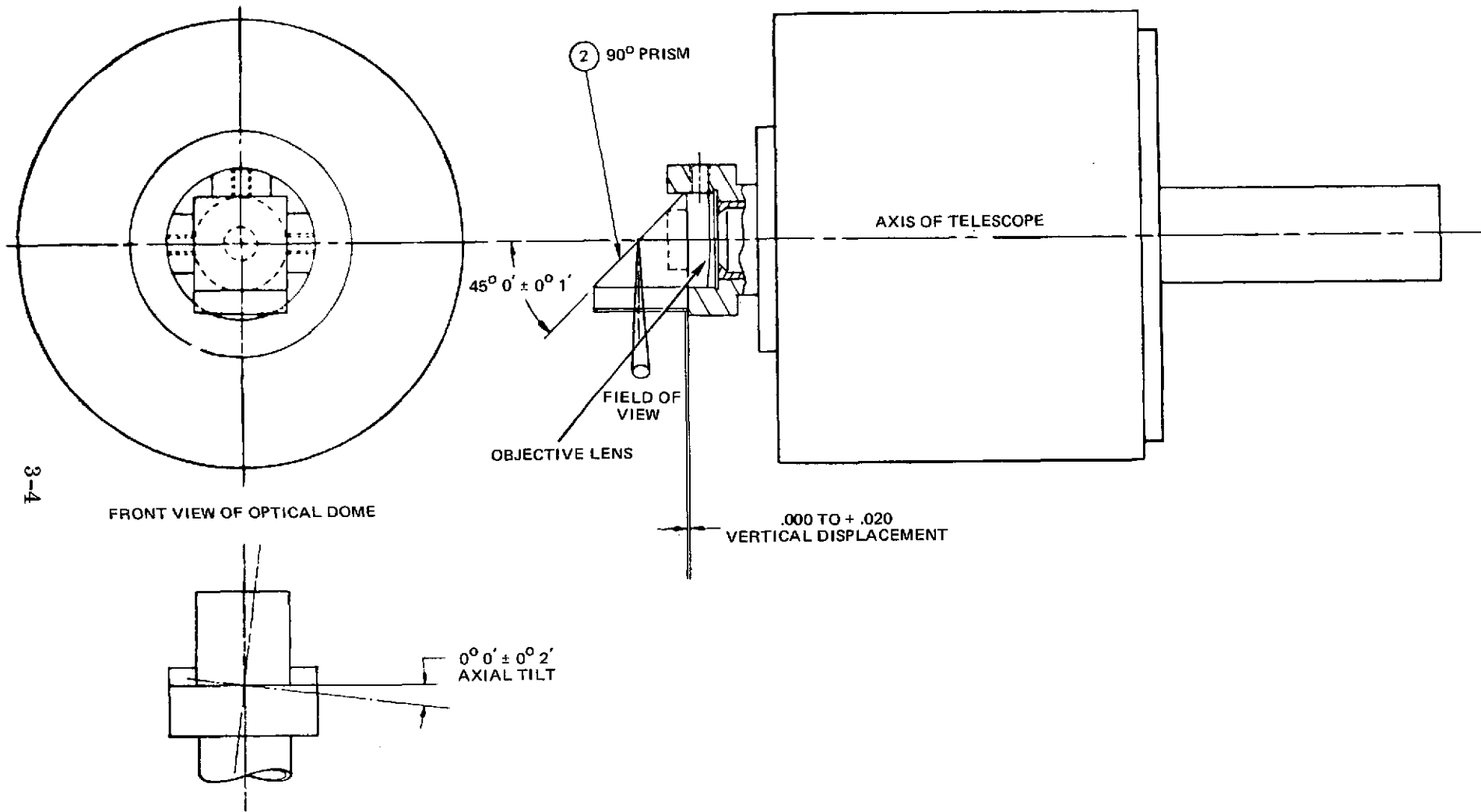
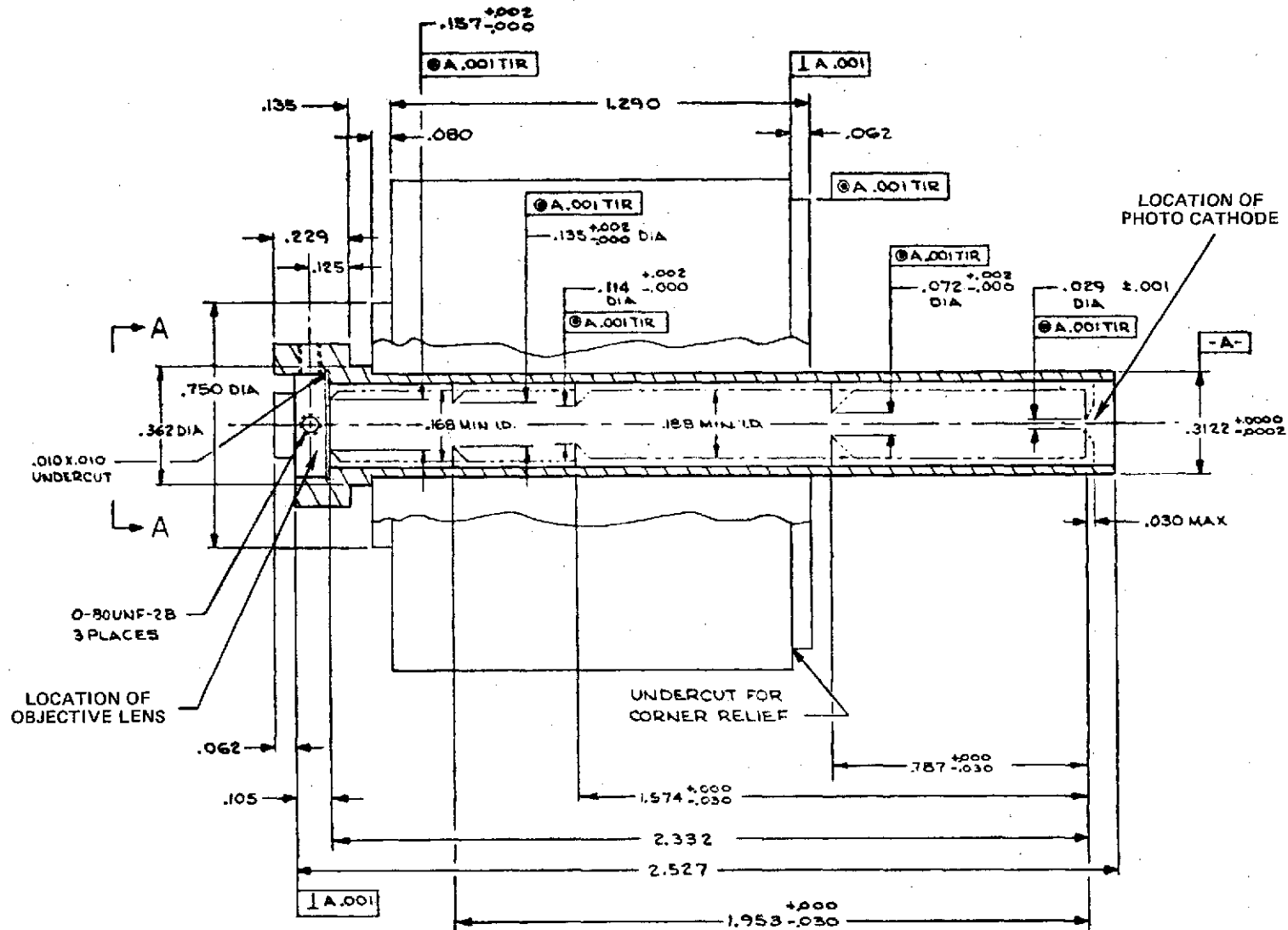


Figure 3-3. PAS Scanner Optics



3-5

Figure 3-4. PAS Telescope and Encoder Details

The following summarizes the azimuthal tolerances for the specified resolution of the PAS system:

<u>RPM</u>	<u>AOS (Degrees)</u>	<u>LOS (Degrees)</u>	<u>AOS to LOS (Degrees)</u>	<u>Spin Rate Percent</u>
50	±0.85	±0.85	±1.3	±0.1
12	±0.85	±0.85	±1.3	±0.1
4	±1.0	±1.0	±1.5	±0.1

The following summarizes the spherical and planar mode elevation tolerances for the specified resolution of the PAS system:

<u>Angle</u>	<u>Tolerance (Degrees)</u>
Z-axis to AOS	±0.45
Z-axis to LOS	±0.45
AOS to LOS	±0.90

The scanner stepping logic in spherical (spin) mode is described in detail in Reference 2. However, a brief description of the stepping logic is included here for background information.

The measure cycle comprises the interval between the first and second Sun pulses within a PAS telemetry frame.

Until an illuminated target is detected, the scanner operates in the search mode, advancing one step each time a Sun pulse occurs, except the scanner does not advance on the Sun pulse which begins each measure cycle. When a target is acquired, whether during the measure cycle or at any other time during the 15.36-second frame period, the scanner switches to the measure mode, and remains in that mode until the next end of measure cycle Sun pulse occurs. While in the measure mode, no scanner advance occurs. However, at the end of each measure cycle, the scanner switches from measure mode to search

mode and advances a single step. If a target is again detected, the scanner switches to measure mode and performs another measurement during the next cycle.

Thus, in the continuous presence of a target, the scanner advances one step and performs one measurement for each measure gate cycle. When a target is present intermittently, as in the case of spacecraft wobble, the probability of making a measurement is maximized because any target detected during a cycle is measured, whether it was detected during a preceding cycle or not. When no signal is acquired by the scanner during a measure cycle, the readout of the AOS will be the spin period (time from Sun pulse to Sun pulse).

The AOS time is stored in a 10-bit counter whose rate is adjusted according to the following inequality so that overflow will not occur:

$$C \leq \frac{S}{60} (1023)$$

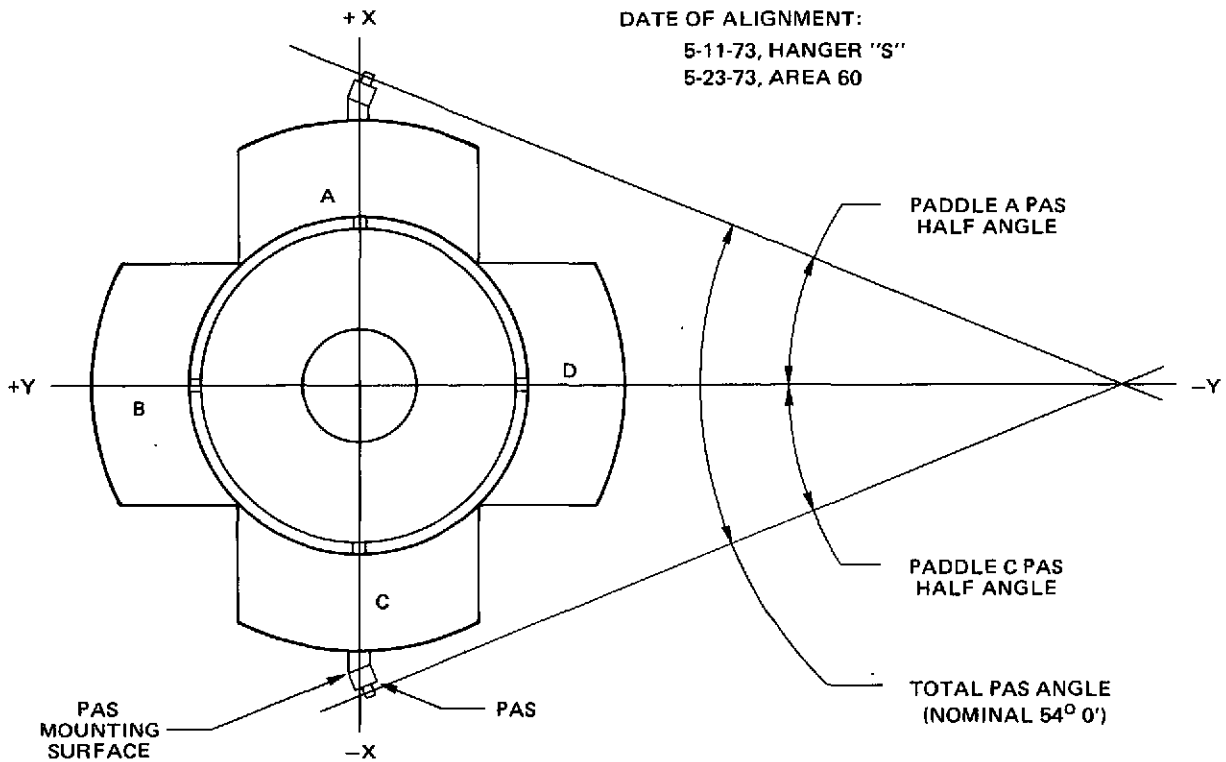
where S is the spin rate (rpm)

C is the clock rate (Hertz)

The time from AOS to LOS is stored in a 7-bit counter. Loss of most-significant bits may occur; the AOS-LOS time is known only modulo (t_o) , where $t_o = 128/C$. The problem of overflow in the LOS register was mitigated by software design (Reference 3).

Both scanners were tested by the manufacturer using flight electronics and met or exceeded the design specifications.

The hardware was mounted on the spacecraft and aligned at the launch site approximately one month before launch (Reference 4). With the exception of the PAS Sun slit parallelism with the Z-axis, all angles were within expected limits and the measured biases were negligible compared to sensor resolution. Figure 3-5 summarizes the results of the alignment procedure.



SPACECRAFT TOP VIEW (+Z UP OUT OF FIGURE)

PADDLE A, PAS BRACKET A, PAS S/N 8
 PADDLE A PAS HALF ANGLE, 5-11-73
 PADDLE A PAS MOUNTING PLANE
 Z-AXIS PARALLELISM, 5-23-73
 PADDLE A PAS SUN SENSOR SLIT
 PARALLELISM WITH THE Z-AXIS,
 5-23-73

$26^{\circ} 56' 50''$
 PLANE TIPS $10'$ TOWARD $-Z$ -AXIS
 TOP OF SLIT TILTED $1^{\circ} 45'$ TOWARD
 $+Y$ -AXIS

PADDLE C, PAS BRACKET B, PAS S/N 9
 PADDLE C PAS HALF ANGLE, 5-11-73
 PADDLE C PAS MOUNTING PLANE
 Z-AXIS PARALLELISM, 5-23-73
 PADDLE C PAS SUN SENSOR SLIT
 PARALLELISM WITH THE Z-AXIS,
 5-23-73

$27^{\circ} 3' 8''$
 PLANE TIPS $10'$ TOWARD $-Z$ -AXIS
 TOP OF SLIT TILTED $2^{\circ} 0'$ TOWARD
 $-Y$ -AXIS

TOTAL ANGLE BETWEEN PAS FIELDS OF
 VIEW, 5-11-73

$53^{\circ} 59' 58''$

Figure 3-5. PAS Alignment Details

The SAS in spherical mode consists of a pair of digital solar sensors (Figure 3-6) mounted above and below the PAS head on paddle A as shown in Figure 3-7. An upper or lower sensor measures the angle between the Sun and the spin axis when the Sun is in the Northern or Southern Hemisphere of the spacecraft, respectively. The Sun angle output is in 1-degree increments (± 0.5 -degree resolution).

Figure 3-8 summarizes the alignment obtained for the SAS system. The measured zenith angles deviated from the nominal 30-degree value by 9 and 3 minutes for the upper and lower sensors, respectively; the azimuthal biases were 45 and 0 minutes toward the +Y-axis. No tilt of the horizontal slits was observed.

3.2.2 Postlaunch Sensor Operation

All measured biases and resolutions were input to the MAPS/RAE-B system with the exception of the 10-minute PAS scanner plane tilt and the PAS Sun slit tilt which could not be accommodated in the spin mode attitude system. It was assumed that the measured PAS Sun slit tilt was equivalent to a PAS scanner zero offset angle because of the PAS head design which implied that the 0-degree scanner line of sight was normal to the plane of the Sun sensor slit.

Attitude data was received 15 minutes after a nominal injection at 1429 GMT on June 10 with an initial hardware configuration of PAS2-SAS(upper) and the 200-Hertz clock. The Moon was acquired at 1457 GMT at an angle $\gamma = +33.6$ degrees ; the Sun angle was $\beta = 92.5$ degrees and a single frame attitude of $\alpha \cong 165$ degrees and $\delta \cong -15$ degrees was obtained.

The Moon acquisition was for only one step, as expected, because the Moon at launch has an angular radius of 0.5 degree and the PAS stepsize is 0.7 degree. After leaving the Moon, the scanner made several automatic advances (no target in view) before acquiring the Sun at 50 degrees just prior to the spacecraft clock being switched to 800 Hertz.

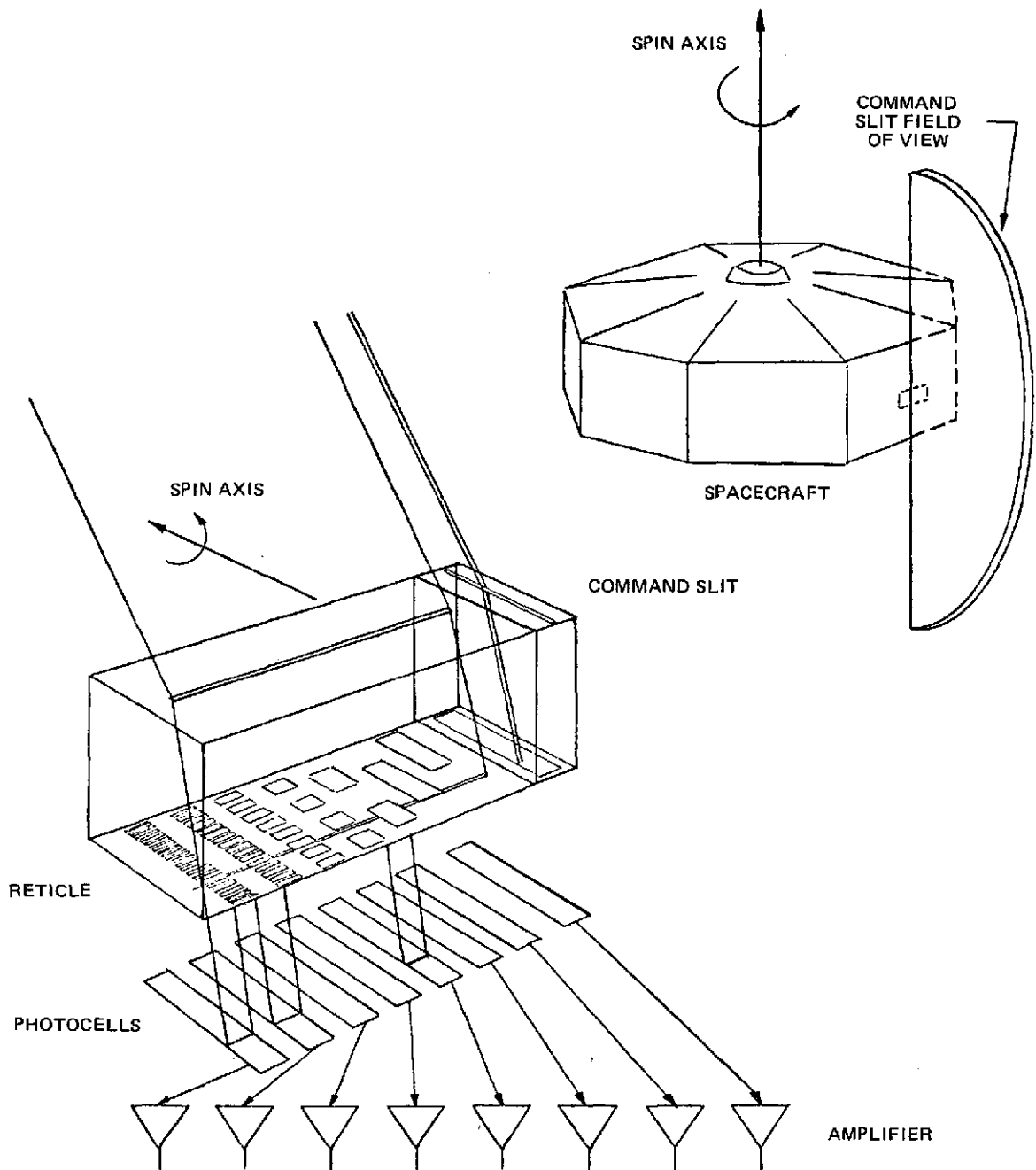
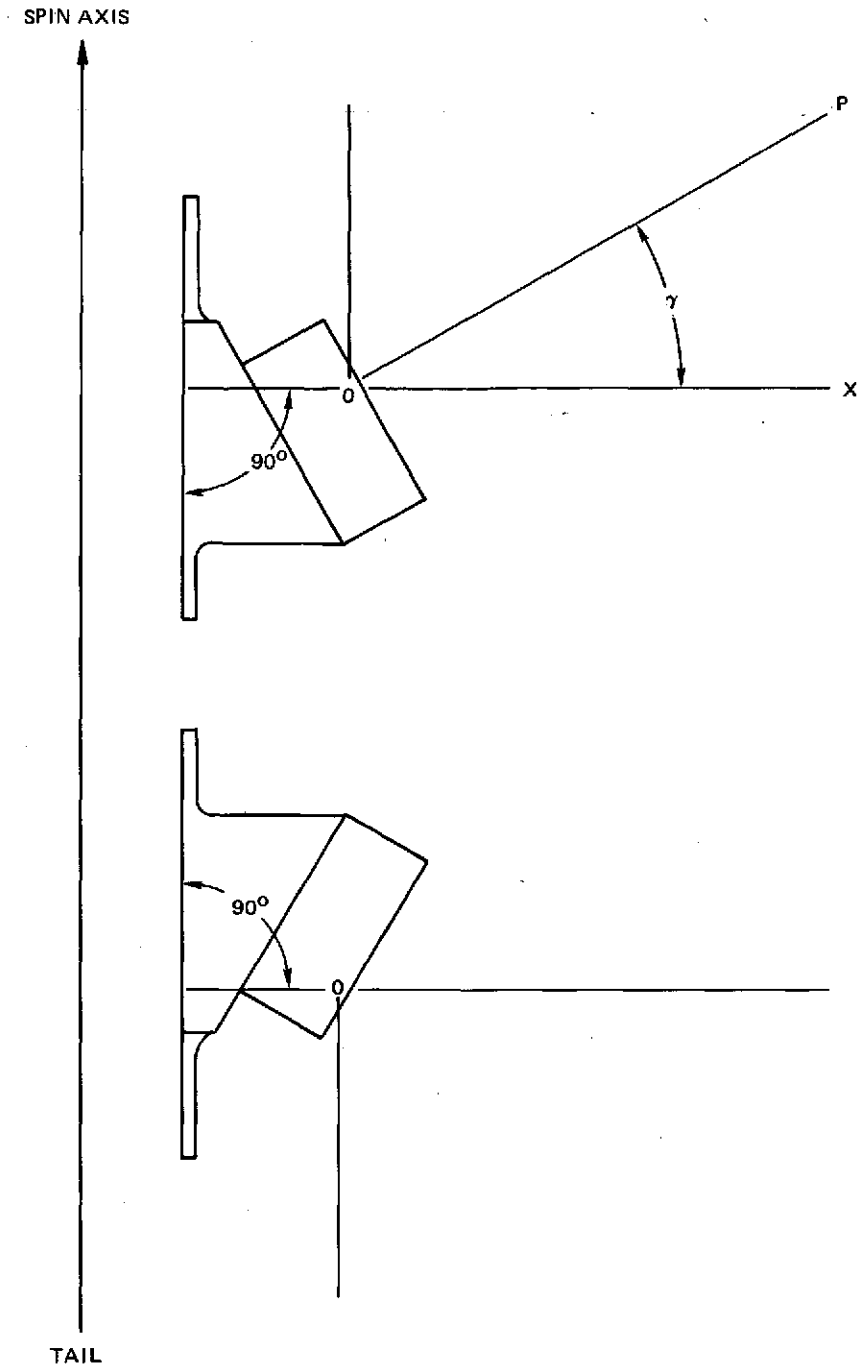


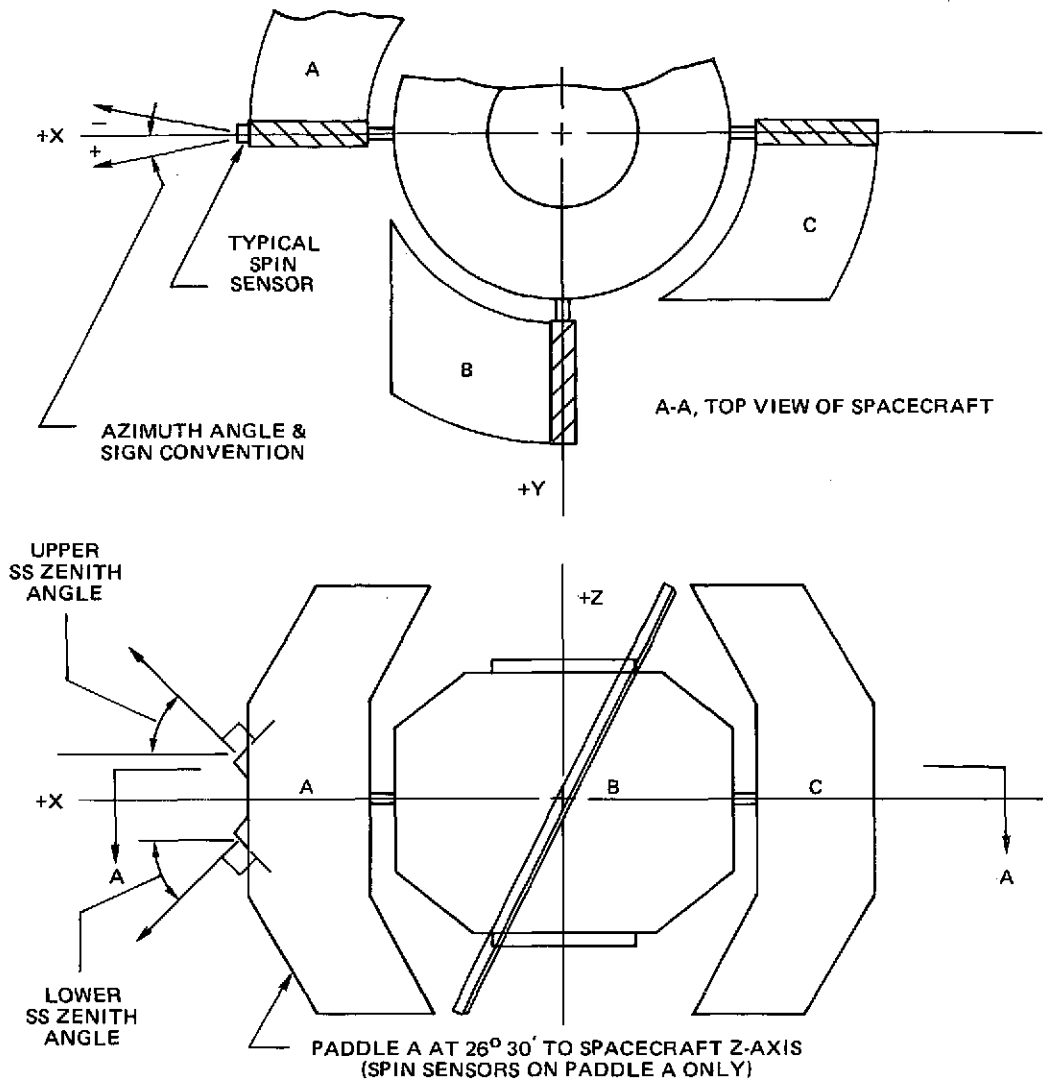
Figure 3-6. Spherical Mode Sun Sensor Operation



ROTATION CLOCKWISE
LOOKING AT TAIL

Figure 3-7. Upper and Lower Spherical Mode Sun Sensor Alignment

DATE OF ALIGNMENT:
 5-11-73, HANGER "S"
 5-23-73, AREA 60



	ZENITH ANGLE, 5-23-73	AZIMUTH ANGLE, 5-11-73	DEVIATION OF HORIZONTAL SLIT FROM THE HORIZONTAL (X-Y) PLANE, 5-11-73
UPPER SS	$29^{\circ} 51'$	$+0^{\circ} 45'$ (TOWARD +Y)	$0^{\circ} 0'$
LOWER SS	$29^{\circ} 57'$	$0^{\circ} 0'$	$0^{\circ} 0'$

Figure 3-8. Spherical SAS Alignment Details

The scanner stepped off the Sun at $\gamma = 132$ degrees and acquired the Earth at 1523 GMT for about 2 minutes. An asymmetric Sun acceptance angle, $A = -1$ degree ± 14 degrees and $\gamma = 92$ degrees ± 40 degrees was observed.

Figure 3-9 shows the locus of the Sun with the locus of the nominal 15-degree acceptance angle. This behavior was in qualitative agreement with the results of the spin functional test where it was found that the dihedral angular acceptance was approximately one half of the nadir angle acceptance. Several automatic advances were made after the initial Earth pass, and after stepping through the dark Earth, the Sun was reacquired at $\gamma = -158$ degrees as illustrated in Figure 3-10. This indicated that the Sun acceptance differed for positive and negative encoder angles. Earth horizons were reacquired at $\gamma = -142$ degrees, and considerable Earth-Sun interference was observed as shown in Figure 3-11.

Because it was clear that the Earth geometry was unfavorable for attitude determination, the scanner was repeatedly stepped to $\gamma \approx \pm 33$ degrees where the Moon was acquired. This geometry is illustrated in Figure 3-12 where a number of lunar events can be seen in the lower right-hand side of the figure and the Sun and Earth appear in the upper left-hand side. An attitude was obtained from this series of Moon sightings, and an effort was then made to determine PAS sensor biases prior to the midcourse correction.

The zero offset for the scanner could be easily found because lunar acquisitions were obtained for both positive and negative mounting angles. Data were received at $\gamma = +18.6$ degrees and $\gamma = -15.2$ degrees using the measured angle of 92 degrees for the angle from the Z-axis to the scanner 0-degree line of sight. This 2-degree bias was clearly too large. Biases of 1.7 degrees and 0.7 degree are displayed in Figures 3-13 and 3-14. The dihedral and mounting angle resolutions of ± 0.85 and ± 0.45 degree are shown as horizontal and vertical

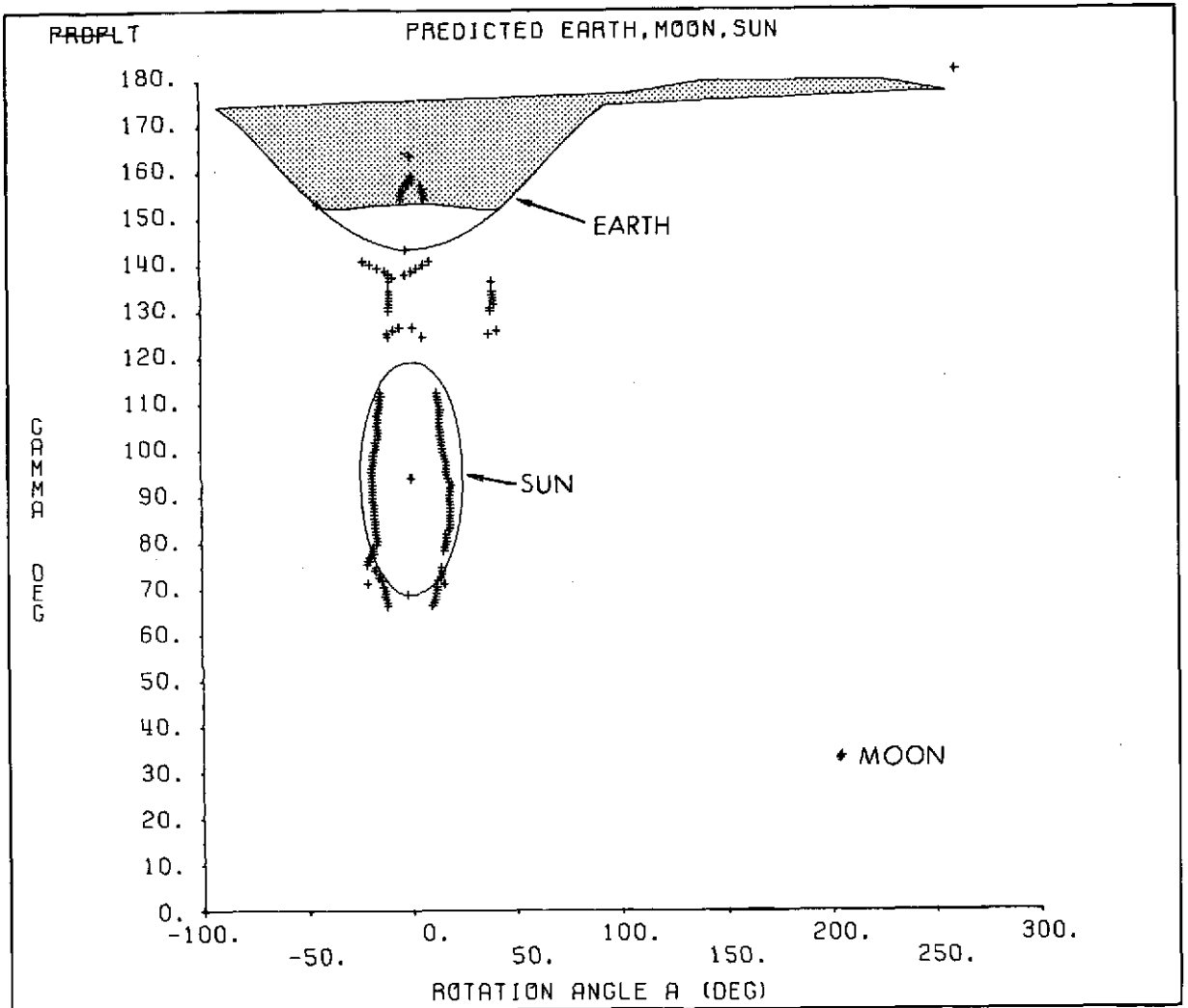


Figure 3-9. Central Body Geometry at Launch

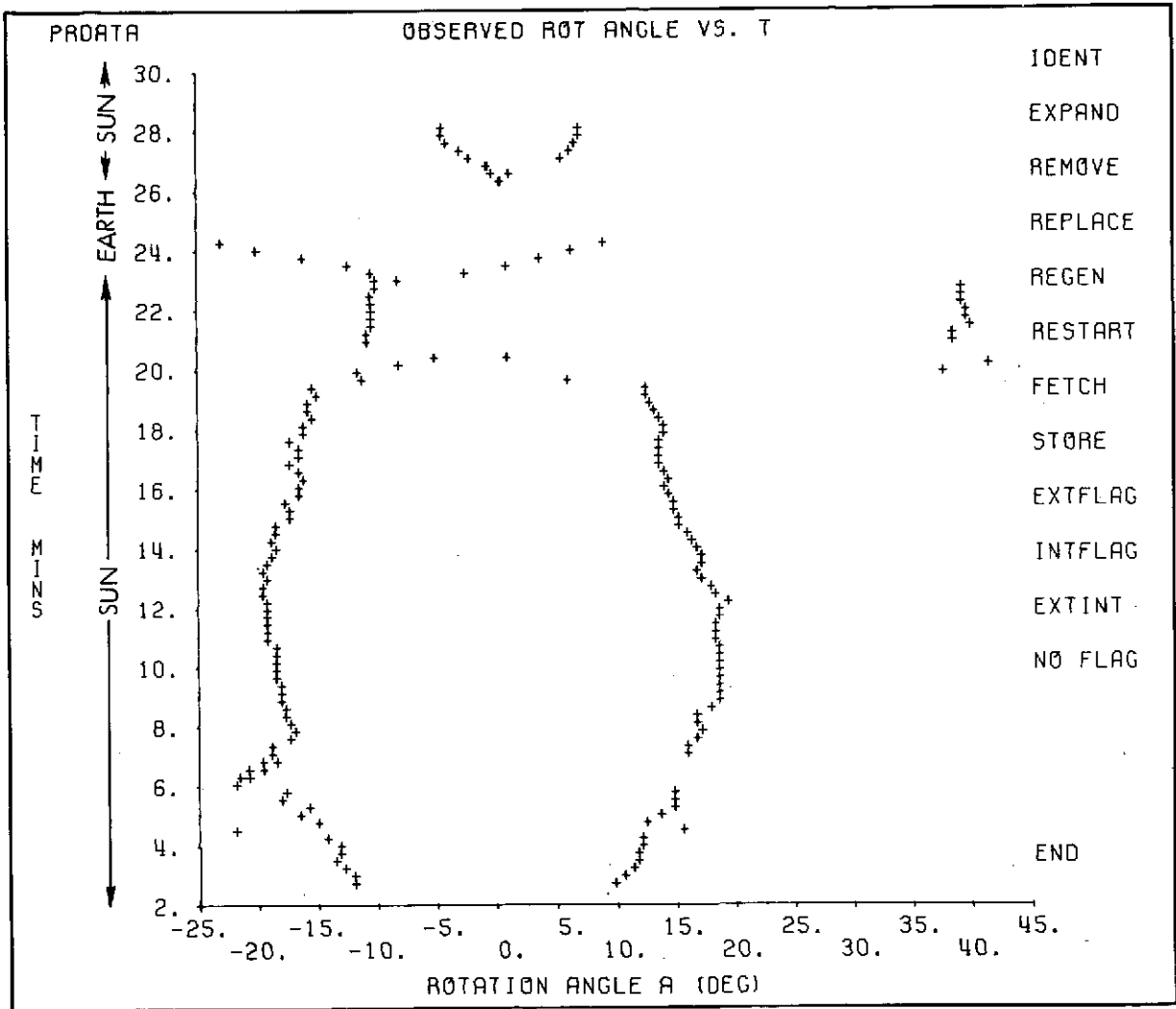


Figure 3-10. Azimuth Angles Versus Time at Launch

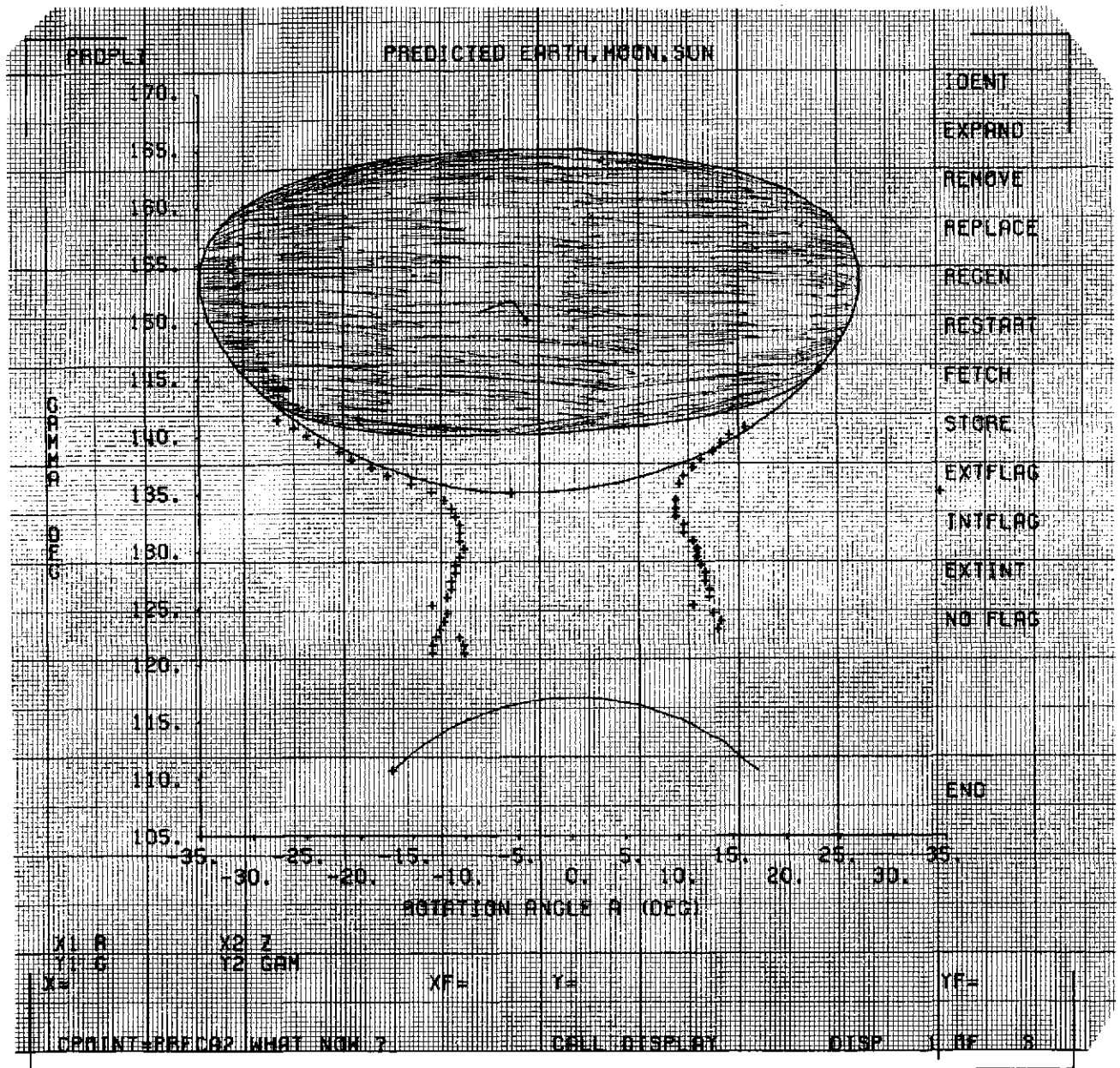


Figure 3-11. Earth-Sun Interference at Launch

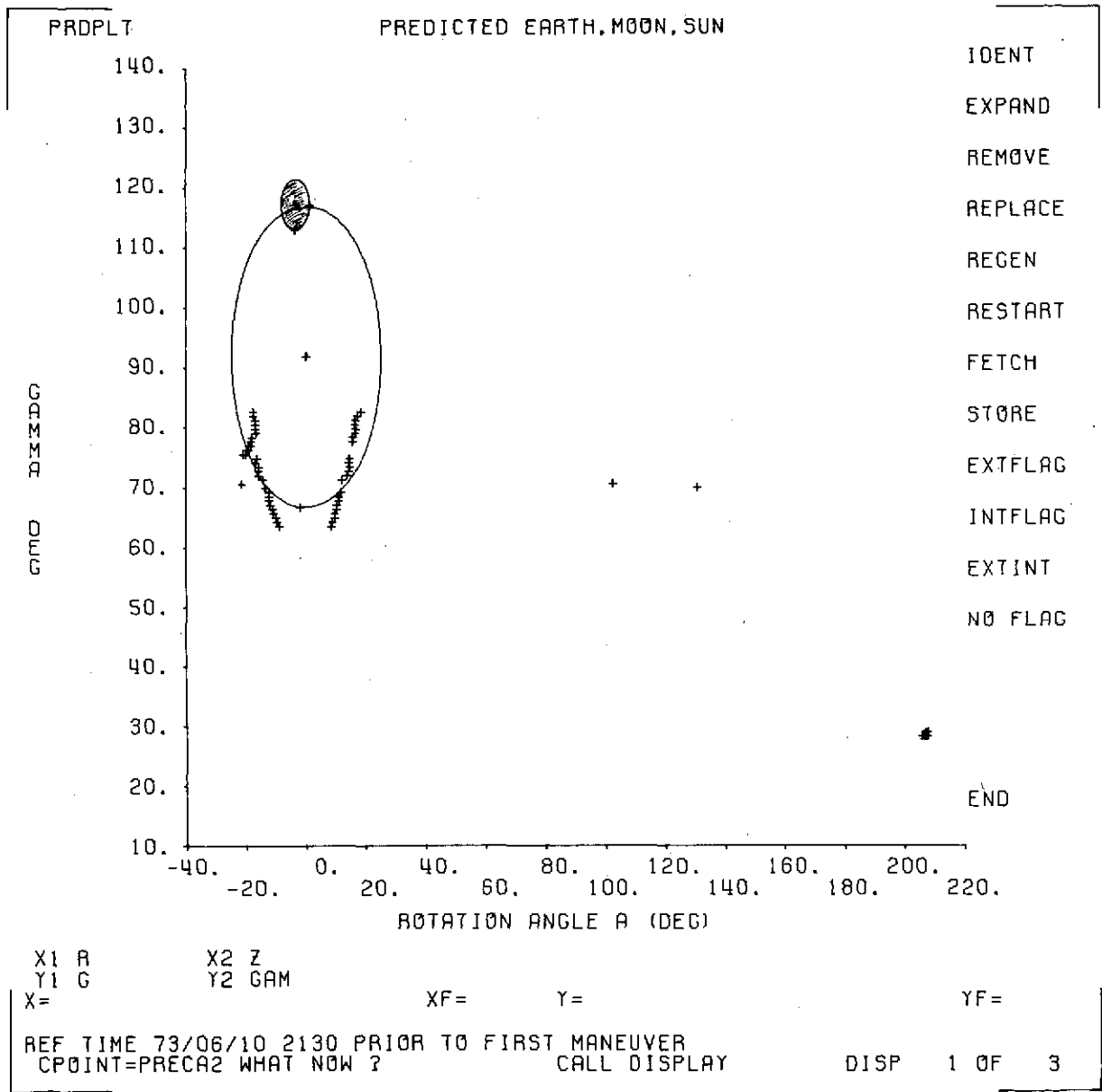


Figure 3-12. Moon Data at Launch

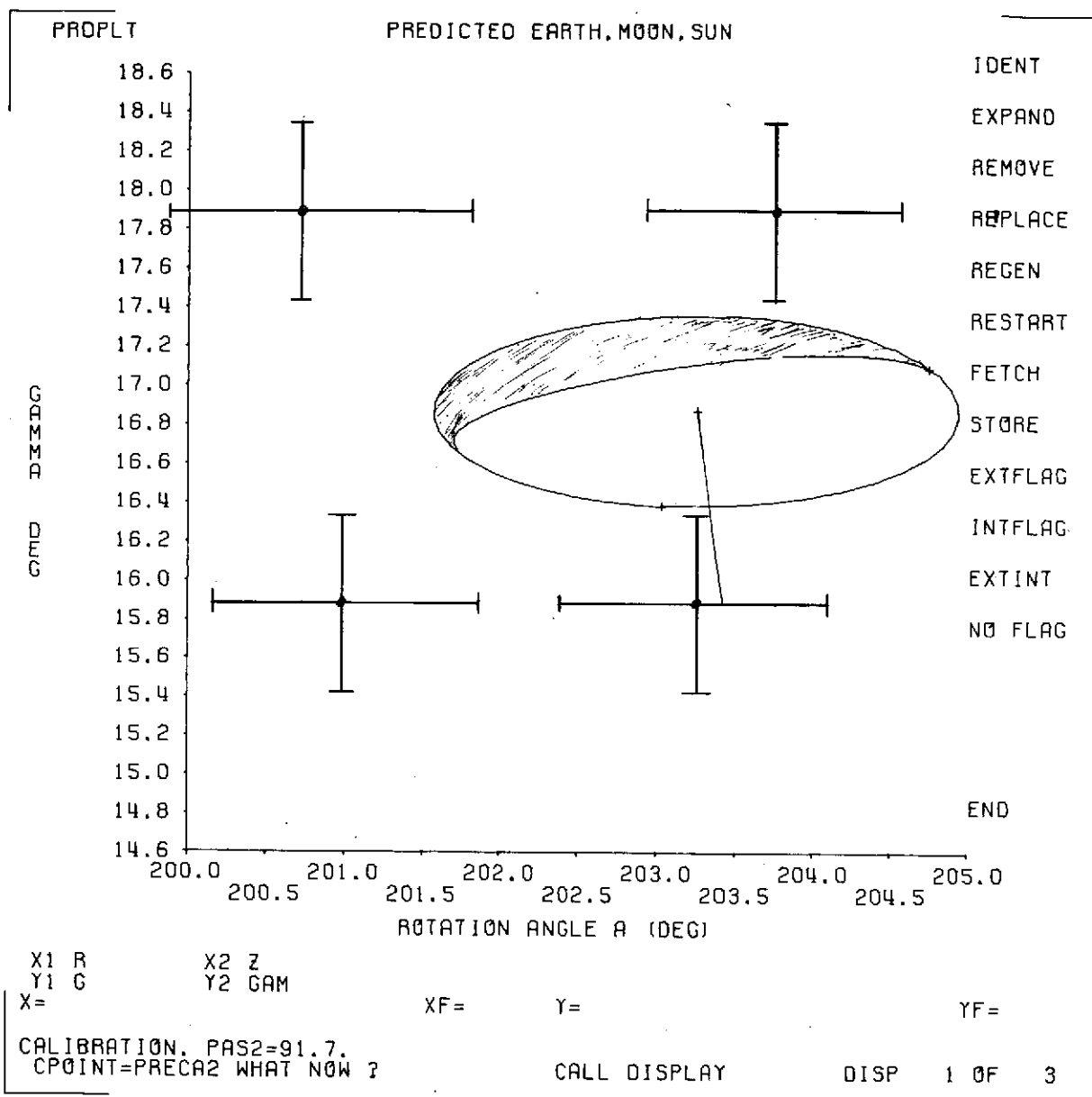


Figure 3-13. Moon Data, 1.7-Degree PAS2 Zero Bias

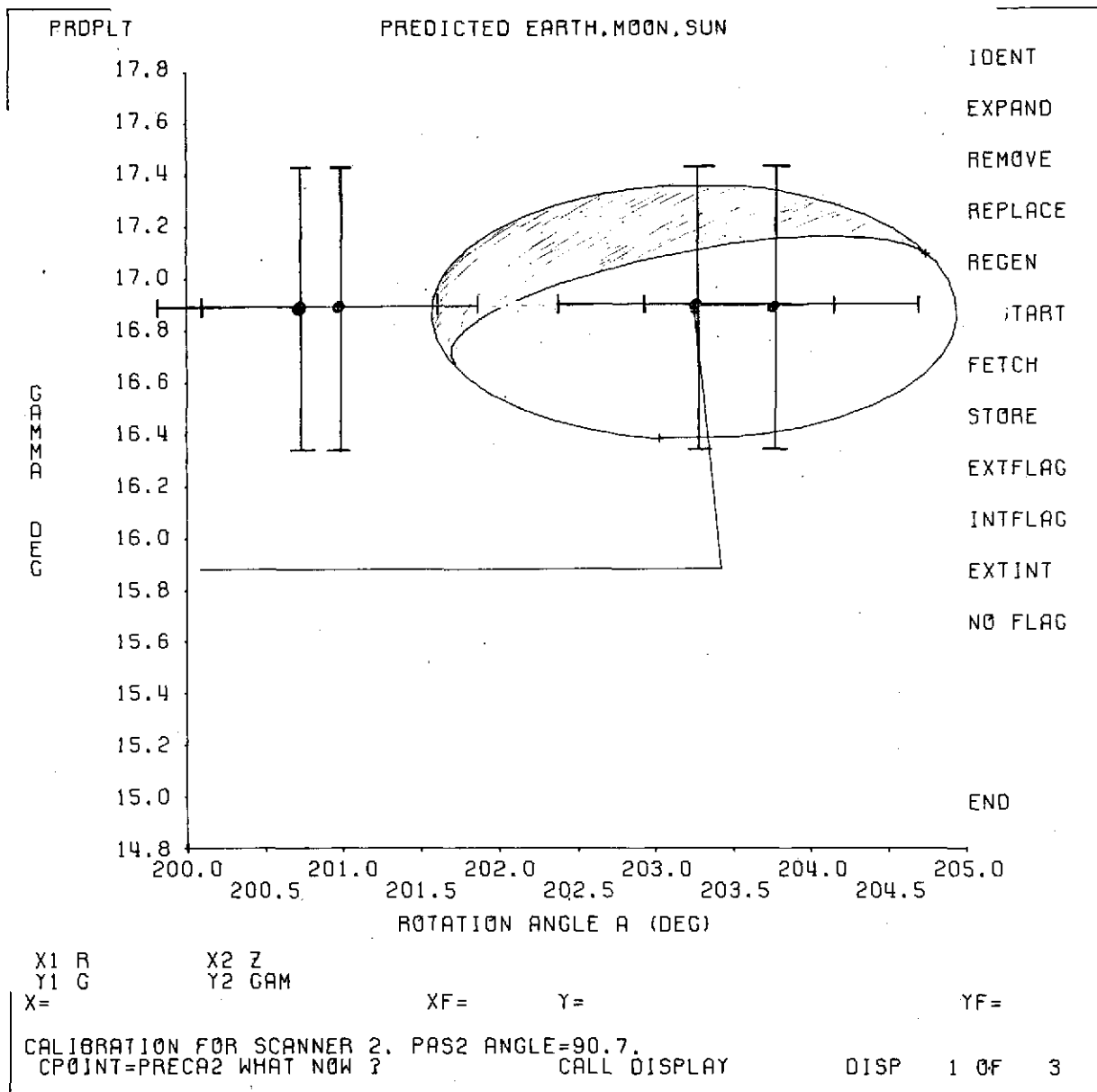


Figure 3-14. Moon Data, 0.7-Degree PAS2 Zero Offset

bars about the four PAS transitions in the figures. In light of the ± 0.85 -degree resolution of the scanners the bias was estimated to be $+0.7$ degree ± 0.4 degree. Although it would appear from the previous figures that there is a dihedral angle bias of approximately 1 degree, it should be noted that this is not significant compared to the 1.3-degree dihedral angle resolution. A series of Moon sightings between 1604 and 1710 GMT was used to check the dihedral angle bias. The MOD3 double-cross solutions, which are independent of the dihedral angle (cones intersection assuming the radius of the Moon is negligible) and MOD2 double-cross solutions, which are independent of the nadir angle (using the dihedral angle and nadir angle from the Sun to the central body), are shown in Figure 3-15.

The averages are as follows:

<u>Solutions</u>	<u>α</u> (Degrees)	<u>δ</u> (Degrees)	<u>Standard Deviation</u> (Degrees)
MOD2	166.0	-12.0	0.4
MOD3	165.7	-12.6	0.1

It was concluded that the dihedral angle bias for PAS2-SAS(upper) was nominal. Note that a 1-degree uncertainty in the declination translates into a 3.2-degree uncertainty in the dihedral angle (see Figure 3-13).

At 1737 GMT the configuration was changed to PAS1-SAS(upper), and PAS1 was found to be acquiring a target independent of the encoder angle as illustrated in Figure 3-16. A target was observed on all steps, including the poles. It was observed that whenever the projection of the Sun vector on the spacecraft equatorial plane was within 0 degree ± 15 degrees or 180 degrees ± 15 degrees of the PAS1 scan plane (see Figure 3-1), a Sun image would be observed independent of the encoder angle. As a consequence of the PAS1 malfunction, the

```

*****
**** M S A D *****
**** D I S P L A Y ***** 73.240.17.15.42 ****
**
** CBLRES DOUBLE CROSS SOLUTIONS **
**
** IDBL - DBLCRS IND. (NC,MOD1,MOD2,MOD3) MOD1 **
**
** IWEGHT - WEIGHTING OPT. (1-SFIN,2-ARC) 1 **
** TRMCHK-HORIZON CHECK(0-H,1-H+U,2-ALL) 1 **
** CBWID - MIN. RHO FOR TRMCHK (DEG) 0.500 **
**
** BLOCK REFERENCE TIME (YYDDD) 73161 **
**
** BLOCK LIMITS - ICUT1 1 **
** ICUT2 12 **
**
** F TIME C H SUN SCL. ONE SOL. TWO R NO. **
** L HMMSS B T BETA GAMMA ALPHA1 DELTA1 WGT1 ALPHA2 DELTA2 WGT2 F SOL **
** 160431 M T 92.4 31.6 166.03 -11.84 0.07 165.28 -13.55 0.04 2 **
** 160736 M T 92.4 31.6 165.83 -12.30 0.03 165.39 -13.30 0.04 2 **
** 163459 M T 92.4 30.9 166.39 -11.00 0.07 165.60 -12.82 0.04 2 **
** 165137 M T 92.4 30.9 165.97 -11.57 0.04 165.49 -13.02 0.04 2 **
** 165442 M T 92.4 30.9 165.69 -12.62 0.17 999.00 999.00 0.0 * 1 **
** 171003 M T 92.4 30.9 165.71 -12.57 0.05 165.24 -13.65 0.05 2 **
**
*****
**** M S A D *****
**** D I S P L A Y ***** 73.240.17.16.17 ****
**
** CBLRES DOUBLE CROSS SOLUTIONS **
**
** IDBL - DBLCRS IND. (NC,MOD1,MOD2,MOD3) MOD2 **
**
** IWEGHT - WEIGHTING OPT. (1-SFIN,2-ARC) 1 **
** TRMCHK-HORIZON CHECK(0-H,1-H+U,2-ALL) 1 **
** CBWID - MIN. RHO FOR TRMCHK (DEG) 0.500 **
**
** BLOCK REFERENCE TIME (YYDDD) 73161 **
**
** BLOCK LIMITS - ICUT1 1 **
** ICUT2 12 **
**
** F TIME C H SUN SCL. ONE SOL. TWO R NO. **
** L HMMSS B T BETA GAMMA ALPHA1 DELTA1 WGT1 ALPHA2 DELTA2 WGT2 F SOL **
** 160431 M T 92.4 31.6 351.43 -13.28 0.65 165.87 -12.21 0.04 2 **
** 160736 M T 92.4 31.6 351.33 -13.07 0.66 165.57 -11.58 0.04 2 **
** 163459 M T 92.4 30.9 351.45 -13.34 0.66 166.00 -11.50 0.05 2 **
** 165137 M T 92.4 30.9 351.63 -12.74 0.66 165.53 -12.07 0.05 2 **
** 165442 M T 92.4 30.9 351.57 -12.60 0.67 165.99 -11.92 0.05 2 **
** 171003 M T 92.4 30.9 351.69 -13.89 0.66 165.95 -12.02 0.05 2 **
**
*****
**** M S A D *****
**** D I S P L A Y ***** 73.240.17.13.53 ****
**
** CBLRES DOUBLE CROSS SOLUTIONS **
**
** IDBL - DBLCRS IND. (NC,MOD1,MOD2,MOD3) MOD3 **
**
** IWEGHT - WEIGHTING OPT. (1-SFIN,2-ARC) 1 **
** TRMCHK-HORIZON CHECK(0-H,1-H+U,2-ALL) 1 **
** CBWID - MIN. RHO FOR TRMCHK (DEG) 0.500 **
**
** BLOCK REFERENCE TIME (YYDDD) 73161 **
**
** BLOCK LIMITS - ICUT1 1 **
** ICUT2 12 **
**
** F TIME C H SUN SCL. ONE SOL. TWO R NO. **
** L HMMSS B T BETA GAMMA ALPHA1 DELTA1 WGT1 ALPHA2 DELTA2 WGT2 F SOL **
** 160431 M T 92.4 31.6 165.64 -12.72 0.15 999.00 999.00 0.0 1 **
** 160736 M T 92.4 31.6 165.60 -12.81 0.15 999.00 999.00 0.0 1 **
** 163459 M T 92.4 30.9 165.98 -11.94 0.14 999.00 999.00 0.0 1 **
** 165137 M T 92.4 30.9 165.72 -12.54 0.16 999.00 999.00 0.0 1 **
** 165442 M T 92.4 30.9 165.68 -12.63 0.16 999.00 999.00 0.0 1 **
** 171003 M T 92.4 30.9 165.47 -13.13 0.18 999.00 999.00 0.0 1 **
**
** CPOINT=OBLCRO WHAT NGW CALL DISPLAY DISP 1 OF 1 **
**
*****
**** M S A D *****
**** D I S P L A Y *****

```

Figure 3-15. Double-Crossing Solutions (MOD1, MOD2, and MOD3)

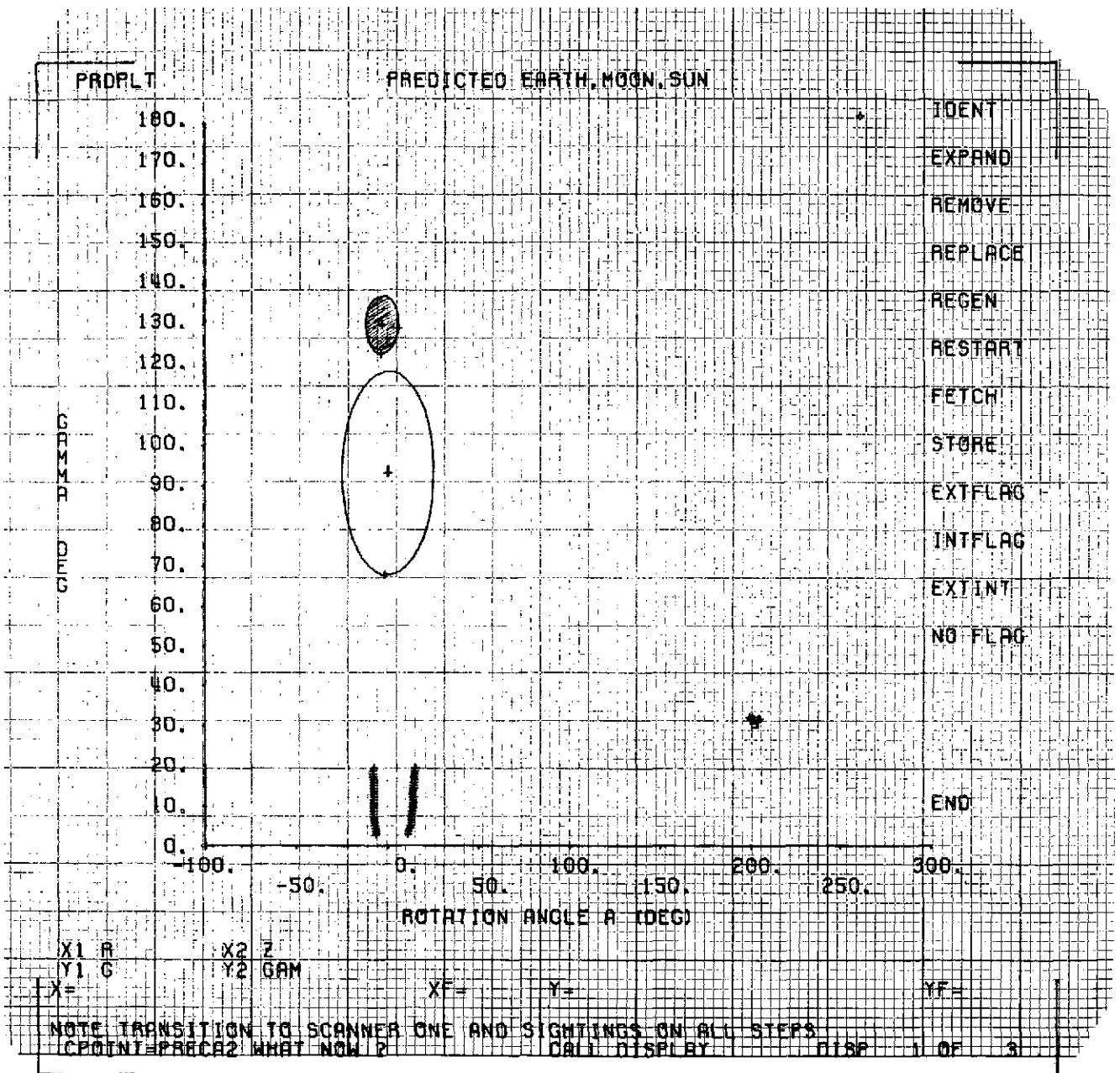


Figure 3-16. PAS1 Malfunction

following severe limitations were placed on the attitude system using this scanner:

1. A large region of phase space, approximately 40 percent, was completely inaccessible for target acquisition.
2. As a result of the electronic logic which recorded only the first AOS and LOS for a given scan, a valid target had to be acquired before the scanner saw the Sun. The range of valid dihedral angles was found to be

<u>Range</u>	<u>Configuration</u>
$63 < A < 165$	PAS1-SAS; $\gamma > 0$
$243 < A < 345$	PAS1-SAS; $\gamma < 0$
$90 < A < 165$	PAS1-PAS; $\gamma > 0$
$270 < A < 345$	PAS1-PAS; $\gamma < 0$

3. The automatic stepping logic (no target in view) was inoperative, and extensive use of the manual advance was required.
4. Bias determination for PAS1 was greatly hindered by the lack of data for negative mounting angles.

Because of the problems encountered, the attempt to calibrate PAS1 was abandoned, and the configuration PAS2-SAS was selected at 1900 GMT. After several maneuvers to calibrate the ACS, the configuration PAS2-PAS was selected, and an attempt to determine biases was made. Because the PAS2 Sun slit was found to be tilted during the May alignment and this was not provided for, the resulting dihedral angle bias would be dependent upon the angle γ . In any event, the determination of any dihedral angle biases during the translunar phase was extremely difficult because of the Moon's nadir angle as shown in Figure 3-17. Note that a 1-degree uncertainty in the spacecraft declination is equivalent to a 5-degree uncertainty in dihedral angle bias; or equivalently,

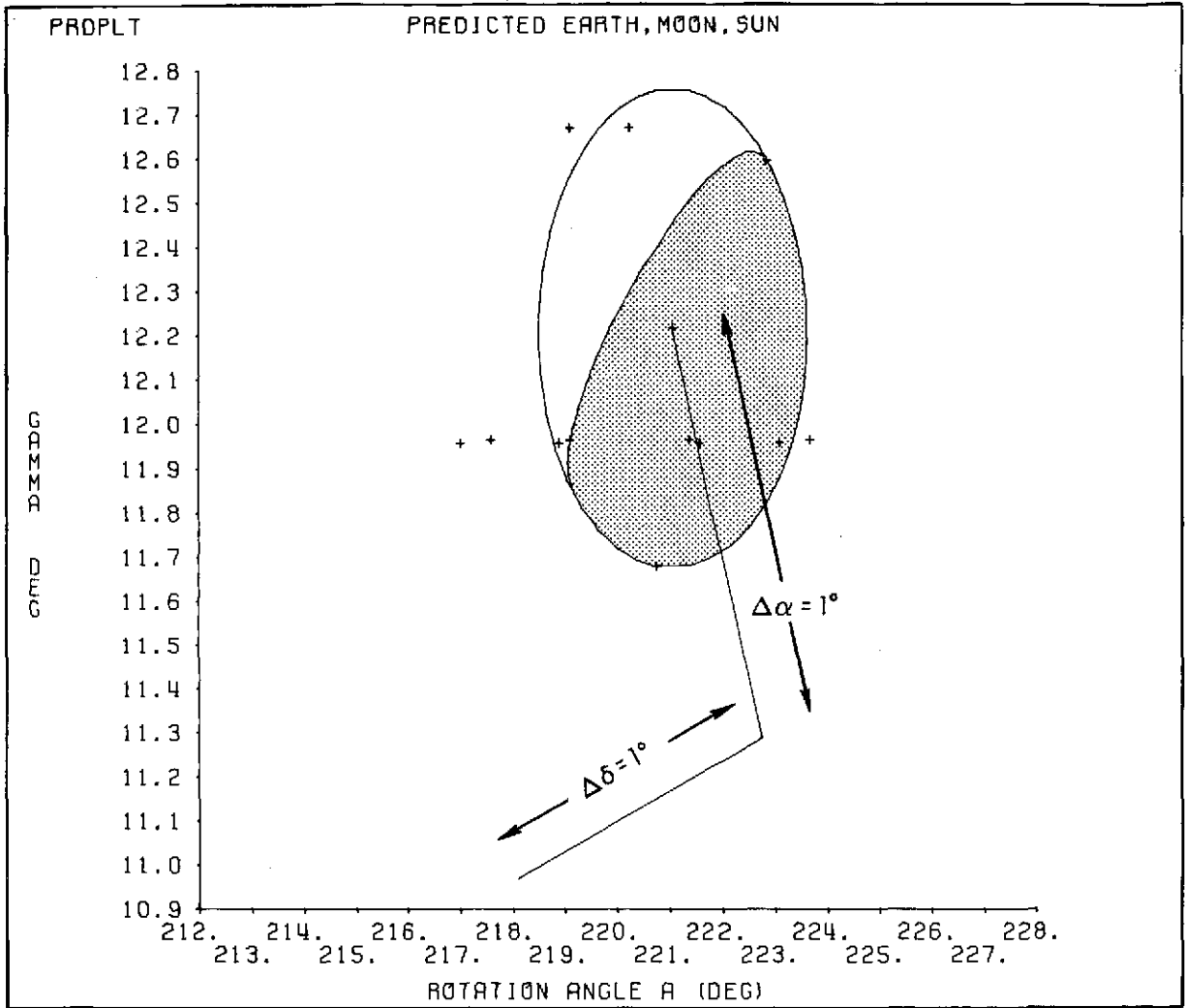


Figure 3-17. Attitude Determination Off Moon

to determine a 1-degree dihedral bias one would need an independent attitude measurement good to 0.2-degree accuracy. Clearly such precision was not possible in light of the Sun and PAS sensor resolution.

No further attempts at bias determination were made and only periodic checks of sensor performance and spacecraft attitude were planned until just prior to lunar insertion at 0400 GMT on June 15. Figure 3-18 illustrates the peculiar behavior of PAS2 for positive and negative mounting angles at the edge of the effective Sun. This behavior was noted at launch in Figure 3-9. By symmetry, one would expect an equivalent sensor response for positive and negative angles because the geometry is equivalent except for a 180-degree rotation of the spacecraft (the zero bias was found to be less than 1 degree). The observed asymmetry suggests two following possible explanations for the PAS2 behavior:

1. The optical dome contains some deposit or reflecting property which differs for the eastern and western quadrants.
2. Reflections off the spacecraft trigger the PAS scanner. This behavior would be strongly dependent on the Sun angle.

A slow degradation of the PAS2 sensor performance became evident early on June 12, manifested by a further enlargement of the effective vertical (γ direction) Sun acceptance angle. Figure 3-19 shows the nominal behavior of PAS2 at 2145 GMT on June 11, and Figure 3-20 shows the response 22 hours later. This anomalous behavior consists in part of AOS and LOS counts independent of encoder angle; the apparent shift in Figure 3-21 from (-90 degrees and -10 degrees) to (+90 degrees and +170 degrees) is an artifact resulting from the sign change in encoder angle. The transitions near $A = 0$ and 180 degrees indicate a vertical Sun acceptance angle greater than ± 90 degrees, and may result from reflections within the scanner head. The transitions near $A = \pm 90$ degrees correspond to the PAS2 line of sight at the time the PAS2 Sun slit views the Sun,

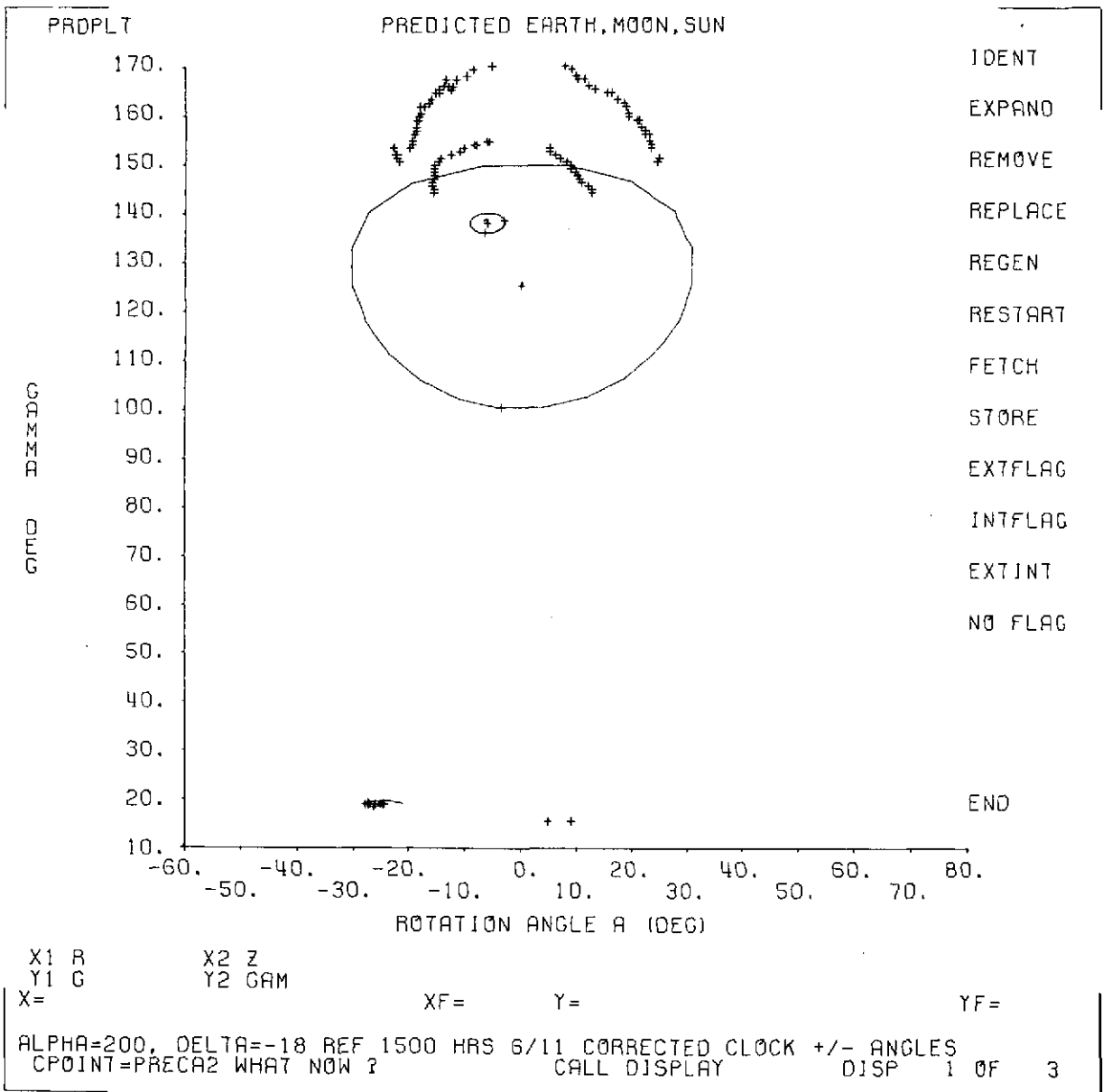


Figure 3-18. PAS2 Asymmetric Sun Acceptance for Positive and Negative Encoder Angles (1500 GMT on June 11) (1 of 2)

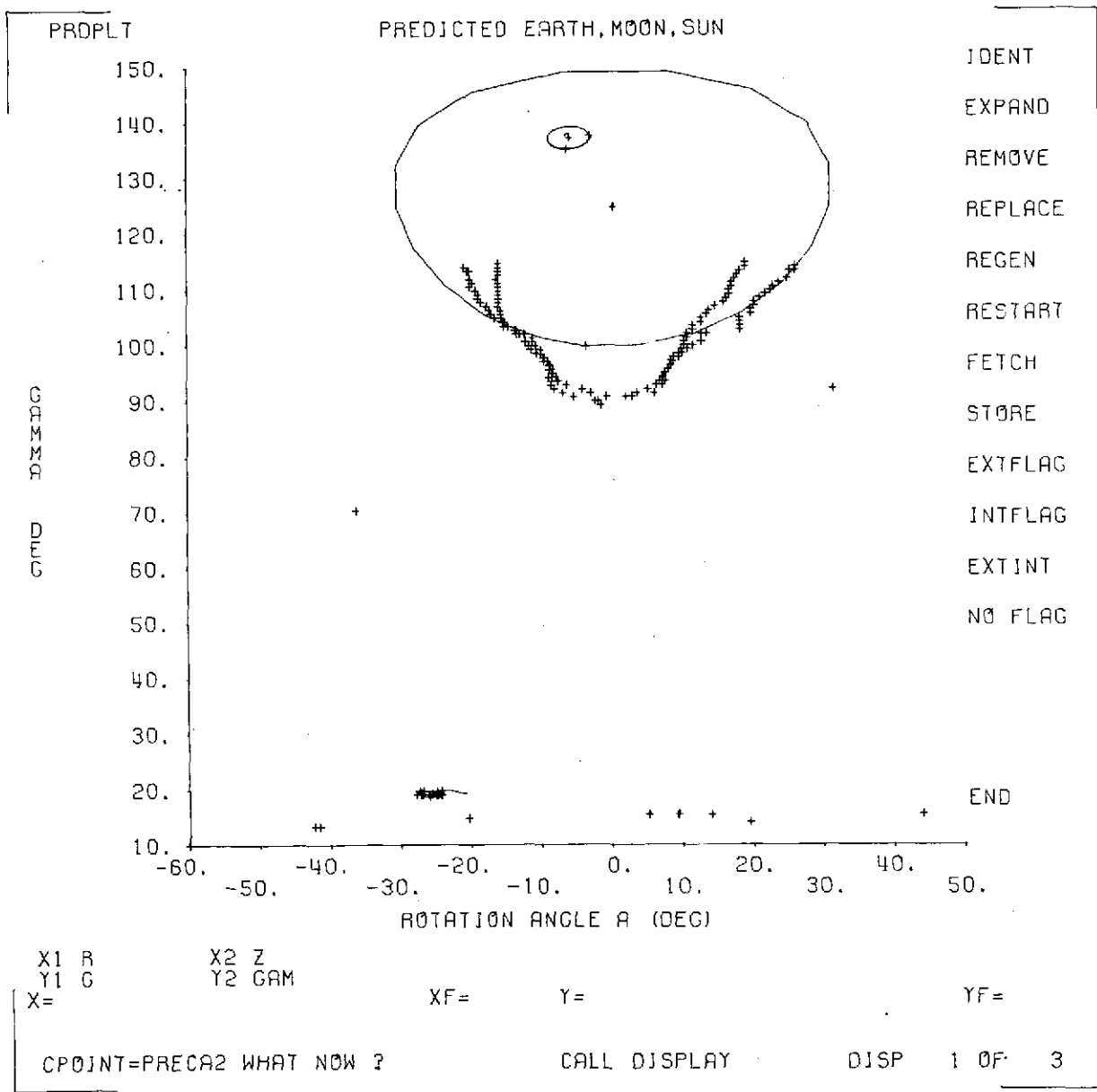


Figure 3-18. PAS2 Asymmetric Sun Acceptance for Positive and Negative Encoder Angles (1500 GMT on June 11) (2 of 2)

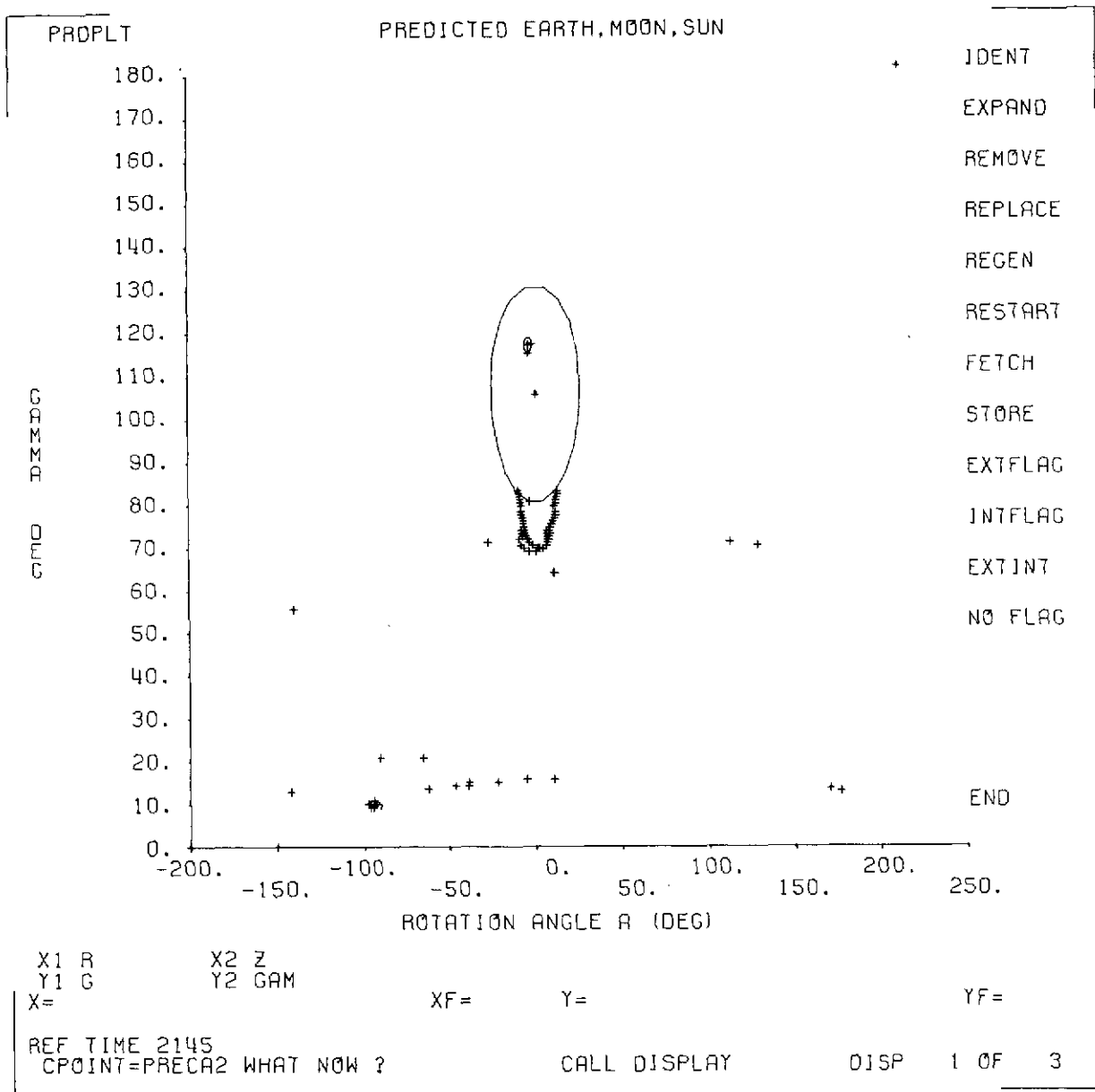


Figure 3-19. PAS2 Performance at 2145 on June 11

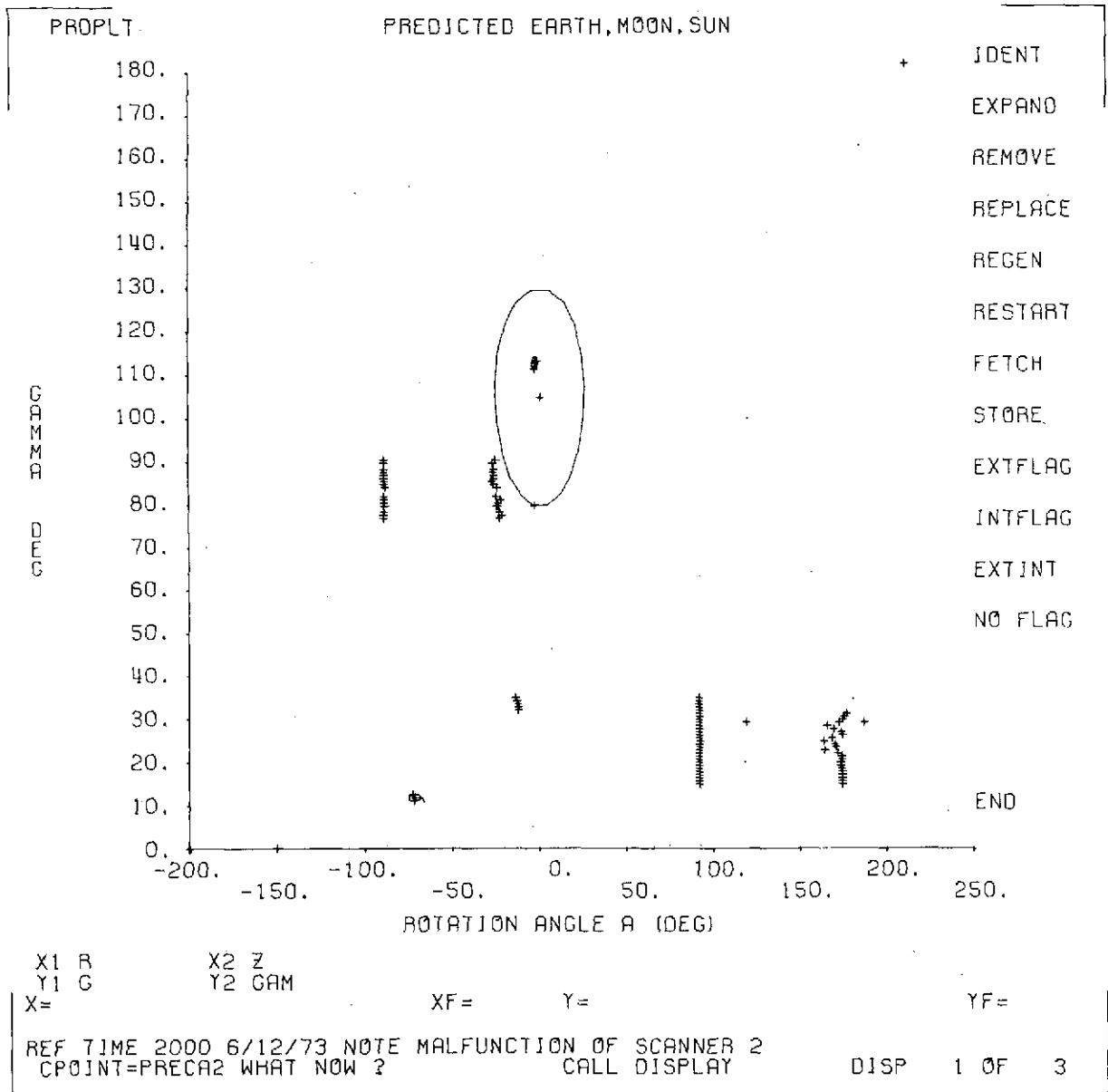


Figure 3-20. PAS2 Performance at 2000 on June 12

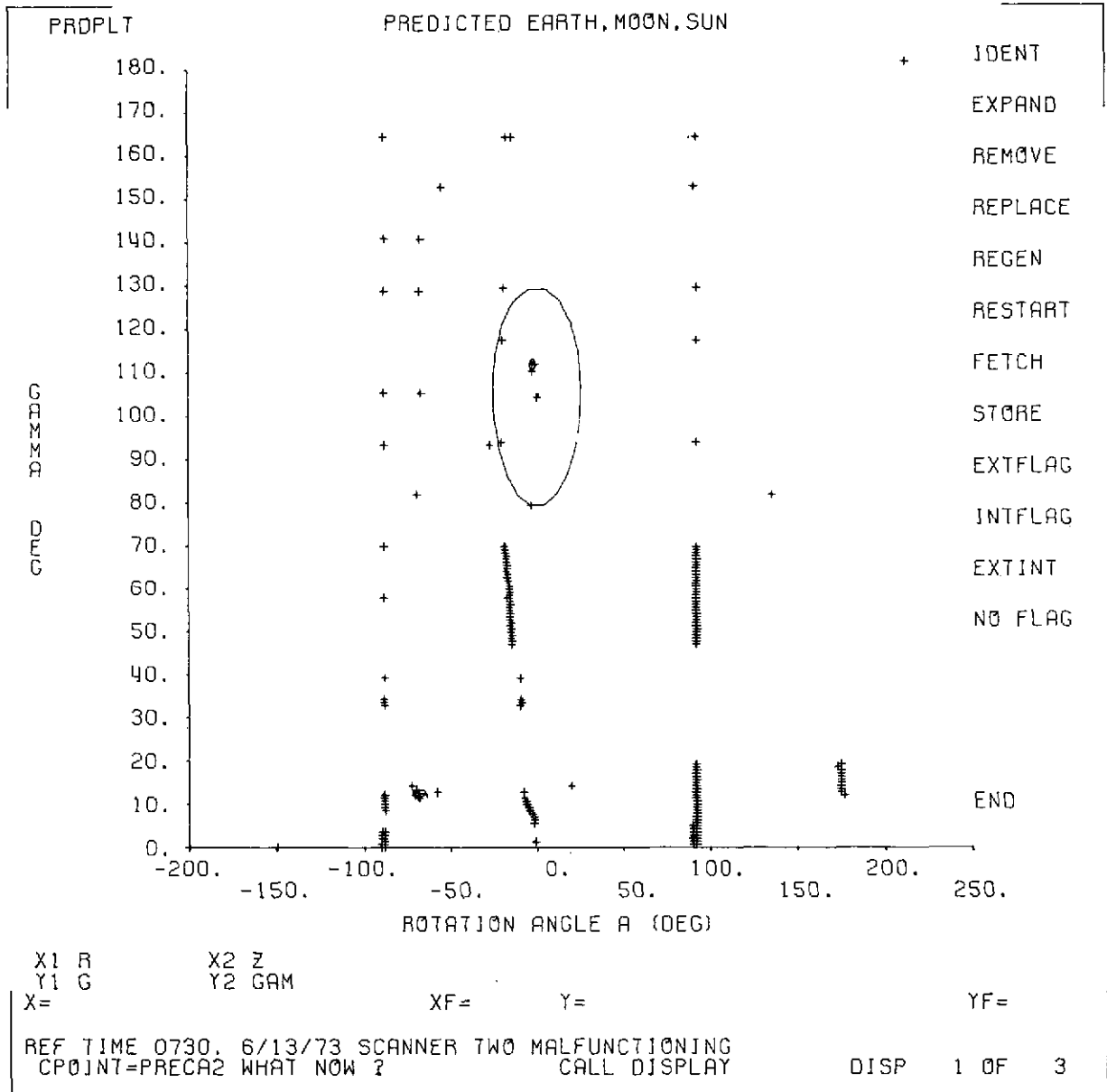


Figure 3-21. PAS2 Performance at 0730 on June 13

and are believed to arise from a coupling between the PAS2 solar gate and the PAS2 detector.

The scanner configuration was changed to PAS1-SAS(lower) at approximately 2000 GMT on June 14 for attitude determination prior to the critical lunar insertion VCS maneuver. This configuration was adequate for attitude determination for $63 \text{ degrees} < A < 165 \text{ degrees}$ and positive encoder angles. Figures 3-21 through 3-24 illustrate the attitude obtained prior to, and just after, the ACS trim maneuver to the lunar insertion attitude. The measured PAS1 zero bias of +2 degrees was used together with a PAS1 dihedral angle of 64.3 degrees in this figure. The nominal and aligned dihedral angles were 63 degrees. Note that although for this geometry the dihedral angle is observable (a 1-degree uncertainty in declination corresponds to approximately 1.7-degree dihedral angle uncertainty) other combinations of biases could also fit the observed data. At approximately 0220 GMT, the dihedral angle from the Sun to the lit lunar horizon became less than 64 degrees, and the PAS1 scanner initiated each scan on the lit Moon. As expected, the anomaly flag was set; the LOS register contained the dihedral angle of the lunar terminator; and the AOS register contained the terminator to Sun dihedral angle. Figures 3-25 and 3-26 indicate this geometry. Note that a dihedral angle of +65 degrees was observed, but that an expected AOS at 64.3 degrees was not observed. These observations tend to support the observed dihedral angle bias.

During the dipole calibration portion of the mission, June 20 through July 10, one orbit per day was devoted to attitude determination. Typically, a very crescent Moon was encountered during half of this orbit, and no reliable attitude results were obtained. This was partly a result of the small lit lunar area, but primarily because AOS was generally off the Sun and LOS off the lunar terminator. During the remaining half of the orbit, the Moon was nearly full and satisfactory attitude results were obtained. Figure 3-27 illustrates the favorable Earth-Moon geometry. The sensor configuration was PAS1-SAS (upper)

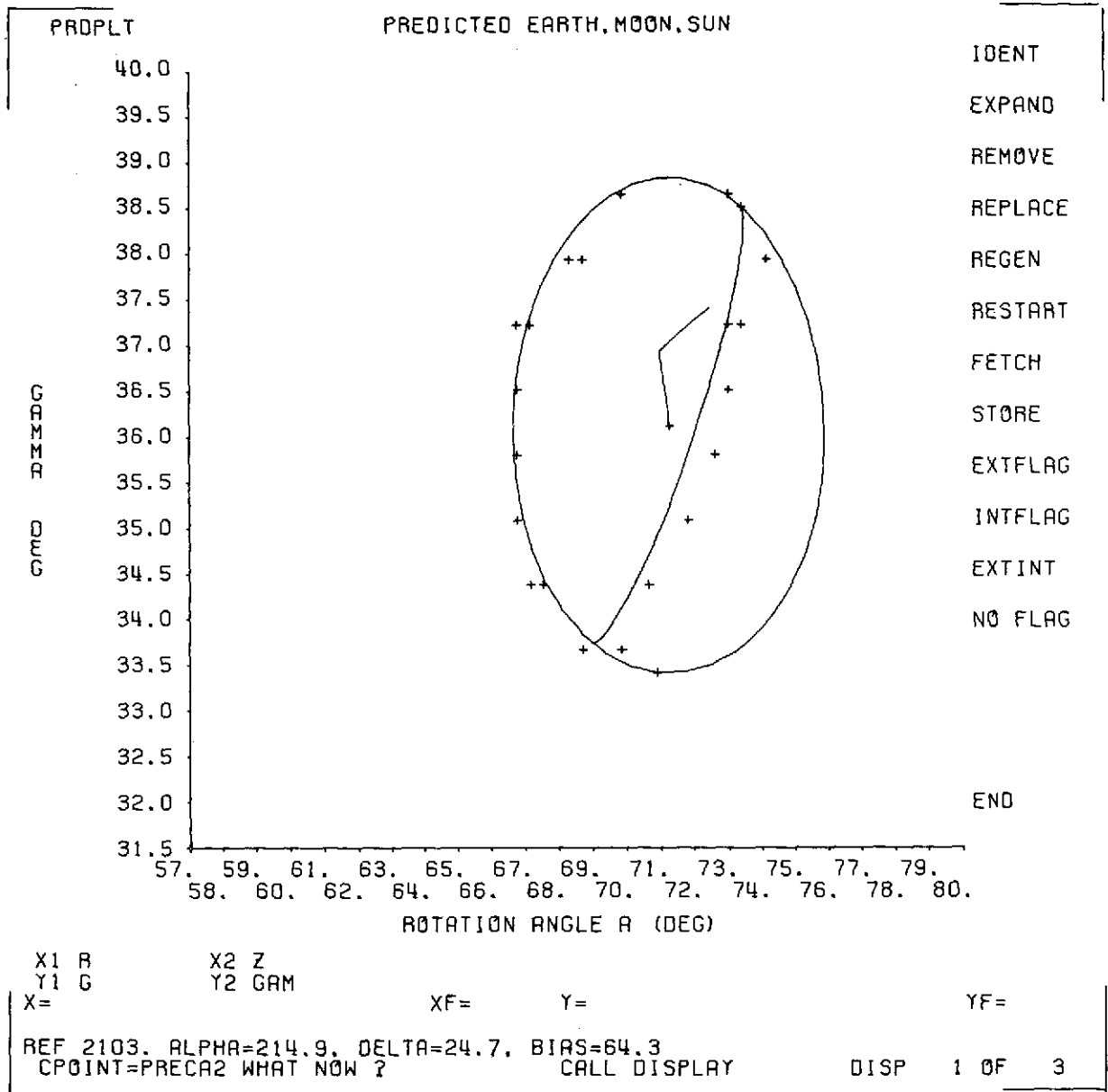


Figure 3-22. Attitude Determination Off Moon at 2103 GMT June 14
 Before Lunar Insertion Trim

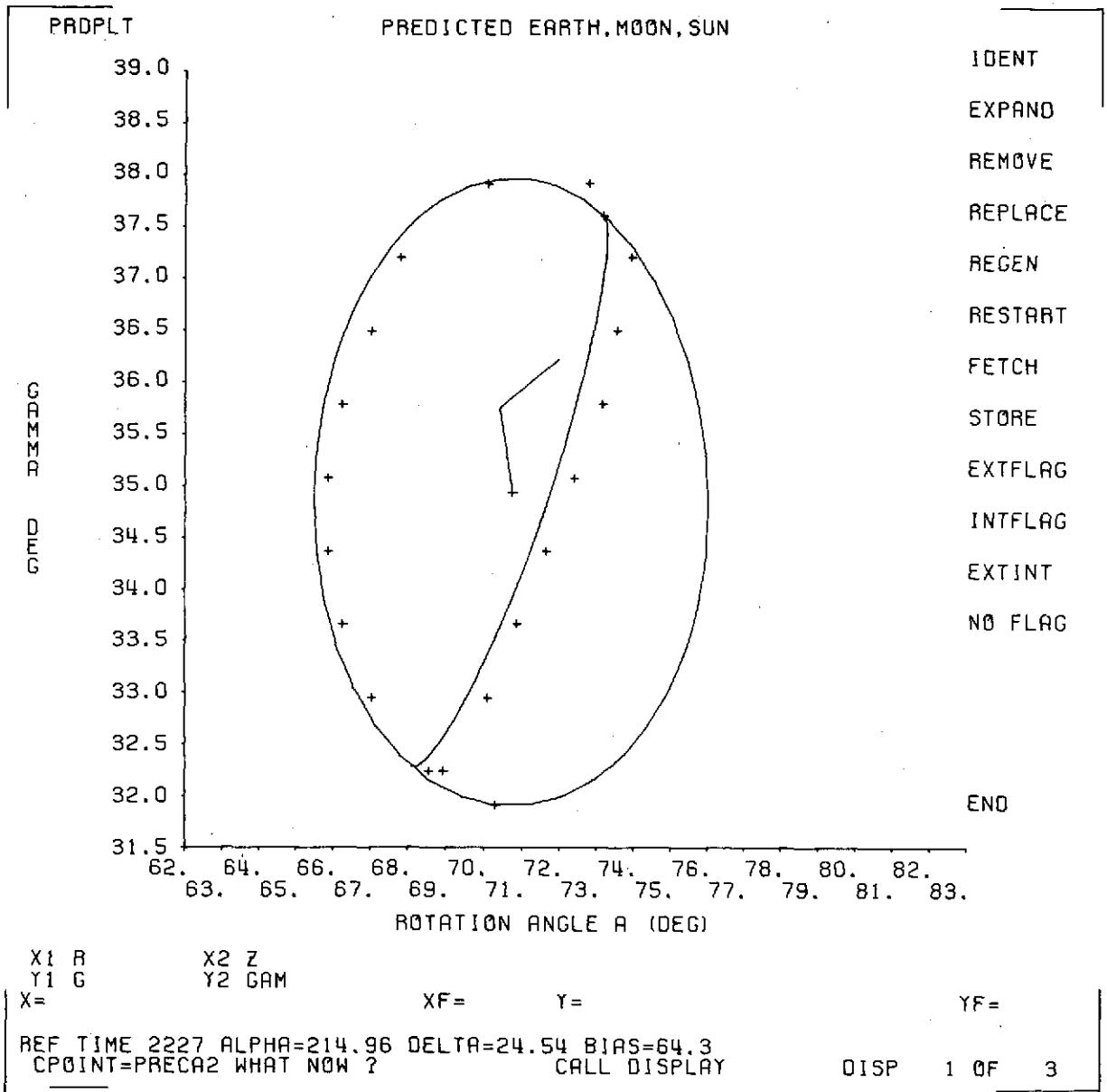


Figure 3-23. Attitude Determination Off Moon at 2227 GMT June 14
 Before Lunar Insertion Trim

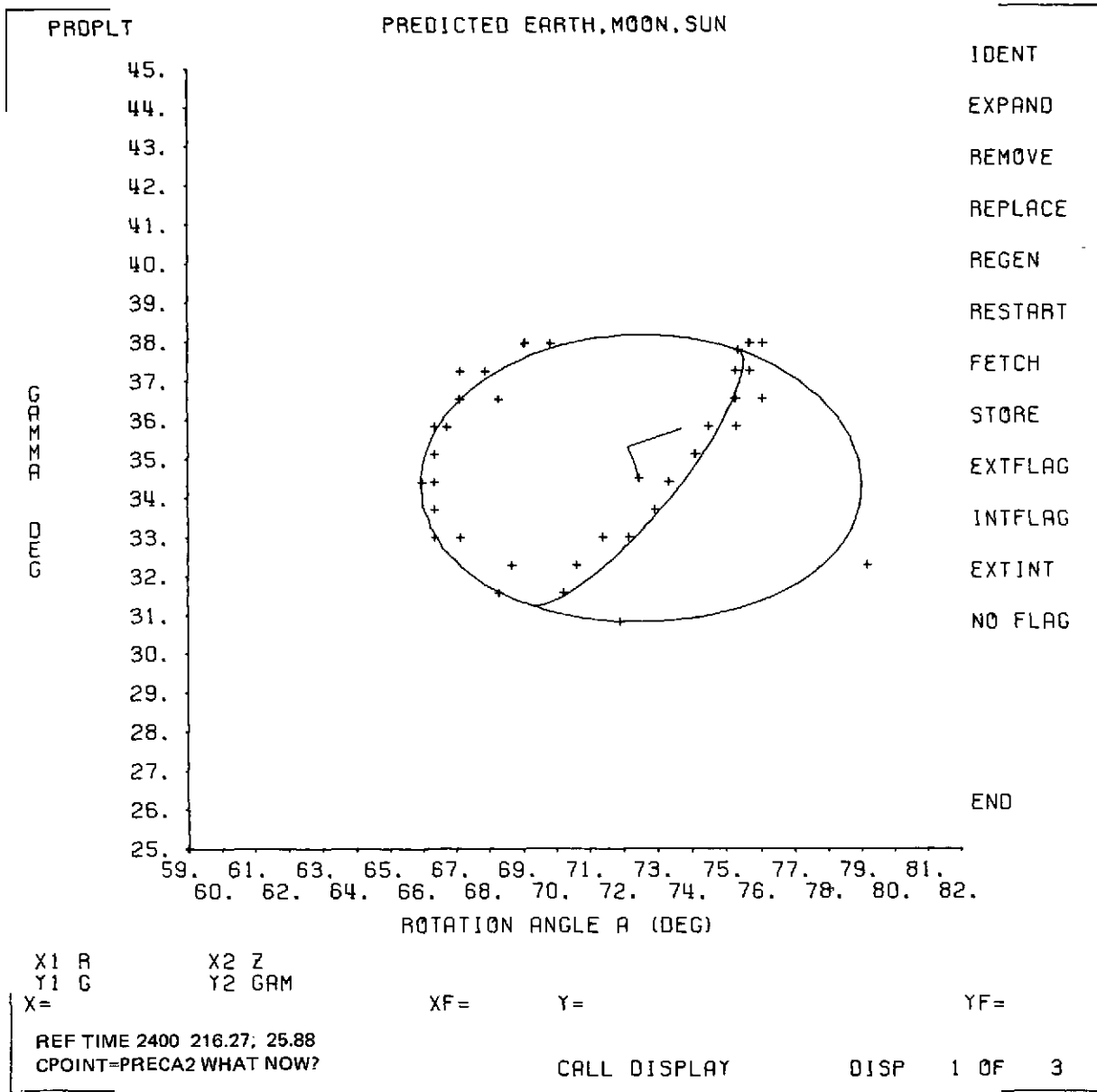


Figure 3-24. Attitude Determination Off Moon at 2400 GMT June 14 After Lunar Insertion Trim

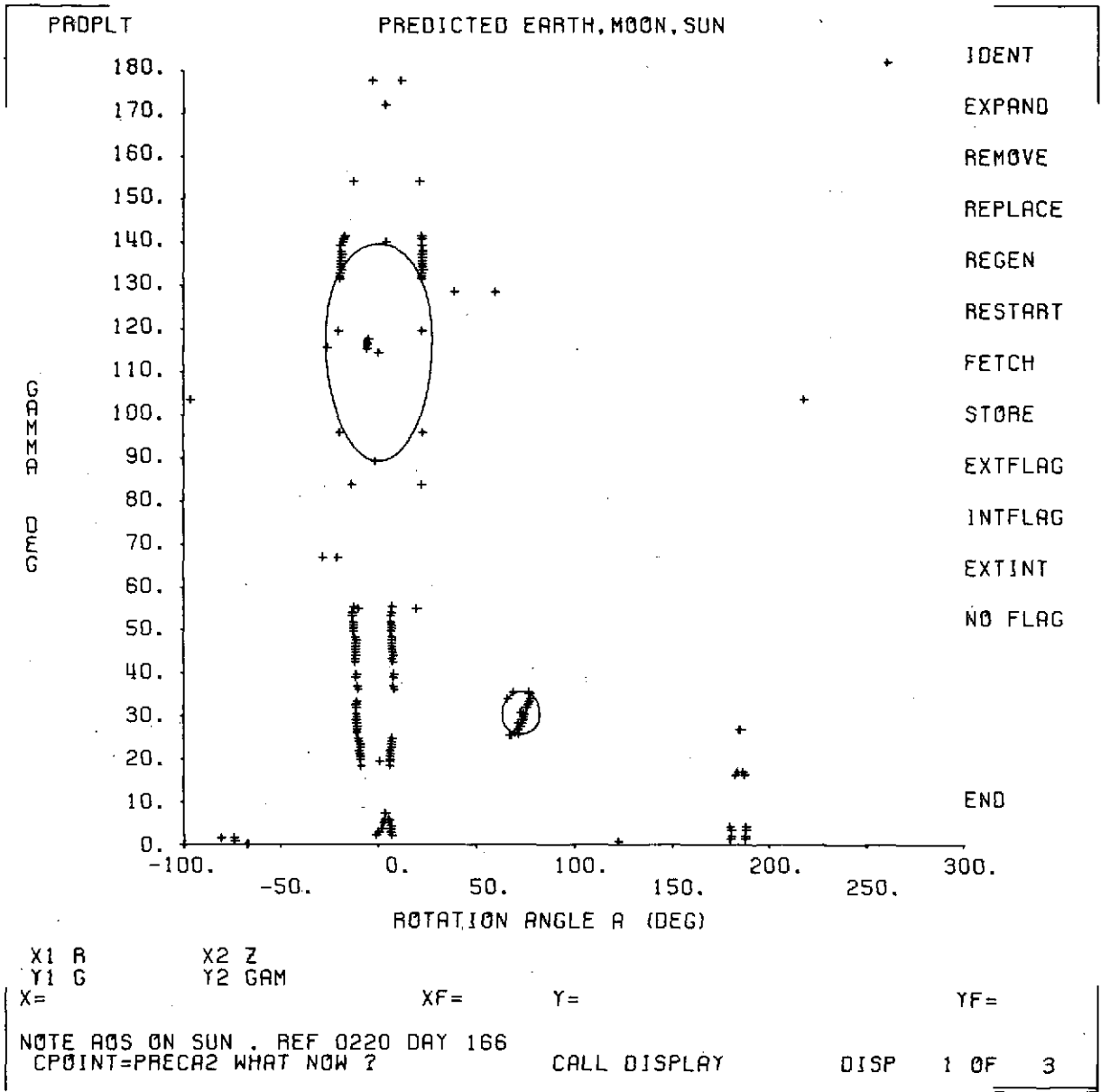


Figure 3-25. Geometry Prior to Lunar Insertion (First AOS Off Sun)

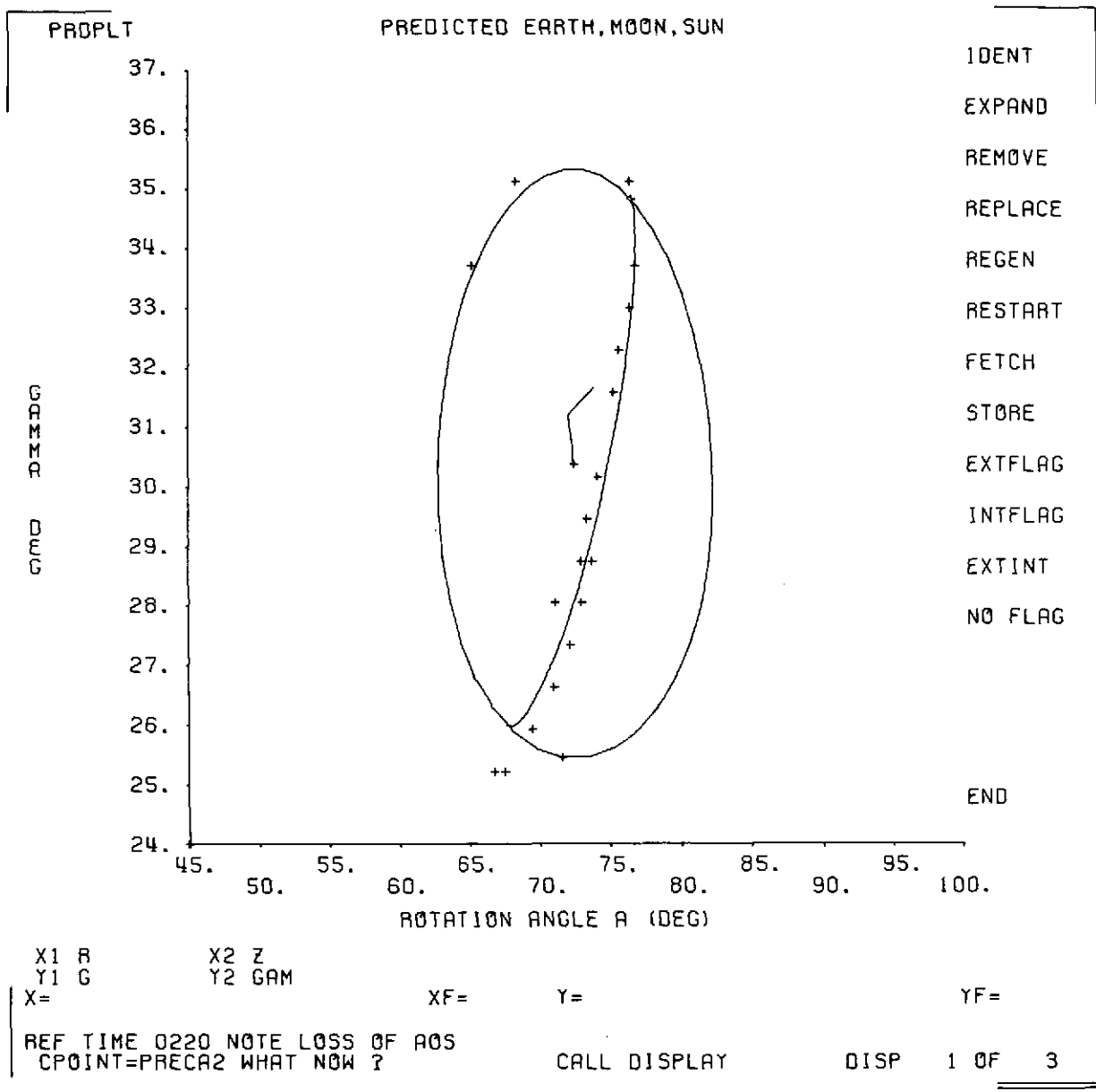


Figure 3-26. Graphical Attitude Determination Off Lunar Terminator

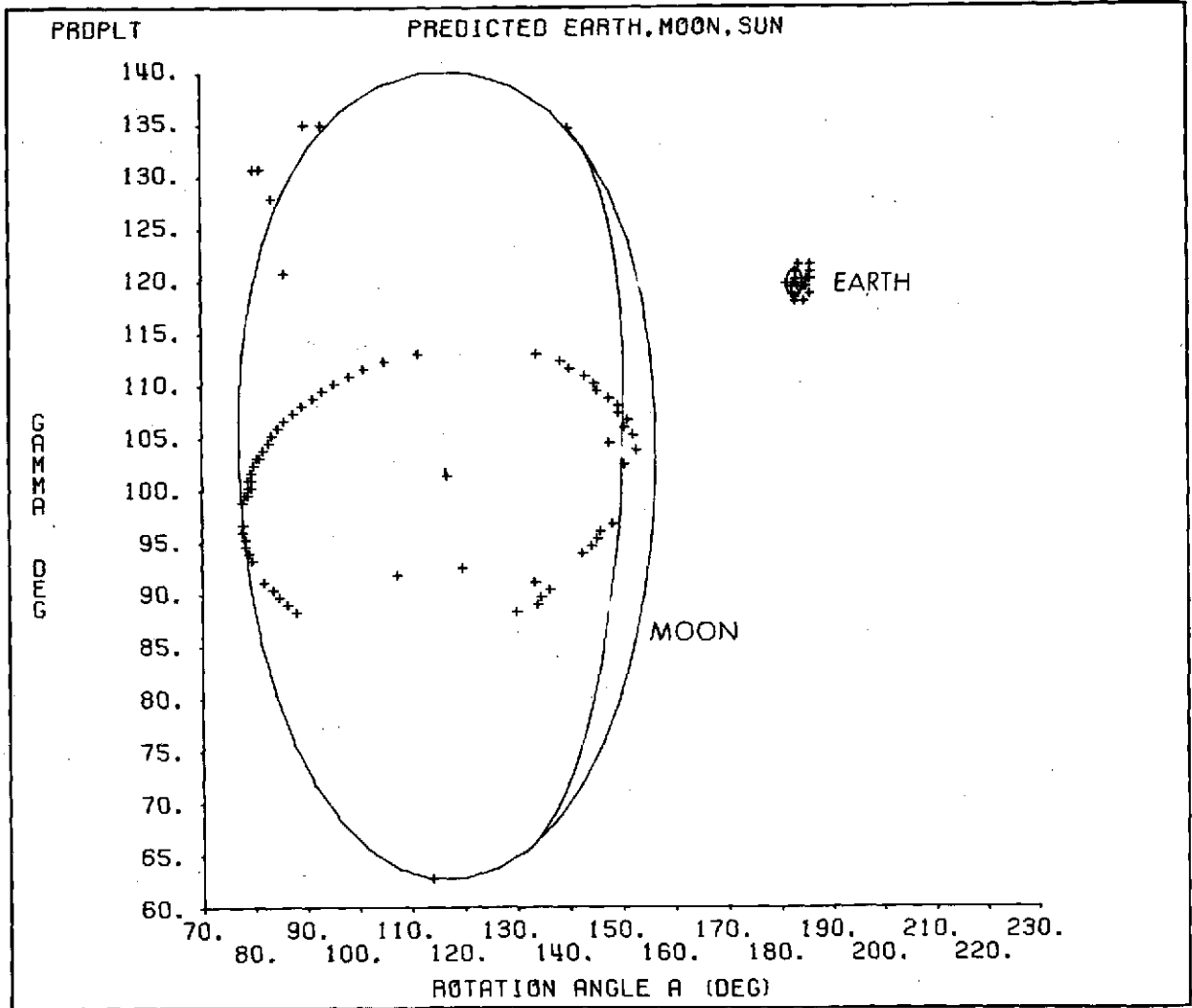


Figure 3-27. Central Body Geometry During Dipole Calibration

(Sun angle = 87.5 degrees) at 1356 GMT on June 28. Because the Earth was an acceptable small target, an attempt was made to investigate sensor biases. Use of MOD3 double cross implied an attitude of $\alpha = 5.9$ degrees and $\delta = 8.4$ degrees and a +3-degree dihedral angle bias. This was unacceptable because the attitude was in marked disagreement with the attitude obtained from Moon data and the bias was far greater than that indicated from earlier analyses and OABIAS results. Use of MOD2 double cross implied an attitude of $\alpha = 8.5$ degrees and $\delta = 2.4$ degrees and a -0.3-degree sensor zero (γ) bias. This result was within acceptable limits and is illustrated in Figure 3-28. The attitude using all Moon and Earth data was $\alpha = 7.9$ degrees and $\delta = 4.0$ degrees. It must be noted that the overall quality of the approximately 40 Moon samples was poor; a standard deviation of 5 degrees was obtained, and consequently the biases obtained are not unique.

Table 3-1 summarizes the biases obtained from spin-mode processing and includes the OABIAS results (Reference 5). It must be emphasized that only the PAS2 null direction of 90.7 degrees and to a lesser degree the biases in the Earth and Moon radii, can be regarded as definitive. In all other cases, the results obtained were constrained by assuming some other parameter or set of parameters were known. However, this set does adequately explain all observed spin-mode data.

3.3 ATTITUDE DETERMINATION SENSORS--PLANAR MODE

3.3.1 Prelaunch Specifications and Alignment

The RAE-B spacecraft uses the same PAS scanners in planar mode as in spin mode. Detailed information for the scanner's specifications and alignment can be found in Section 3.2.1. The major difference between spin and planar mode is in the mode of operation of the scanners. In the planar mode, either one of the two scanners receives a start pulse at frame time and begins a sweep at 100 steps per second in its scan plane from its nominal zero position in the

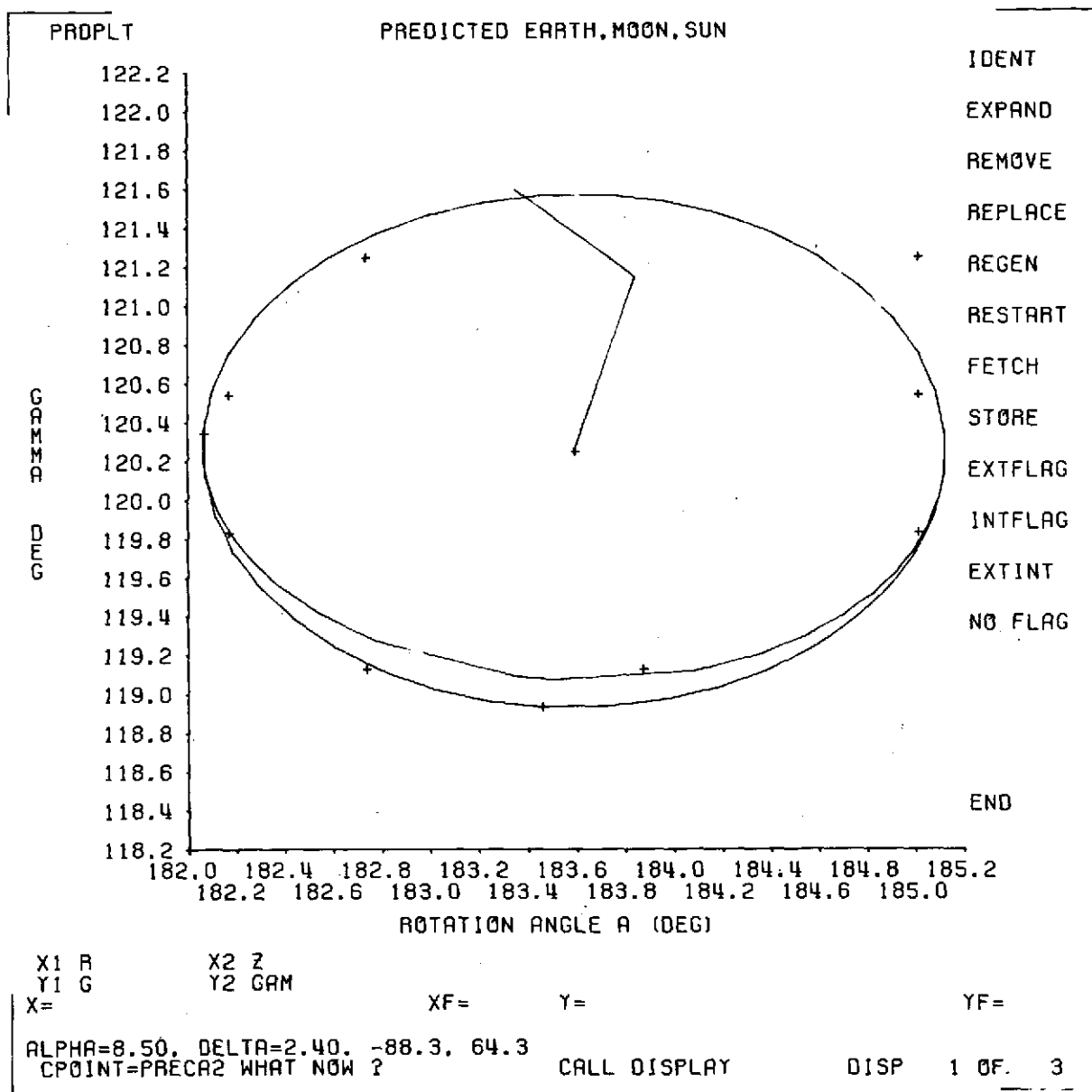


Figure 3-28. Attitude Determination Off Earth From Lunar Orbit

Table 3-1. RAE-B Biases--Spin Mode

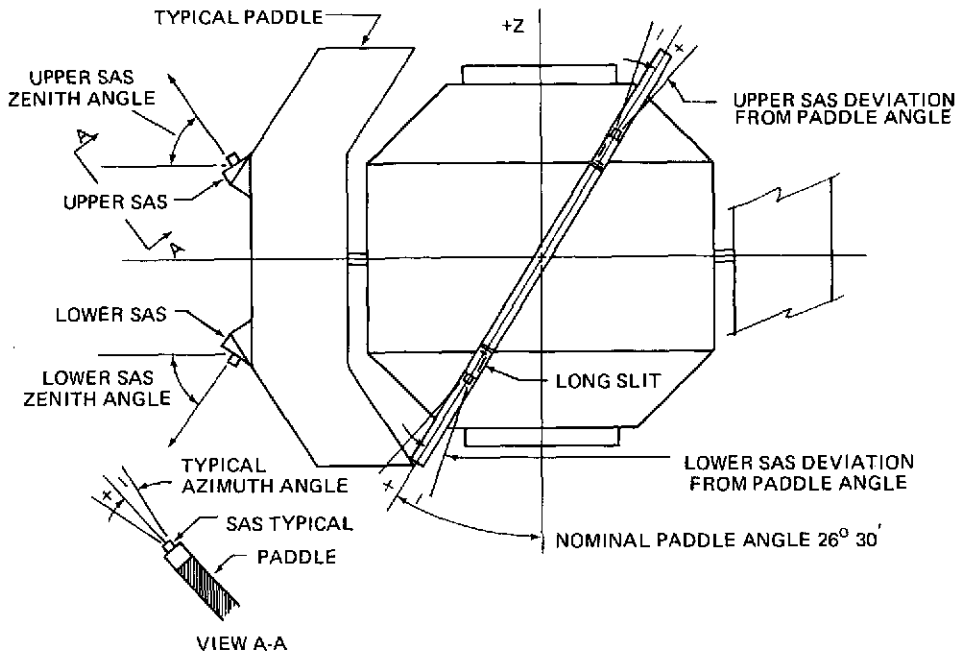
DESIGNATION		NOMINAL SPACECRAFT (DEGREES)	CALIBRATED SPACECRAFT (DEGREES)	OABIAS (DEGREES)	MAPS/RAE-B (DEGREES)	CONSENSUS (DEGREES)
RHOE:	BIAS IN EARTH RADIUS	0.0	0.0	0.30	0.3	0.3
RHOM:	BIAS IN MOON RADIUS	0.0	0.0	0.17		0.17
SASU:	+90° DIRECTION FROM +Z	+90.0	+90.15			90.15
SASL:	+90° DIRECTION FROM +Z	+90.0	+89.95			89.95
PAS1:	NULL DIRECTION FROM +Z	-90.0	-88.25		-88.3	-88.3
PAS2:	NULL DIRECTION FROM +Z	+90.0	92.00	90.7	90.7	90.7
SASU:	+90° DIRECTION FROM +X	0.0	0.75			0.75
SASL:	+90° DIRECTION FROM +X	0.0	0.0			0.0
PAS1:	NULL DIRECTION FROM +X	63.0	63.05	64.3	64.3	64.3
PAS2:	NULL DIRECTION FROM +X	297.0	297.05		297.05	297.05
PAS1:	SUN DIRECTION FROM +X	333.0	333.05			333.05
PAS2:	SUN DIRECTION FROM +X	207.0	207.05			207.05

spacecraft X-Y plane. The sweep continues for 512 steps or 5.12 seconds, terminating at the scanner zero position. The circuit registers onboard the spacecraft record the number of counts from the start position to the first AOS and to the last LOS. The scan takes place during an even, or SAS, telemetry frame and is held until the next, or odd (PAS), telemetry frame at which time the scanner identification and counts are read out as telemetry data. Two other bits of information are recorded and sent in telemetry. If the sensor was off the zero position when the scan was initiated, a telemetry flag is set indicating this. Also, if the first four consecutive steps after scan start indicate a lit target, an anomaly flag is set. Once the sequence is complete the alternate scanner is selected, and at the next frame time the scan procedure is repeated.

The solid mode Sun sensors onboard the RAE-B spacecraft are distinct from and operate in a different manner than the spin mode SAS sensors. Reference 6 presents detailed information on the specifications and operation of the SAS solid mode sensors. Final alignment measurements were taken shortly prior to launch and Figure 3-29 presents a summary of these measurements. Eight solid mode SAS sensors (labeled 1 through 8) are mounted two on each paddle. Paddle A contains sensors 1 and 2; sensor 1 is mounted so that its viewing range is predominantly in the upper hemisphere of the spacecraft body coordinate system, and sensor 2 is mounted so that its viewing range is predominantly in the lower hemisphere. Sensor pairs 3-4, 5-6, and 7-8 are mounted similarly on paddles B, C, and D, respectively.

The eight sensors are scanned sequentially from 1 through 8. The scan is started by the positive going transition of a sample pulse. As each sensor is scanned, the magnitude of the output voltage is compared with the sum of the output voltages from all eight sensors. When these two compared voltages are equal to each other and exceed a reference voltage, the scan process is terminated. Then, the two 7-bit Gray-coded numbers (N_a and N_b), plus the sensor

DATE OF ALIGNMENT: 5-11-73
HANGER "S"



PADDLE	SENSOR	ZENITH ANGLE (RELATIVE TO PADDLE EDGE)	AZIMUTH ANGLE	DEVIATION FROM PADDLE ANGLE (LONG SLIT RELATIVE TO PADDLE ANGLE)
A	LOWER SAS	35° 50'	-0° 30'	0° 0'
A	UPPER SAS	35° 59'	+0° 21'	-0° 8'
D	UPPER SAS	35° 40'	-0° 12'	-0° 16'
D	LOWER SAS	35° 22'	+0° 12'	-0° 16'
C	LOWER SAS	35° 36'	-0° 30'	-0° 24'
C	UPPER SAS	35° 46'	+0° 30'	-0° 6'
B	UPPER SAS	35° 18'	+0° 15'	+0° 7'
B	LOWER SAS	35° 30'	-1° 5'	0° 0'

Figure 3-29. Summary of RAE-B Solid Angle Sensor (SAS) Alignment Checks

number, are gated into and held in a shift-count register for later readout into the telemetry stream. If no sensor is selected, the sensor number portion of the register should contain a value of either 9 or 11, and the contents of the N_a and N_b portion of the register are unreliable. The scan nominally occurs at the beginning of every even telemetry frame and takes approximately 80 milliseconds, each sensor being interrogated for approximately 10 milliseconds.

3.3.2 PAS Hardware Malfunctions

The large Sun acceptance angle noted in spin mode continued to be a problem in planar mode. The impact is to some extent minimized by the fact that in planar mode the scan is nearly in a plane containing the spacecraft Z-axis. When the dihedral angle about the Z-axis between the Sun vector and the PAS rotation axis is less than approximately 60 degrees, little or no Sun interference is expected; whereas in spin mode, a Sun transition is expected on every scan, and only the scanner acquisition logic allows other transitions to be seen.

Another malfunction was noted, relating to scanner selection. Nominally, alternate scanners are selected for alternate PAS frames. However, long sequences occur in telemetry in which scanner 1 appears in every PAS frame. The anomaly flag is always set in these frames. Usually the associated AOS and LOS do not yield calculated attitudes. These sequences occur when Sun sightings by scanner 1 are expected, and may be related to the Sun sightings. Data loss results because scanner 2 would not be expected to see the Sun at the same time as scanner 1.

3.3.3 SAS Hardware Malfunctions

During the dipole calibration phase of the mission, the spacecraft was operated for extended periods at 4.706(4.7) and 3.062(3.1) rpm. The attitude sensors were periodically operated in spin mode to monitor spin axis attitude, but were operated in planar mode most of the time to obtain Sun angle data from which phase (rotation) angle information could be derived. Though the spin rate was

higher than that for which the sensors were designed, it was anticipated that there would be a consequent loss of accuracy, but an acceptably accurate phase angle could nonetheless be calculated. However, this was not the case; the data as received could not be processed with the attitude system.

The nominal sensor data permit calculation of the Sun vector right ascension and declination in body coordinates. The actual data was of two types: (1) a valid sensor identification with the values of N_b and N_a inconsistent with the Sun declination angle (known from spin mode measurements); and (2) a sensor identification of nine with values of N_b and N_a generally consistent with the Sun declination angle.

Although there was no clear indication that the malfunction was spin-rate dependent, the sensors began to operate normally when the spacecraft was despun prior to main boom deployment. A sensor identification of nine was still common at 0.39 rpm, but enough valid data was received to calculate attitudes in planar mode.

The cause of the malfunction has not been explained. Data analysis indicates that the N_b and N_a associated with sensor identification nine is valid, and that it is possible to reconstruct a consistent sensor identification. The analysis is described in Appendix B.

3.4 ATTITUDE CONTROL HARDWARE EVALUATION

The RAE-B spacecraft is equipped with a cold-gas ACS capable of performing spin axis reorientations and spin rate changes. Pressurized gas (CF_4 + 10 percent He at 40 pounds per square inch) is released from one of six thruster nozzles. One precess nozzle plus a spin-up/spin-down pair is mounted on each of two ACS booms. All nozzles are 0.2-pound thrust nominal except one precess nozzle is 0.1-pound thrust nominal. Spin-up/spin-down nozzles may be operated continuously or by individually commanded pulses of 300-millisecond duration. The two precess nozzles are fired in short pulses: one pulse per spin period.

An electronic pulse width of 80, 350, or 950 milliseconds may be selected. Each pulse is initiated at a specified time delay following receipt of a Sun-reference pulse from a preselected sensor (SAS, PAS1, or PAS2). Operation in this fashion results in attitude maneuver trajectories which are Sun-referenced rhumb lines. Further description of the ACS is provided in Section 1.2.5.

The ACS performed generally as expected during the RAE-B mission. Two notable hardware malfunctions resulted in some unforeseen problems, which are discussed in the following section. In addition, preflight calibration of the thruster strengths and pulse centroids were rather poorly defined in some cases. The resulting problems were effectively resolved by the capability for in-flight updating of ACS performance characteristics provided in the ACS software. Preflight measurements of nozzle misalignment proved to be quite satisfactory. Approximately half of the usable ACS fuel was consumed during the mission. The average specific impulse for all the ACS maneuvers was 3.2 percent greater than preflight estimates had indicated.

3.4.1 Hardware Malfunctions

3.4.1.1 ACS Register Shift

For a precess maneuver, the initiation of each ACS pulse is timed from the Sun-reference pulse. The timing, which determines the direction of precession of the spacecraft angular momentum vector, is performed in the following manner. The ACS register (8 bits) is loaded by ground command with a preselected value. On receipt of the Sun-reference pulse, a counter is incremented at the ACS clock rate until the counter matches the ACS register. At this time, an ACS pulse is initiated, and the counter is reset to zero and remains in that state until receipt of the next Sun pulse. The ACS clock rate is selected from 200, 50, 12.5, or 0.78125 Hertz. The Sun pulse is selected from the SAS or from the solar gate of either PAS.

Early in the mission, it was decided to test the ACS system with a small (10.6 degrees) precess maneuver toward the attitude required for the first mid-course correction (Table 2-1). The hardware selected (ACS number 1, 350-millisecond pulse width) was optimal for the 50-rpm spin rate, which was maintained throughout the translunar phase. The 277-second maneuver was initiated and monitored on a real-time display of predicted versus observed Sun angles. This display is reproduced in Figure 3-30. Initially the Sun angle increased at approximately the predicted rate, but then failed to increase further and finally dropped back one Sun bucket. This was due to a shift in the ACS register from the preset value of 66 to 132 at 162 seconds into the maneuver. With the 200-Hertz ACS clock rate and the PAS2 Sun pulse, this register shift resulted in a 100-degree change in the direction of precession from approximately south with respect to the Sun as the North Pole to slightly north of east. The ACS register value was monitored during the maneuver, and eventually its shift was noted, but the maneuver timed out before any decisive action was taken.

Approximately 14 hours later, another maneuver to the first midcourse correction attitude (Table 2-1) was initiated using the same hardware (ACS number 1, 350-millisecond pulse width). This time the ACS register was carefully monitored, and when the register shifted from 59 to 119 after 1.5 minutes, the maneuver was immediately terminated. Because the required time for VCPS firing was rapidly approaching, the failure of the ACS register to hold its preset value presented a significant problem. The spacecraft attitude was quickly redetermined, and a maneuver to the desired attitude was computed using a different hardware combination (ACS number 2, 80-millisecond pulse width). This maneuver was executed with no problems. The hardware combination for which the register shift occurred (ACS number 1, 350-millisecond pulse width) was never used again during the mission, and no further problems with the ACS register were encountered. It was noted that the new register value was in one

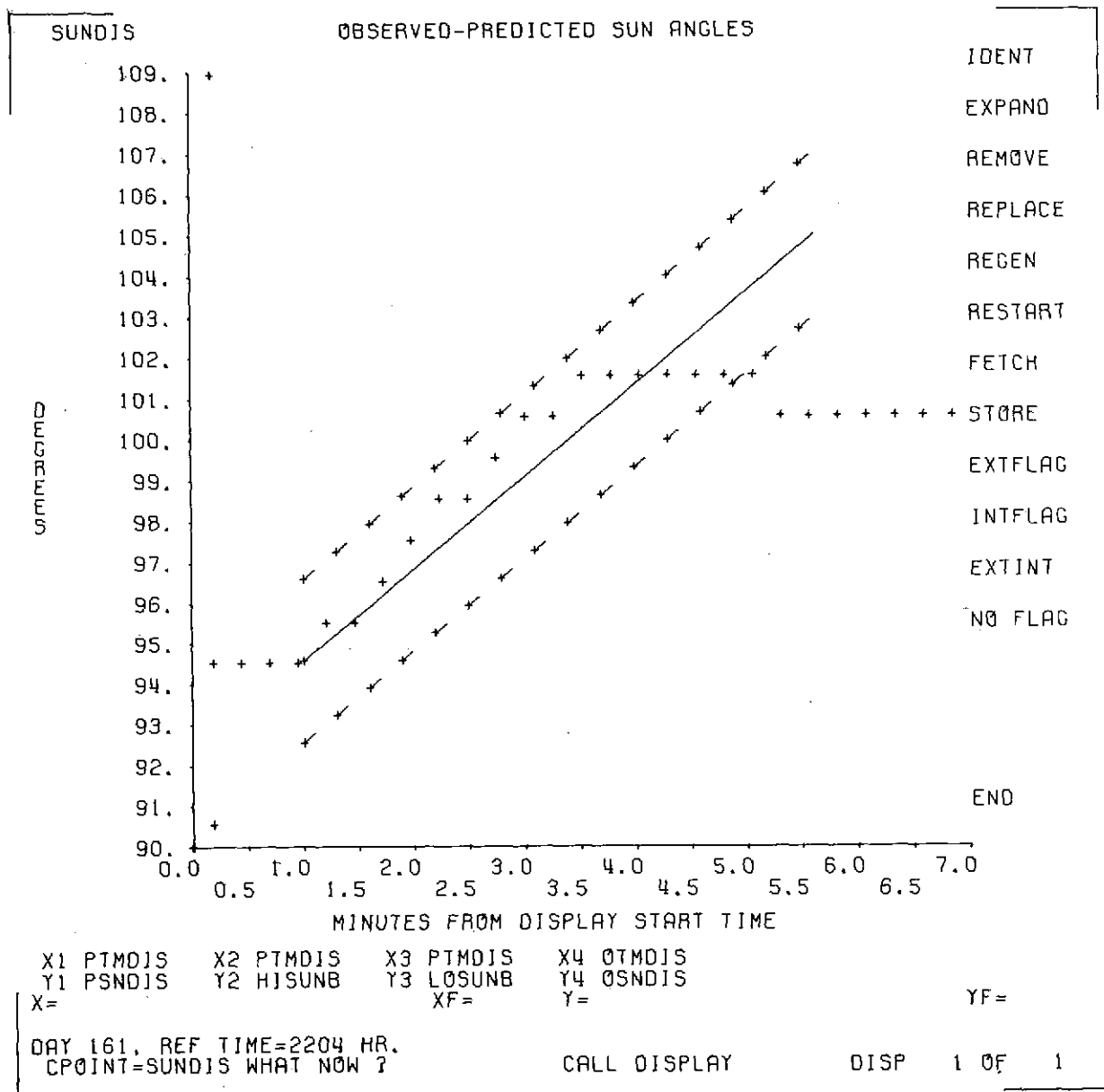


Figure 3-30. ACS Register Shift During Small Precess Maneuver

case twice the old value, and in the other, one greater than twice the old value. This indicates a left shift of the register bits by one bit, with the new, least significant bit being random.

3.4.1.2 Faulty Operation of Pulsed Mode Spin Control

The spin-up/spin-down nozzles may be operated in a pulsed mode for which each ground command causes the selected valve to open for approximately 300 milliseconds. This produces a spin rate change of 0.06 rpm to 0.09 rpm depending on the spacecraft Z-moment of inertia. Thus small changes in spin rate may be accomplished by a series of individually commanded pulses.

Prior to dipole calibration, it was decided to increase the spacecraft spin rate from 12.6 rpm to 15.0 rpm using a series of pulsed spin commands (Table 2-1). Thirty pulses were sent at 15-second intervals. Initially the spin rate increased as predicted, but as the last few pulses were sent, the spin rate suddenly jumped from 14.5 rpm to 17.5 rpm. An examination of the telemetry data at a later time showed that the spin nozzle remained on for approximately 15 seconds following the initiation of the 27th command. Apparently the 28th command (15 seconds after the 27th command) executed properly and terminated the continuous operation of the nozzle. The final two pulsed spin commands apparently also executed properly.

Just prior to main boom deployment, the spacecraft had to be despun to approximately 0.25 rpm. Following a continuous despin from 12 rpm to 3.8 rpm, the final descent was performed using a series of pulsed spin commands. The final spin-down procedure was further complicated because reliable spin-rate data was unavailable below approximately 3 rpm. In this range, the spin rate was indirectly monitored by observing on a stripchart the periodic pattern of the antenna signal strength. On the 37th of 39 planned pulsed spin commands, the ACS stuck on. The spin rate decreased through zero to -6.48 rpm before the ACS could be shut off. A continuous spin-up maneuver was then performed,

sending the spin rate back through zero to a value of +1.11 rpm. Eight pulsed spin commands were then executed, reducing the spin rate to 0.39 rpm. Although no problems were encountered in this series of pulses, it was decided to deploy the booms from this spin rate.

3.4.2 Hardware Calibration

The ACS software provides the capability for determining biases to the nominal ACS performance characteristics, based on the actual in-flight performance of the ACS. These biases are in the form of a set of performance parameters which were chosen to be as independent as possible and determinable from the observed results of an ACS operation. In addition, the performance parameters are independent of spacecraft spin rate and moments of inertia so that the performance parameters determined from one maneuver evaluation may be applied later under a different set of conditions. Individual performance parameters are computed for each ACS hardware combination to update the following characteristics:

1. Effective torque level
2. Rate of fuel consumption
3. Spin component of torque
4. Location of pulse centroid

The last two are applicable only to the precess combinations. Parameter updating was performed throughout the RAE-B mission with very good results. Using the updated performance parameters determined from previous maneuvers, commands could be generated for future maneuvers with a high level of confidence in the predicted spacecraft response.

The first use of ACS number 2 with the 950-millisecond pulse width occurred in lunar orbit for the coarse precession to the attitude required for the second orbit circularization (Table 2-1). The large precession trajectory (180 degrees) and the relatively low spin rate (12.3 rpm) made this the chosen combination. ACS

commands and the associated prediction were generated for the maneuver using 1.10 for the effective torque performance parameter and -10 milliseconds for the centroid offset performance parameter. These values were chosen based on previous experience with other hardware combinations and a desire not to overshoot the maneuver. Nominal values were used for the other two performance parameters. Plots of predicted versus observed Sun angles and spin rates were monitored in real time during the maneuver. These plots are reproduced in Figures 3-31 and 3-32. It is apparent from Figure 3-31 that the Sun angle is not decreasing as rapidly as predicted. During the maneuver, it was judged that the spacecraft was precessing very nearly in the desired direction, but that the effective torque performance parameter should be near the nominal value (1.0) rather than the conservative value of 1.1 used in the prediction. Consequently the maneuver time was extended from 27.0 minutes to 29.25 minutes. The resulting final attitude was within 2 degrees of the targeted position, confirming the judgment made during the maneuver. A postmaneuver performance evaluation was carried out, and the resulting input and output displays are reproduced in Figures 3-33 and 3-34. The updated performance parameters recommended in Figure 3-34 were used to regenerate the predicted spacecraft response for the implemented command. The resulting plots of predicted versus observed Sun angles and spin rates are shown in Figures 3-35 and 3-36. The predicted values now match the observed data very well, representing a significant improvement over the results plotted in Figures 3-31 and 3-32.

The performance parameters determined for the hardware combination discussed above (ACS number 2, 950-millisecond pulse width) were reasonably close to the nominal values determined from preflight calibration testing. However, this was not the case for the hardware combination (ACS number 2, 80-millisecond pulse width) used throughout the translunar phase of the mission. In-flight performance evaluations for this combination showed the pulse centroid offset to be 40 milliseconds shorter and the torque impulse to be 11 percent

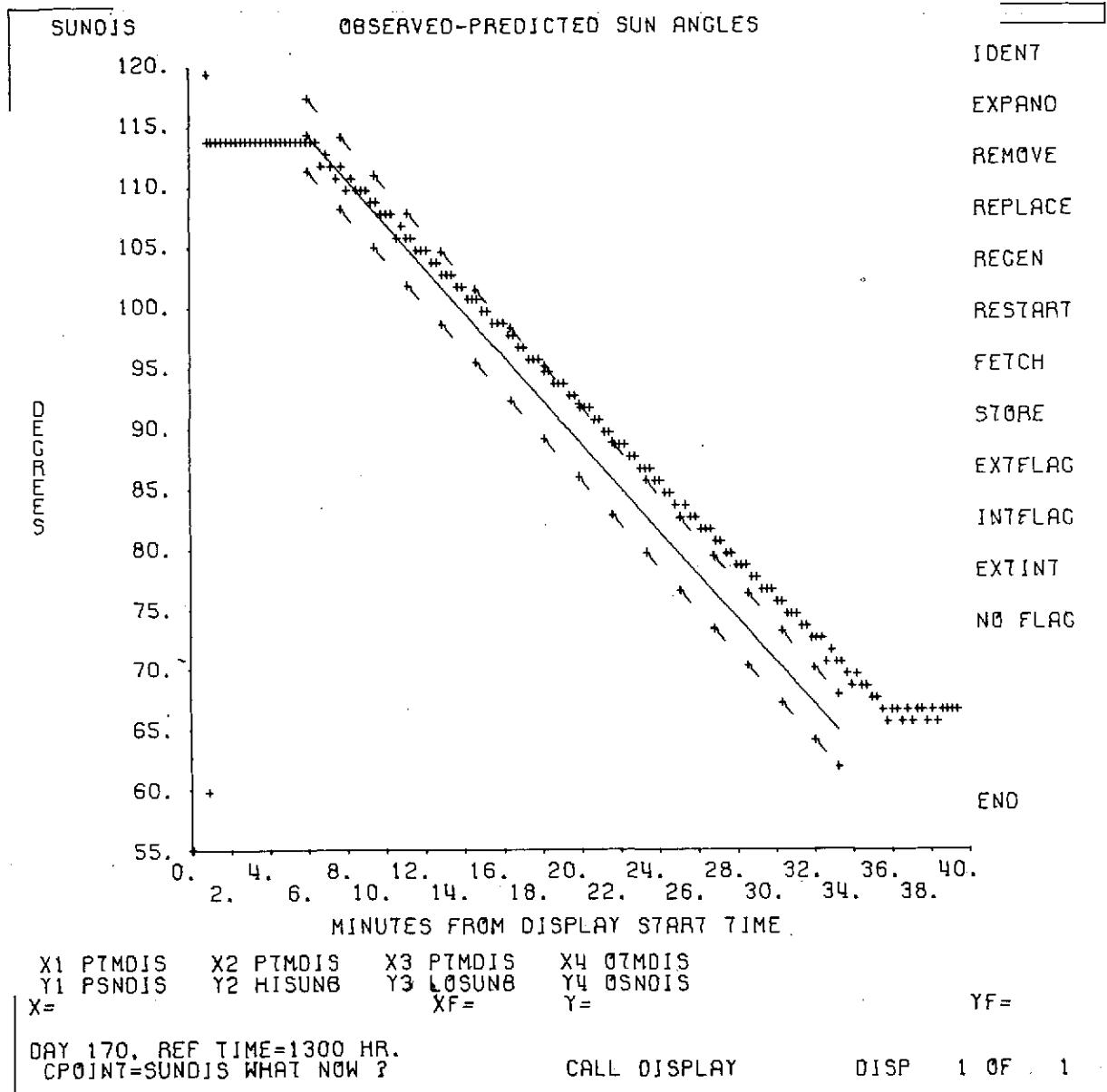


Figure 3-31. Predicted-Observed Sun Angles During ACS Maneuver
Using Uncalibrated Hardware

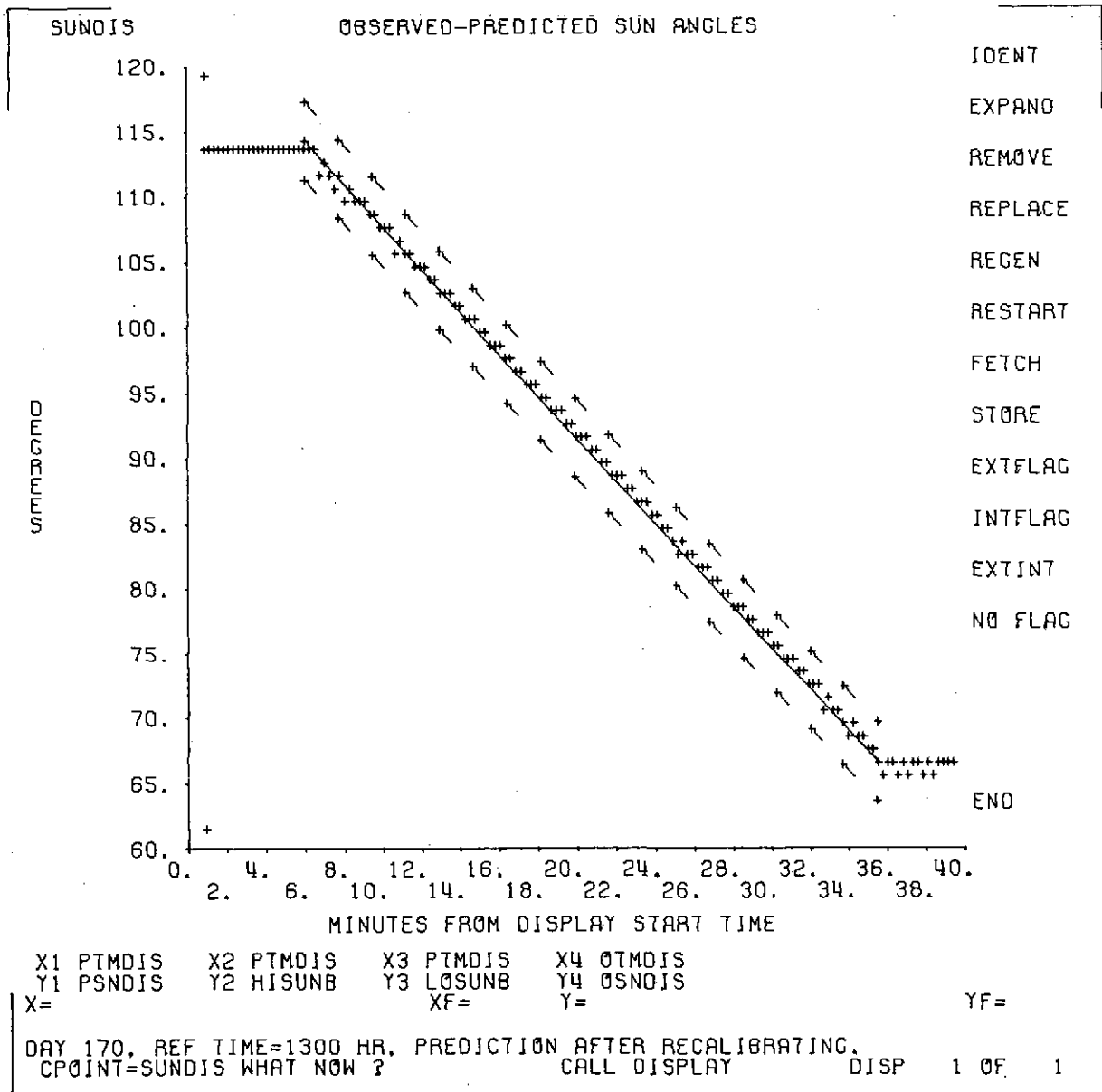


Figure 3-35. Predicted-Observed Sun Angles Following ACS Performance Evaluation

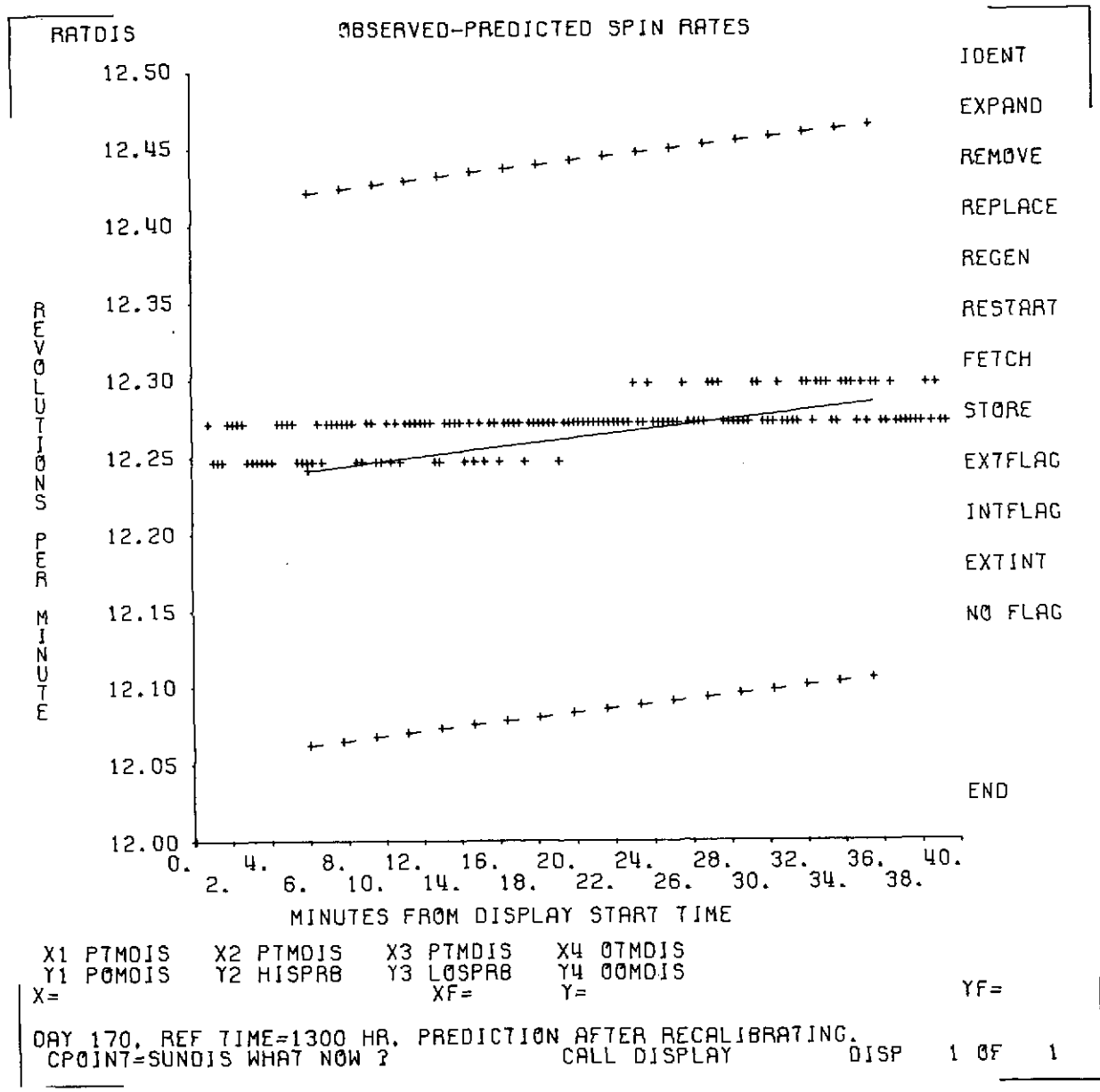


Figure 3-36. Predicted-Observed Spin Rates Following ACS Performance Evaluation

smaller than the values provided from preflight calibrations. The centroid discrepancy results in a 12-degree error in the precession direction at 50 rpm. The effectiveness of in-flight updating of the ACS performance characteristics is demonstrated for this hardware combination (ACS number 2, 80-millisecond pulse width) in the first precess maneuver in lunar orbit (Table 2-1). This maneuver came within a few tenths of a degree of the targeted attitude even though it was computed using performance parameters determined from previous maneuvers with a very different spin rate and Z-moment of inertia (due to fourth-stage firing and ejection).

The results of all hardware evaluations performed during the mission are summarized in the following discussion. The four spin nozzles plus the ACS number 1 precess nozzle are nominally identical. These were apparently under-rated (in thruster strength) by approximately 10 percent in preflight calibrations.

Preflight tests showed the pulses for all pulse widths to have approximately the same 300-millisecond tail following shut off of valve current. The fall-off rate of this tail is rather sensitive to the operating environment of the nozzle, and, of course, test conditions could not exactly duplicate the actual operating environment. Centroid locations and torque impulses for the various pulse widths were computed based on the pulse shapes determined from these tests. It is believed that the pulses tailed off more rapidly than indicated in the tests for the following reasons.

1. The centroid offsets for all pulse widths were shorter than the computed values.
2. The torque impulses for all pulse widths were smaller than the computed values.
3. The first two effects were much more apparent for the short pulse widths than for the longer ones.

The characteristics of a tail, which may be as long as 300 milliseconds, can obviously have a great effect on the performance of an 80-millisecond pulse. This effect resulted in significant errors in the initial predictions using the 80-millisecond pulse width.

The preflight calibration for the misalignment of the precess nozzles was very good. Spin-rate changes during precess maneuvers were computed by the Attitude Control software, taking into account angular momentum and moment of inertia changes during the maneuver and nozzle misalignment. The resulting predicted spin rates agreed quite well with the observed values. Spin-rate changes caused no problems in predicting spacecraft response for precess maneuvers.

The rate of fuel consumption could not be accurately calibrated for individual maneuvers. Actual fuel consumption was determined as the difference between the premaneuver and postmaneuver fuel mass remaining in the ACS tanks. Uncertainties in the tank temperatures and pressures resulted in rather large uncertainties in the initial and final masses compared to the small amount of fuel used in a single maneuver. However, the total fuel consumption and average specific impulse for the entire mission has been calculated. A total of 2.71 kilograms (5.97-pound of mass) of ACS propellant was consumed. This is approximately half of the usable fuel carried on the mission. The average specific impulse for all the ACS maneuvers was computed to be 403-Newton seconds per kilograms (43.8-pound thrust-seconds per pound of mass) This value is 3.2 percent greater than the value of 42.5-pound thrust-seconds per pound of mass provided from preflight calibrations.

SECTION 4 - SOFTWARE EVALUATION

4.1 MAPS/RAE-B SYSTEM EVALUATION

The MAPS/RAE-B Attitude Support System is a large, complex system designed to satisfy nominal and in some cases non-nominal attitude determination and attitude control requirements for the RAE-B mission. The system operated in an exceptional manner throughout the translunar and boom-deployment phases of the mission and is currently being used to satisfy weekly operational and definitive requirements.

The system possesses many highly desirable characteristics and capabilities to monitor and control the satellite's attitude behavior. The system was designed in a modular fashion under the Multi-Satellite Attitude Determination Executive System and provides great flexibility for processing attitude data and refining attitude solutions. Many graphic displays are incorporated in the system which aid the user both analytically and operationally in ensuring reliable attitude accuracies.

The sophistication and complexity of the system was necessitated by the intricate spacecraft hardware and demanding mission requirements. New attitude determination algorithms were developed and incorporated within the system to determine attitude using data obtained from the panoramic scanners and solid angle Sun sensors. The real-time operational support of boom deployment necessitated the design and development of a dynamic model to monitor the spacecraft motions.

Many mission and spacecraft hardware contingency conditions were anticipated in the design phase of the system, and the system was developed to accommodate these. The system illustrates the demanding analytical and software requirements placed on the Attitude Determination and Control Section in supporting future missions. Careful planning in the analysis and design phases of

the software system generation cycle must be taken to develop systems to meet these complicated requirements and, also, to avoid complex operational problems. Systems should be designed to accommodate some contingencies; however some contingencies should be treated as such. Systems should be designed to ease the testing of the system to develop high system integrity such as in the RAE-B Attitude Support System.

4.2 PERFORMANCE EVALUATION OF ANALYTICAL ALGORITHMS

Four special algorithms were incorporated into the RAE-B system: solution restoration, analytic identification of horizons and terminators, pairing of solutions for unidentified crossings, and bit overflow restoration. The analysis for these algorithms is found in References 7, 8, 9, and 3, respectively. In addition, the capability for calculating and modifying ACS performance parameters was included, and a predicted-observed telemetry data plot was developed.

4.2.1 Solution Restoration

Poor geometry or small and crescent targets frequently yield inconsistent data, manifested by square roots of negative numbers, cosines with magnitude greater than 1, or nonintersecting cones when the data are processed with the standard optical aspect algorithm (Reference 10). Such data are rejected in the course of processing. Methods described in Reference 7 for analyzing and restoring these data were implemented in the MAPS/RAE-B modules SGLCRS and DBLCRS. Actual RAE-B sensor data included many such inconsistencies. The modified algorithms were generally able to compute a valid attitude.

Examples of solutions restored for single horizon crossings from Moon sightings during the early translunar cruise are illustrated in Figure 4-1. The second and fourth solutions were restored (denoted by the asterisk in the column headed RF) and an accurate attitude was obtained. Note that in this case the restored solutions have a weight approximately one-fourth that of the normal solutions. An additional feature, which is characteristic of small targets,

is that the restored solutions resulted in unambiguous attitudes whereas the normal solutions do not. In this instance, the restored solutions determine the choice (believed correct on the basis of other data) between the ambiguous pairs of solutions which are based on consistent data.

4.2.2 Horizon-Terminator Checking

The MAPS/RAE-B utilized the analytic method for central body and horizon-terminator identification described in Reference 8. This method achieved results essentially identical to those obtained using a data predictor at a considerable savings in both processing time and core usage. The tolerances on intermediate attitude calculations, provided as a part of solution restoration discussed above, allowed correct identification of central bodies in cases for which a data predictor would indicate that a scan with the computed attitude would (narrowly) fail to intersect the central body.

4.2.3 Solution Pairing

Solution pairing is a term used to describe a particular set of circumstances in which solutions from the two transitions within a scan should be treated as a pair of ambiguous attitudes rather than as distinct solutions. The analysis leading to this treatment is contained in Reference 9. The conditions are that the horizon-terminator identification method described above be unable to determine whether either of the transitions corresponds to horizon or terminator, and that each transition give rise to a single attitude solution. The scan geometry and the first-AOS/first-LOS logic of the scanner circuitry make it highly likely that one transition is a horizon, the other a terminator in this case. Therefore, one solution (from the horizon crossing) is correct while the other is incorrect. The two are treated in MAPS/RAE-B as an ambiguous pair; only one of the two is included in any block-averaging iteration.

During the RAE-B mission this procedure did not prove particularly useful. The large Sun acceptance angle of the PAS and the problems which developed with the PAS during the mission, combined with the central body geometry, limited the number of frames in which the technique could be applied. Figure 4-2 does illustrate several unknown (UU) crossings in actual RAE-B data. Note that the crossing from 153059 to 153216 are all UU pairs. In the five cases in which the AOS and LOS (first and second, respectively, of the two with the same time label) transitions each yield one attitude, the AOS solution is the correct attitude whereas the LOS solution is erroneous. Clearly these are all horizon-to-terminator scans, although a data predictor would identify each transition separately as a horizon crossing. Figure 4-3 illustrates the correct block-averaging procedure for these data. The paired frames are numbers 39, 41, 45, 47, and 49, and are denoted by an S. The block-averaging procedure selects the correct attitude solution from each frame.

4.2.4 Bit Overflow Restoration

It was realized well in advance of launch that most-significant bits might be lost in the LOS register from the PAS, and several algorithms were designed to detect and, if possible, restore missing bits (see Reference 3). In none of these was knowledge of an a priori attitude fully exploited. This was a deficiency in the program. Few overflows occurred with the Earth as a target because the Earth was not a useful target after the first hours of the mission. By the time the Moon appeared large enough to cause overflows, the attitude was well established. The known attitude was used with the plot of predicted versus observed telemetry data to manually restore the overflowed bits in the latter case, however, so no serious difficulties resulted.


```

***** M S A D *****
*** DISPLAY ***** 73.240.16.43.47 ***
**
**      BLKINT          BLOCK AVERAGE INPUT ARRAYS      **
**
**      IBLK - ELCKC AVERAGE INDICATOR          CS      **
**      (NC,D,DS,DIN,OCUT,S,IN,OUT)            **
**      ICBL - DBLCRS IND. (NC,MOD1,MOD2,MCD3)  MOD1     **
**      ISGL - SGLCRS IND. (NO,YES)            YES      **
**      REFERENCE DATE (YYDD)                  73161    **
**      A PRICRI RIGHT ASCENSION              164.500   **
**      A PRICRI DECLINATION                   -15.000   **
**
**      IAPICR - A PRIORI ATTITUDE INDICATOR    8        **
**      (0-NCNE,4-USE LAST,8-USE FIRST)        **
**      BLKAVE ARRAY POINTERS                  **
**      IESTRT - START ELEMENT                  1        **
**      IEND - ENDING ELEMENT                  26       **
**      INPUT ARRAY POINTERS IBOUT1            1        **
**      IBOUT2                                  52       **
**      GEN. BLKAVE DISPLAY ARRAYS (YES,NO)     YES      **
**      FRAM FR NO. SOL. CNE. SOL. TWO CHOIC SPNDEV    **
**      NO. ID SOL ALPHA1 DELTA1 WT81 ALPHA2 DELTA2 WT82 **
**      7 S 2 156.60 -31.23 1.41 170.87 -0.28 1.39 0 ***** **
**      9 S 2 156.77 -30.92 1.40 170.71 -0.66 1.38 0 ***** **
**      11 S 2 157.06 -30.40 1.38 170.61 -0.89 1.36 0 ***** **
**      13 S 2 157.18 -30.18 1.35 170.49 -1.16 1.33 0 ***** **
**      15 S 2 157.22 -30.12 1.32 170.44 -1.2E 1.30 0 ***** **
**      17 S 2 157.26 -30.03 1.28 170.30 -1.60 1.26 0 ***** **
**      19 S 2 157.32 -29.92 1.24 170.23 -1.77 1.22 0 ***** **
**      21 S 2 157.40 -29.78 1.19 170.15 -1.96 1.17 0 ***** **
**      23 S 2 157.37 -29.83 1.14 169.89 -2.57 1.12 0 ***** **
**      25 S 2 157.36 -29.85 1.08 170.05 -2.20 1.07 0 ***** **
**      27 S 2 157.47 -29.65 1.03 169.94 -2.46 1.02 0 ***** **
**      29 S 2 157.82 -28.99 0.97 169.54 -3.40 0.96 0 ***** **
**      31 S 2 158.09 -28.50 0.91 169.40 -3.73 0.91 0 ***** **
**      33 S 2 158.37 -27.96 0.85 169.15 -4.32 0.85 0 ***** **
**      35 S 2 158.67 -27.39 0.79 168.89 -4.65 0.80 0 ***** **
**      37 S 2 158.99 -26.76 0.73 168.70 -5.39 0.74 0 ***** **
**      39 S 2 165.62 -12.58 0.91 180.36 20.63 0.93 1 C.22 **
**      41 S 2 165.69 -12.42 0.87 180.13 20.06 0.91 1 C.05 **
**      43 I 2 177.25 14.17 0.04 180.34 20.49 0.05 0 ***** **
**      44 C 1 177.05 13.76 0.7E 999.00 999.00 0.0 0 ***** **
**      45 S 2 165.78 -12.21 0.78 179.08 17.99 0.82 1 C.15 **
**      47 S 2 165.81 -12.14 0.73 177.37 14.43 0.70 1 C.25 **
**      49 S 2 165.77 -12.22 0.67 165.32 -13.27 0.50 1 0.17 **
**      51 D 2 161.32 -22.05 0.02 141.48 -51.05 0.32 0 ***** **
**      51 I 1 165.84 -12.08 0.61 999.00 999.00 0.0 1 0.32 **
**      52 C 1 165.33 -13.23 0.43 999.00 999.00 0.0 1 C.93 **
**
**
**
**      M204 NUMBER(S) TOO BIG FOR FORMAT (*)
**      CPOINT=BLKRES WHAT NOW          CALL DISPLAY          DISP 1 CF 1
**
***** M S A D *****
***** DISPLAY *****

```

Figure 4-3. Block Average Selection of Correct Solutions From Pairs

4.2.5 ACS Performance Parameter Evaluation

The ACS of MAPS/RAE-B included the capability to evaluate ACS performance parameters on the basis of observed attitude changes. The effectiveness of parameter reevaluation can be seen from Table 2-1. Trim maneuvers were performed on three of the precession maneuvers; the later trim maneuvers were much smaller in relation to the initial maneuvers than was the first trim maneuver. Predictions for spin maneuvers also improve with experience. As noted in Section 3.4 significant deviations were determined (and corrected) in effective thrust levels and in the offset between pulse initiation and pulse center.

4.2.6 Predicted-Observed Telemetry Data Plot

As an aid in determining attitude and in visualizing data quality, a predicted-observed telemetry data plot was developed. For an example, see Figure 2-11. The predicted portion of the plot consists of a nadir angle versus dihedral angle plot of Moon and Earth horizons and terminators, plus an extended Sun of arbitrary angular radius, as seen from the spacecraft at a particular time for a specified attitude. Lines from the centers of the three bodies indicate approximately the direction of the shift in apparent position of the three bodies for a specified change in spacecraft attitude. The observed portion of the plot consists of mounting angle versus AOS and LOS angles from the PAS.

In translunar orbit, where apparent angular velocities of the central bodies were low, the plot proved useful both in determining attitude and (with various types of attitude solution) in estimating biases in the PAS. In lunar orbit, the plot was less useful because the angular velocity of the spacecraft with respect to the Moon was about 1.6 degrees per minute, or about 0.4 degree per data point. However, the plot could still be used to estimate and correct bit overflows in the LOS register.

APPENDIX A - EXPLANATION OF COLUMN HEADINGS FOR
TABULAR DISPLAYS

A	Dihedral angle about the spin vector from the Sun vector to the horizon vector
AA	PAS anomaly flag: =0, scan does not start on a lit target =1, scan starts on a lit target
ALPHA	Angle between the Sun vector and the horizon vector
BB	See CB
BETA	See SUN BETA
BODY RADIUS	Angular radius subtended by the indicated central body at the position of the spacecraft
CB	Central body indicator for PAS transition: =E, Earth =M, Moon =S, Sun =U, unidentified
CC	See HT
CHOIC	Pointer to selected solution from pair of solutions: =0, no solution selected =1, first (or only) solution =2, second
CLCK RATE	Nominal PAS clock rate; values of 800, 200, and 50 Hertz are allowed

EE Flag to indicate number of times PAS LOS counter has overflowed; values of 0 to 7 are allowed

FL Attitude solution flag:
 =' ' , frame has not been flagged
 ='1', frame has been flagged

FR ID PAS data used for attitude solution:
 =I, AOS
 =O, LOS
 =D, AOS + LOS (double-crossing solution)

FRAM NO. Position of the frame of data in the block of data output from the telemetry processor.

GAMMA Angle between the spacecraft Z-axis and the line of sight of the PAS scanner.

HHMMSS Time (hours, minutes, seconds) of Sun angle for the data frame

HT Indicator for PAS transition:
 =H, horizon
 =T, terminator
 =U, unresolvable between horizon and terminator

KKKK KKKK (0123 4567) LOS overflow indicator:
 =0, number of overflows is not consistent with other data
 =1, number of overflows is consistent with other data

NO. SOL Number of solutions calculated for this set of data

PAS GAM See GAMMA

RF	Solution restoration flag: =' ', solution calculated normally ='*', inconsistencies within estimated error limits were eliminated during processing
SOL. ONE (ALPHA1, DELTA1, WTB1)	See SOLUTION ONE (ALPHA1, DELTA1, WGHT1)
SOL. TWO (ALPHA2, DELTA2, WTB2)	See SOLUTION TWO (ALPHA2, DELTA2, WGHT2)
SOLUTION ONE (ALPHA1, DELTA1, WGHT1)	First (or only) spin axis right ascension (degrees), declination (degrees), and solution weight calculated from the frame of data
SOLUTION TWO (ALPHA2, DELTA2, WGHT2)	Second spin axis right ascension (degrees), declination (degrees), and solution weight calculated from the frame of data; =999.00, only one solution calculated
SPNDEV	Arc difference (degrees) between the calculated attitude and the average attitude
SPNRT (RPM)	Measured spin rate for the data frame
SUN BETA	Measured angle between the spacecraft axis and the Sun vector
SUN-CBDY	Calculated angle between the Sun vector and the vector to the center of the central body.

APPENDIX B - DIPOLE CALIBRATION DATA ANALYSIS

B.1 INTRODUCTION

During the dipole calibration phase of the RAE-B mission, the spacecraft attitude sensors were operated in solid/planar mode much of the time to obtain Sun angle data from which phase (rotation) angle information could be obtained. The spin rate (3-5 rpm) was higher than the sensors were designed for; it was anticipated that there would be a consequent loss of accuracy but that an acceptably accurate phase angle could nonetheless be calculated. This was not the case; the data as received could not be processed with the attitude system. It is the purpose of this memorandum to describe the data received and the regularities in the data which indicate that it may be possible to calculate the spacecraft phase angle.

B.1.1 Nominal Sensor Data

Sensor data returned in the telemetry include a sensor ID between 1 and 8 (9 or 11 indicate no data), and two angles (N_B and N_A) from which the Sun vector can be obtained with respect to the particular Sun sensor coordinate axes. From these three numbers, the Sun vector, or equivalently the right ascension and declination of the Sun vector, can be calculated with respect to the spacecraft body coordinate axes. The Sun vector right ascension can then be combined with the spin axis attitude and Sun vector in inertial coordinates to obtain the spacecraft rotation angle at the time the data was taken.

B.1.2 Actual Sensor Data

Prior to main boom deployment, the spacecraft was operated for extended periods at 4.706 (4.7) and 3.062 (3.1) rpm, and for a short time at 0.392 (0.39) rpm. Data from all three spin rates has been analyzed.

At 4.7 and 3.1 rpm, only two types of data are seen: a valid sensor ID, in combination with values of N_B and N_A inconsistent with the known body Sun declination angle,¹ from which no attitude can be calculated, and a sensor ID of 9, in combination with values of N_B and N_A generally consistent with the known body Sun declination angle. Because in the latter case no valid sensor ID is present, no attitude can be calculated.

At 0.39 rpm, the two types of data above are present, along with a third: a valid sensor ID along with values of N_B and N_A consistent with the known body Sun vector declination angle. As there was considerable nutation at 0.39 rpm (approximately 5- to 10-degrees cone half-angle) the statement about declination angle is not definitive; however, the correct spacecraft attitude was calculated for many frames of data, using the associated panoramic scanner data.

B.2 ANALYSIS

The fact that the values of N_B and N_A associated with the sensor ID 9 are generally consistent with the known body Sun declination angle led to further analysis to determine whether a valid sensor ID could be associated with each 9. The body Sun right ascension angle could then be calculated by interpolation, and the phase angle calculated. Four tests were developed and applied to blocks of data at each of the three spin rates mentioned above to determine whether the IDs of 9 could be restored to valid IDs.

B.2.1 Validity Tests

Two tests use only data from the frames with a Sun sensor ID of 9. The first requires that the body Sun declination angle, calculated using N_B , N_A , and

¹The values of N_B and N_A unambiguously determine the body Sun declination angle if it is known whether the associated sensor ID is even or odd; otherwise, two possible values are calculated. The body Sun declination angle is known from spin/spherical mode measurements.

the (assumed) valid ID, agree with the value obtained during the times when the spacecraft was operating in spin/spherical mode. Except when the Sun angle is close to 90 degrees, this also identifies the sensor as even or odd.

The second test requires that the difference in body Sun right ascension angle between two consecutive frames with a sensor ID of 9 be consistent with the spacecraft spin rate, which is also known from spin/spherical mode measurements. Once a single sensor has been tentatively identified, this test will generally eliminate at least all but one possibility for the next sensor.

The tests described above must be satisfied for the data associated with the ID 9 to be considered valid. Because the eight Sun sensors possess fourfold rotational symmetry about the Z-axis, the tests are insufficient to unambiguously identify the Sun sensors: if a given sequence of sensor IDs satisfies the tests, another sequence in which each ID is increased by two (modulo eight) will satisfy the tests as well. Two additional tests can be used to resolve the ambiguity.

The third test assumes that the valid IDs in telemetry indicate approximately the location of the Sun vector in body coordinates, even if the associated N_B and N_A are invalid. The position of the Sun vector can be predicted by interpolation or extrapolation from the tentatively identified sensors, and a corresponding prediction made of the Sun sensor which should have triggered. This ID can be compared with that in telemetry. The one of the four sequences of tentatively identified 9s which can be used to correctly predict the largest number of valid IDs is assumed correct.

The fourth test uses interpolated Sun angles together with panoramic scanner data to calculate the spacecraft spin axis attitude, which is then compared with the attitude calculated from spin/spherical mode data. Although the solid/planar mode attitude system was not intended to be used at 3-5 rpm, it should give results in reasonable agreement with spin/spherical mode results. The interpretation of results is complicated by the large Sun acceptance angles of the panoramic scanners.

B.2.2 Results of Analysis

At all three spin rates, the Sun angle data associated with sensor ID 9 satisfies the first two tests, although the nutation at 0.39 rpm results in a corresponding deviation in body Sun declination. The body Sun right ascension can be made to fit a linear curve with slope equal to the negative of the spin rate at all three spin rates, the nutation at 0.39 rpm having little effect because the Sun vector lies close to the spacecraft x-y plane.

The third test is satisfied qualitatively at all three spin rates, but there are quantitative aspects to the results which may be important. A block of 30 telemetry records containing 18 valid Sun sensor IDs and with 12 ID 9s, was processed from an interval during which the spacecraft was rotating at 4.7 rpm. By straightforward prediction of Sun sensor IDs, one of the four tentative sequences of IDs for the 9s was selected; however, only 3 of the 18 valid IDs were correctly predicted. (The other three sequences yielded one or no correct predictions.) A systematic deviation was noted; as a result, the analysis was extended to associate a triggering delay with the valid IDs. If it is assumed that the 9s represent data taken at frame time, but valid IDs represent triggering at frame time +1.35 seconds, all valid IDs are correctly predicted (using the same sequence of IDs for the 9s as when 3 of 18 IDs were correctly predicted).

At 3.1 rpm, the results are qualitatively the same. An assumed delay of 3.30 seconds is needed to correctly predict all valid sensor IDs.

At 0.39 rpm, one of the four sequences of tentative IDs was selected without resorting to a time delay. The spacecraft was rotating slowly enough that a time delay of the order of the frame interval (7.68 seconds) would have little effect on sensor ID predictions. The occurrence of apparently valid combinations of Sun sensor ID with N_B and N_A provided an indirect indication of a time delay. The curve fitted to valid Sun data differed from the curve fitted to

the data frames with restored sensor IDs by 9 degrees, the two curves being evaluated at the same time. This difference, given the spacecraft spin rate, is equivalent to a triggering delay of 3.84 seconds for the valid IDs relative to the (restored) 9s. The data points for valid IDs showed a greater scatter about the fitted curve than did the data points for restored 9s.

The fourth test, on calculated attitudes, is not generally useful. The restored sensor IDs can be used to calculate Sun angles from which valid attitude solutions can be computed, but valid solutions can also be computed from some of the rejected ID sequences. This occurs because of false PAS triggerings from the Sun and probably also because of geometry at certain points in the orbit.

B.3 CONCLUSIONS

The linear fits that can be obtained to restore sensor data at all spin rates indicate that data associated with sensor ID 9 is valid and is measured at a nearly fixed time with respect to the frame time. This indicates that the spacecraft phase angle can be determined up to a multiple of 90 degrees (plus any error arising from incorrect triggering times). The spin rate is constant enough that different blocks of data will not have a relative phase shift if there is no data dropout exceeding an hour between blocks.

To resolve the fourfold ambiguity in phase, it is necessary to make some assumption regarding the valid IDs in telemetry. Assuming that the valid IDs represent the approximate position of the Sun vector at frame time, and using data from restored IDs to predict sensor IDs for those frames, generally one of the four possible sequences of restored IDs will be selected as providing the best prediction. This prediction cannot be guaranteed to be consistent from one data block to the next. A better prediction occurs if it is assumed that valid IDs correspond to SAS triggerings which are delayed from frame time (or restored

ID triggering time) by a spin-rate dependent amount ≤ 3.84 seconds (see Table B-1). The possibility of such a delayed triggering is supported by data at 0.39 rpm, where curves fit to restored sensor data and to valid sensor data differ by 9 degrees (3.84 seconds). Scatter in the valid points at 0.39 rpm indicates that a delay, if present, is not constant.

Table B-1. Spin Rate Versus Time Delay for Valid Sensor IDs

<u>Spin Rate</u>	<u>Time Delay</u>
0.392	3.84 seconds
3.062	3.30 seconds
4.706	1.35 seconds

REFERENCES

1. Computer Sciences Corporation, 3000-05300-02TN, Radio Astronomy Explorer-B Dipole Calibration Data Analysis, R. Berg and R. Williams, November 1973
2. EMR Aerospace Sciences, 6341-2045, Panoramic Attitude Sensor for Radio Astronomy Explorer B, R. Thomsen, June 1973
3. Computer Sciences Corporation, Memorandum (Task Assignment No. 075), Bit Overflow in the LOS Register of the PAS Sensor on RAE-B, G. Lerner, July 1972
4. Goddard Space Flight Center, RAE-B Alignment Summary (Launch Site), W. P. Sours and K. E. Gardner, May 1973
5. Computer Sciences Corporation, 3000-06000-01TM, OABIAS Test Results I, T. Shinohara, October 1973
6. Goddard Space Flight Center, X-711-68-349, Solar Aspect System for the Radio Astronomy Explorer, E. John Pyle, Jr., September 1968
7. Computer Sciences Corporation, Memorandum (Task Assignment No. 075), Methods for Increasing Data Availability During the Trans-lunar Mode of RAE-B Mission, G. Lerner, March 1973
8. --, Memorandum (Task Assignment No. 075), RAE-B Terminator Checking, R. Williams, July 1972
9. --, Memorandum (Task Assignment No. 031), Extended Capabilities of RAE-B Terminator Checking, R. Williams and G. Lerner, April 1973
10. --, 9101-13300-03TR, Optical Aspect Attitude Determination System (OASYS), M. Joseph and M. Shear, October 1972